NATIONAL AERONAUTICS AND SPACE ADMINISTRATION

Technical Report 32-1560

Attitude Propulsion Technology for TOPS

Philip I. Moynihan

JET PROPULSION LABORATORY
CALIFORNIA INSTITUTE OF TECHNOLOGY
PASADENA, CALIFORNIA

November 1, 1972

Technical Report 32-1560

Attitude Propulsion Technology for TOPS

Philip I. Moynihan

Preface

The work described in this report was sponsored by the National Aeronautics and Space Administration Office of Advanced Research and Technology and was performed by the Propulsion Division of the Jet Propulsion Laboratory. The Thermoelectric Outer Planet Spacecraft (TOPS) advanced technology project provided a design point about which the Attitude Propulsion System technology presented herein was focused for a more meaningful outcome.

Acknowledgments

Contents

Tables

Contents (contd)

Tables (contd)

Figures

Contents (contd)

Figures (contd)

Contents (contd)

Figures (contd)

Abstract

This report summarizes the JPL Thermoelectric Outer Planet Spacecraft (TOPS) attitude propulsion subsystem (APS) effort. It includes the tradeoff rationale that went into the selection of an anhydrous hydrazine baseline system, followed by a discussion of the 0.22-N (0.05-lb$_f$) JPL-developed thruster and its integration into a portable, self-contained propulsion module that was designed, developed, and "man-rated" to support the TOPS single-axis attitude control tests in the JPL Celestarium. The results of a cold-start feasibility demonstration with a modified JPL thruster are presented. A description of three types of 0.44-N (0.1-lb$_f$) thrusters that were procured for in-house evaluation is included along with the results of the test program. This is followed by a description of the APS feed system components, their evaluations, and a discussion of an evaluation of elastomeric material for valve seat seals. The report concludes with a list of new technology items which will be of value for application to future systems of this type.

Attitude Propulsion Technology for TOPS

I. Introduction: TOPS Advanced System Technology Project

The purpose and objectives of the Thermoelectric Outer Planet Spacecraft (TOPS), as defined in Ref. 1, were:

Purpose

(1) To develop and demonstrate the capability to perform missions to the outer planets; specifically, the Grand Tour type of mission.

(2) To develop understanding of the necessary system capabilities for this class of mission.

(3) To provide design, development, and test experience in several new technologies critical to this type of mission.

(4) To develop an understanding of the required subsystems and their interactions so that realistic performance, reliability, schedule, and cost estimates could be made. New spacecraft technology was to be emphasized.

Objectives

(1) To design a Grand Tour mission compatible with a radioisotope thermoelectric generator (RTG) powered ballistic spacecraft for the 1976–1979 launch opportunities.

(2) To develop a spacecraft system design concept emphasizing the long-life, environment immunity,

and emergency adaptability characteristics required for the Grand Tour and other outer planet missions. The system design should represent a proven technology for the 1976–1979 period.

(3) To develop techniques for assuring compatibility between the RTG radiation field and the remainder of the mission systems and subsystems, and to investigate interactions between the spacecraft and science instruments.

(4) To develop advanced designs as required, including the design of the thermoelectric generator of an RTG power subsystem based on system requirements.

(5) To demonstrate, by analysis and test, the validity of design concepts that transcend previous experience or represent major technical innovations. A combination of the results obtained and current experience should establish the feasibility of accomplishing this type of mission with the spacecraft employing the advanced technology.

(6) To develop an understanding of, and possible solutions for, nuclear safety problems associated with an RTG-powered spacecraft. To establish design rules that would ensure compatibility between the launch vehicle and the spacecraft so that operations could be designed to satisfy Atomic Energy Commission (AEC), National Aeronautics and Space Administration (NASA), and Air Force Eastern Test Range (AFETR) constraints.

The outer planet missions that were actually selected for the TOPS technology development where the two multiple-encounter Grand Tour missions, the first being to Jupiter, Saturn, and then Pluto, while the second would explore Jupiter, Uranus, and Neptune. The launch opportunities for these missions are available during the latter half of this decade.

The TOPS advanced system technology project was not, nor was it ever intended to be, a flight project. The final outcome was an identification of required technologies and their status, along with design concepts and some test program results, some of which are synergetic with an ensuing flight project, while others are not.

The Thermoelectric Outer Planet Spacecraft, as perceived at the end of the TOPS Project, is depicted in Fig. 1. As can be seen, the spacecraft concept consists primarily of a skeletal structure, a 4.25-m* (14-ft) deployable antenna, four radioisotope thermoelectric generators, the thermally controlled electronic equipment compartment, the various science instruments, and the propulsion com-

---

*Values in English units are included in parentheses after values in SI (International System) units if the English units were used in the measurements or calculations.

partment. It is in the propulsion compartment that the trajectory correction propulsion subsystem (TCPS) and the attitude propulsion subsystem (APS) are located. The purpose of this report is to describe the efforts related to the attitude propulsion subsystem of TOPS that were active during the TOPS Project.

II. TOPS Attitude Propulsion Subsystem

A. TOPS APS Functional Requirements

The TOPS attitude propulsion subsystem was required to perform the following functions in support of the spacecraft attitude control requirements: (1) tipoff rate reduction and acquisition maneuvers immediately after launch; (2) approximately 2500 momentum wheel unloadings in the yaw axis (1000 each in the pitch and roll axes); (3) commanded turns, consisting of nine positioning maneuvers throughout the 10-year mission to orient the spacecraft for trajectory corrections, of rolling the spacecraft 60 times (once every half AU) and yawing 30 times (once every AU) for calibration of science instruments, and of performing up to 20 re-acquisitions in the event of transient excursions outside the normal operating deadband; and (4) backup limit-cycle control in the event that the two parallel redundant reaction wheels fail in a single axis.
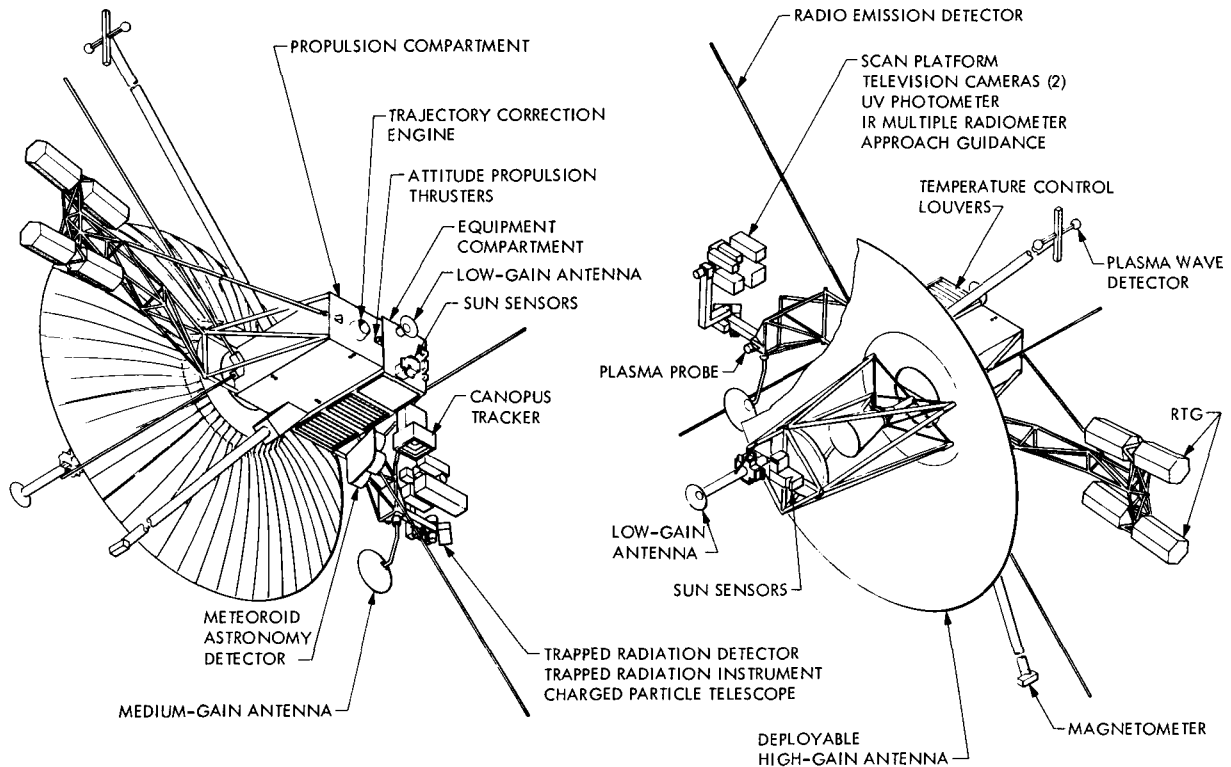
Fig. 1. Thermoelectric Outer Planet Spacecraft

These functions, with the exception of item (4), are summarized in Table 1 in terms of the required torque impulse. Since propellant for the APS function is tanked in common with that used for trajectory corrections, if backup limit-cycle operation were ever required, the necessary propellant would be derived from the trajectory correction 3σ allocation. A spacecraft system-level tradeoff determined that a net mass saving could be realized if the function of performing the various commanded turns was transferred from the reaction wheels to the APS, resulting in a large reduction in reaction wheel mass at the cost of a small increase in propellant mass. The net spacecraft mass saving was on the order of 5.9 kg (13 lb$_m$).

B. Evolution of the TOPS Attitude Propulsion Subsystem

1. Background. The mass expulsion systems for the original TOPS spacecraft consisted of a hydrazine engine for trajectory correction and a gaseous nitrogen source for desaturating (unloading) reaction wheels, which were (and have remained) the primary method of attitude control. This concept presented two separate systems to be packaged into a spacecraft that was volume-limited. The requirements for the nitrogen system, as they were defined at that time, are outlined below.

(1) Reaction wheels to be used for primary attitude control.

(2) Total impulse for attitude control to be 880 N-s (200 lb$_f$-s) with moment arms of 3.1 m (10 ft).

(3) Attitude control system thrust to be in the range of 8.8×10^{-3} to 1.32×10^{-1} N (0.002 to 0.030 lb$_f$) (4.4×10^{-2} N = 0.010 lb$_f$ nominal).

(4) Unloading each reaction wheel to require thrusting for 5 s from the end of a 3.1-m (10-ft) moment arm at 4.4×10^{-2} N (0.010 lb$_f$).

(5) Thruster valves to be cycled 1000 times.

A gaseous nitrogen "torquing" system was consistent with the classical Mariner implementation but had many limitations when applied to a three- or four-planet, 10-year mission. Even very early in the spacecraft design, this attitude propulsion concept offered only limited growth potential. With the relatively low performance and low thrust of a gaseous nitrogen system, long lever arms were required to meet the torquing requirements. This, in turn, necessitated long feed lines that were to be threaded through other subsystems and deployed with the booms, creating a requirement for line thermal control and deployment flexures. The nitrogen gas was to have been tanked at high pressures (on the order of 2.1×10^7 N/m^2 = 3000 psia) and regulated to a nominal thruster valve upstream pressure of approximately 1.72×10^5 N/m^2 (25 psia).

2. Early proposed APS improvements. One of the first suggested improvements to attitude propulsion was to implement a hydrazine plenum system. This system has the primary advantage of tankage commonality with the

Table 1. TOPS APS torque impulse requirements[a]

Function	Pitch		Yaw		Roll	
	m-N-s	(ft-lb$_f$-s)	m-N-s	(ft-lb$_f$-s)	m-N-s	(ft-lb$_f$-s)
Rate reduction (54 mrad/s)	21.76	(16)	110.2	(81)	110.2	(81)
Commanded turns (3 mrad/s)						
Positioning for trajectory correction (9)	—	—	220.3	(162)	220.3	(162)
Science maneuvers (60 roll, 30 yaw)	—	—	734.4	(540)	734.4	(540)
Re-acquisitions (2/year)	48.96	(36)	244.8	(180)	244.8	(180)
Wheel unloadings						
Solar torques	122.4	(90)	613.4	(451)	97.9	(72)
Micrometeoroid	68.0	(50)	68.0	(50)	68.0	(50)
Contingency	78.9	(58)	171.2	(126)	224.5	(165)
Totals	340.0	(250)	2162.3	(1590)	1700.1	(1250)

[a]Required total impulse (based on nominal moment arms for the three axes) = 10,200 N-s (2295 lb$_f$-s).

trajectory correction propulsion system, while in all other respects, it "looks" like a gaseous nitrogen system. However, because it does resemble a nitrogen system, it represents similar implementation complexity. Since the hydrazine plenum system has never flown on a JPL spacecraft, it was not viewed by the Project as a simplification but as an additional unknown. Survivability of the gas generator was questioned, as well as the effect of long-term leakage through valves that would be sealing a hydrogen-rich gas.

A 4.4×10^{-2}-N (0.010-lb$_f$) electrothermal thruster was then considered. It also has the advantage of tankage commonality with the TCPS. Since the decomposition reaction is induced thermally instead of catalytically for this class of thruster, the concern for gas generator or catalyst bed life limitations would be eliminated. In addition, the thruster valves would now seal a liquid instead of a gas. However, at the time when this thruster was proposed, it was not far enough along in development to be a serious contender for the baseline. Because of the low thrust, the configuration of the propellant feed lines for this system, would be similar to both the hydrazine plenum system and the gaseous nitrogen system, and would therefore possess similar problems of deployment and thermal control. The propellant supply lines on the spacecraft appendages would require more extensive thermal control to prevent hydrazine from freezing.

There is a definite advantage to sealing a liquid instead of a gas. The only liquid leakage paths, when a valve poppet and seat are in good contact, are the capillary-size
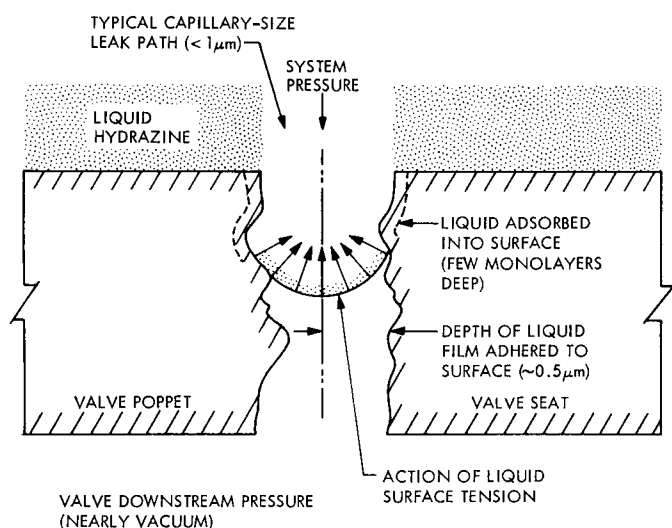
pores that result from microscopic surface irregularities at the seating interface (Fig. 2). When these leakage paths are sufficiently small, the liquid intermolecular cohesive forces, the electropotential adhesive forces between the liquid and the contacted surface, and the liquid surface tension forces all serve to dominate over the upstream pressure forces. A conservative approximation that assumes surface tension effects only can be made by the following relationship:

$$P \leq \frac{4\sigma}{D}$$

where P is the upstream pressure force, σ is the surface tension of the liquid, and D is the "effective" diameter of the leakage path. The leakage path effective diameters are on the order of 1μm or less for the TOPS operating pressure range.

Liquid not only adsorbs into the surface of all materials to the depth of at least a few molecular layers but also forms a film on the order of 0.5 μm thick over the surface. For leak paths on the order of 1 μm across, the films from both surfaces are in intimate contact. The retention forces for this type of contact become very tenacious from both the molecular interaction across such small geometry and the electropotential forces between the liquid and the surface in contact.

For a liquid retained in a capillary-size passage, the actual leakage will be the gas-phase vapors that are generated at the local temperature of the leak point outlet, since the "liquid leakage" driving force is the pressure of the vapor escaping from the surface of the exposed liquid (see Fig. 2). However, the number of active molecules leaving the downstream liquid interface is reduced by the intermolecular cohesive forces and the electropotential liquid-to-wall adhesive forces. This interaction has the effect of reducing the vapor pressure of the liquid for any given temperature. Figure 3 presents the vapor pressure relationship with temperature for a large liquid/vapor interface and represents a conservative estimate for the capillary-size liquid/vapor surfaces. The actual vapor pressure curve will be reduced by the increase of the activation energy needed by the molecule to leave the surface.

For a typical attitude control gas, like gaseous nitrogen, the leakage driving force is the gas pressure itself, since there are no surface tension effects or intermolecular cohesive forces for a gas.

When leakage from a liquid attitude propulsion system is compared with that from a gas system, and if a con-

Fig. 2. Prevention of liquid leakage by surface tension and liquid/wall adhesion
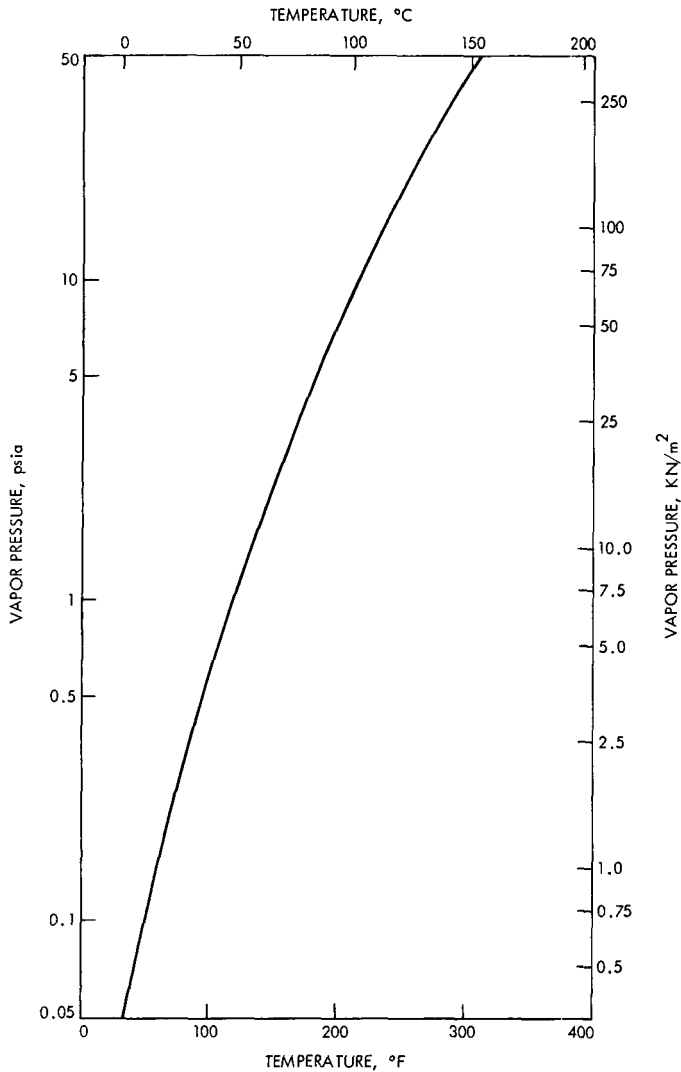
Fig. 3. Vapor pressure of anhydrous hydrazine

Thus, the effect of sealing against a liquid for which the flow passages are small as compared with sealing against a gas for the identical leak paths is approximately as follows:

$$\frac{\dot{m}_{\text{liquid leakage}}}{\dot{m}_{\text{gas leakage}}} \cong \frac{\dfrac{\rho_1 \pi D^4}{128 \mu_1 L}}{\dfrac{\rho_2 \pi D^4}{128 \mu_2 L}} \frac{P_v}{P}$$

where P_v is the hydrazine vapor pressure, P is the gas valve upstream pressure, and the subscripts 1 and 2 refer to the hydrazine vapor and gaseous nitrogen, respectively. Assuming identical geometries and near-equal viscosities for both the hydrazine vapors and the nitrogen gas, the above equation reduces to

$$\frac{\dot{m}_{\text{liquid leakage}}}{\dot{m}_{\text{gas leakage}}} \cong \frac{\rho_1}{\rho_2} \frac{P_v}{P}$$

Since continuum has been assumed for the leakage flows, the densities for both the hydrazine vapors and gaseous nitrogen can be approximated by the ideal gas law, or

$$\rho = \frac{P}{RT}$$

and since the molecular weights of both gases are nearly equal (32 for hydrazine vapor and 28 for nitrogen), the following relationship results (temperatures being assumed equal):

$$\frac{\dot{m}_{\text{liquid leakage}}}{\dot{m}_{\text{gas leakage}}} \cong \frac{\dfrac{P_v}{RT}}{\dfrac{P}{RT}} \frac{P_v}{P} \cong \left(\frac{P_v}{P}\right)^2$$

A gaseous nitrogen attitude control system typically is designed for 1.72×10^5 N/m² (25-psia) nozzle-valve upstream pressure. Hydrazine at 21°C (70°F), however, has a vapor pressure of approximately 1.51×103 N/m² (0.22 psia) (see Fig. 3). Therefore, quantitatively, a conservative estimate of the difference of sealing against liquid with a low vapor pressure as compared with that of a gas is

$$\frac{\dot{m}_{\text{liquid leakage}}}{\dot{m}_{\text{gas leakage}}} \cong \left(\frac{0.22}{25}\right)^2 = (0.0088)^2 = 7.74 \times 10^{-5} \ll 1$$

This ratio will become smaller when the intermolecular cohesive and liquid/wall adhesive forces are considered.

tinuum flow regime is assumed, then the following mass flowrate equation applies for laminar flow:

$$\dot{m} = \frac{\rho \pi D^4}{128 \mu L} \Delta P$$

It can be shown that the maximum Reynolds number is less than 2000 for an assumed gaseous nitrogen valve leakage on the order of 1% of the total flowrate through any specific nozzle. Because of the very low downstream pressure, ΔP is approximately equal to the upstream, or driving, pressure. Therefore,

$$\dot{m} \cong \frac{\rho \pi D^4}{128 \mu L} P$$

Other systems were also considered at that time, including Tridyne (a monopropellant gas consisting of 85% nitrogen, 10% hydrogen, and 5% oxygen by volume) and electrolysis systems; however, they were not competitive after tradeoffs were performed.

3. Final implementation. The final proposed replacement for the gaseous nitrogen APS was a system which utilized hydrazine catalytic thrusters. At the time when these tradeoffs were being made, the state-of-the-art of the 0.44-N (0.1-lb$_f$) catalytic thrusters was sufficiently established, such that this thruster could be a serious contender for baseline. The actual implementation of this subsystem concept was radically different from that of the previous contenders. Because of the higher thrust level and I_{sp} of these hydrazine thrusters, as compared with the then baseline nitrogen system, the moment arms could be reduced from a nominal 3.1 m (10 ft) to a nominal 0.62 m (2 ft). Since these catalytic thrusters also could draw propellant from the TCPS tank, this new concept resulted in locating all APS thrusters, and hence all mass expulsion functions, to within the propulsion bay. In order to maintain the same required torque levels (0.135 N-m = 0.1 ft-lb$_f$ in pitch and 0.27 N-m = 0.2-ft-lb$_f$ in both roll and yaw), the thrust level selected was 0.22 N (0.05 lb$_f$). A 50% reduction in thrust level from an existing design point was considered an acceptable extension of the state-of-the-art. The larger torque levels were obtained within the constraints of the module by angling the thrusters (where required) slightly to present an effectively longer moment arm. Since the TCPS engine was to operate through a 2:1 blowdown mode from beginning to end of mission, this APS concept would function similarly. This eliminated the need for a regulator but necessitated a flow metering/ ΔP device, as the design inlet pressures for the APS thrusters were less than that of the TCPS engine. The effect of the higher thruster performance was nearly offset by the propellant mass penalty that had to be paid by utilizing shorter moment arms; however, the modular concept of combining the TCPS with an APS that was easier to integrate into the spacecraft (as compared with the classical nitrogen APS), combined with the mass savings that would result from storing propellant as a low-pressure liquid instead of a high-pressure gas, was considered a significant simplification and improvement to the overall spacecraft. As a result, the APS with catalytic thrusters was eventually assigned as the new baseline for attitude control thruster-torque functions by the TOPS design team. As the spacecraft requirements and design later changed, the APS thrust level evolved to 0.44 N (0.1 lb$_f$). The details of the system are discussed in later sections.

Prior to the catalytic hydrazine APS becoming the baseline attitude propulsion system, there were many concerns expressed by representatives of other spacecraft subsystems. Some of the primary points in question were:

(1) Exhaust products may affect hydrogen detection science instruments and spacecraft subsystem electronics.

(2) Exhaust plume may thermally or chemically affect sensors and other subsystems.

(3) Long-term materials chemical compatibility with propellants is questionable and must be established.

(4) System implementation must be configured for maximum reliability.

(5) Reliable, low-flow thruster valves of the APS size must be qualified.

(6) Catalytic thrusters of the 0.44-N (0.1-lb$_f$) size must demonstrate that they are capable of performing the TOPS duty cycle.

(7) Personnel hazard may exist during system testing.

Concern about the first point was dispelled quickly when the exhaust product quantities were compared with that from the 110-N (25-lb$_f$) trajectory correction engine, which would be on board and active regardless of the type of attitude propulsion system used. A comparison of the integrated hydrazine exhaust product masses for the combined TCPS and APS, along with the APS alone (as viewed from space and as viewed between the spacecraft and Jupiter from launch to Jupiter encounter) are presented in Figs. 4 and 5. Further calculations of attitude control mass expulsion were performed, and it was concluded that hot-gas and cold-gas attitude propulsion were equally compatible with the TOPS spectroscopic science package. However, nitrogen accumulating from both usage and leakage from a cold-gas system was felt to provide more interference with ultraviolet experiments than hydrogen APS exhaust products.

Possible plume interference with other subsystems was avoided by locating the APS thrusters on the propulsion bay surface at points where the main stream of the exhaust plumes did not impinge directly on any subsystem. Also, at no time did a propellant feed line violate another subsystem interface. The possibility of plume deposition on optics and solid-state detectors could not be quantified at the time of this tradeoff, although Air Force data were available indicating that it should be minimal for the proposed TOPS APS thruster locations. Goddard Space
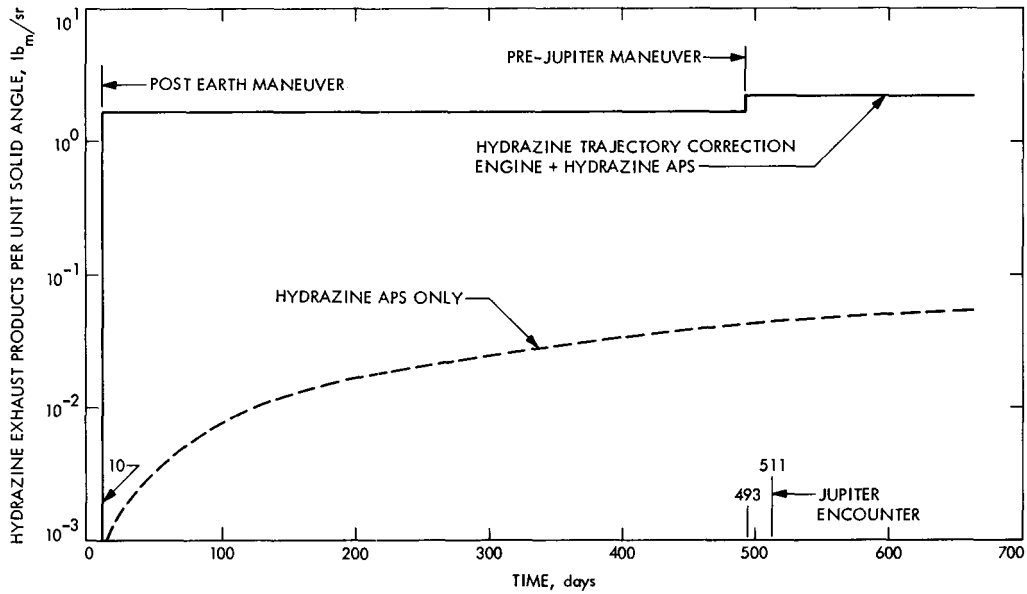
Fig. 4. Hydrazine exhaust products viewed in space from launch to Jupiter encounter
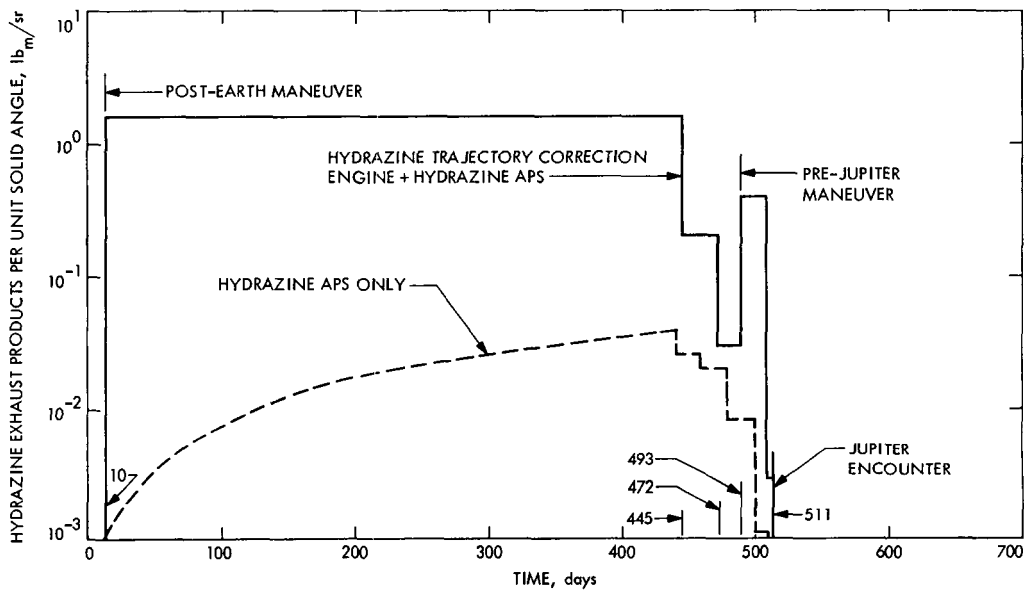
Fig. 5. Hydrazine exhaust products viewed between the spacecraft and Jupiter from launch to Jupiter encounter

Flight Center, however, had some qualitative results indicating an adverse effect of ammonia on solid-state detectors. The technique for predicting ammonia deposits on spacecraft surfaces at different locations was lacking at the time, as was a quantitative feel for the order of magnitude of the exhaust plume backflow. (Recent JPL plume tests have been successful in defining the plume backflow region for small nozzles. The Bibliography presents two references on this work.)

The long-term materials compatibility question must be answered for a hydrazine APS. However, it must also be answered for the TCPS, as this concern is identical for both subsystems. An active materials compatibility program is in effect at JPL, with some 800 candidate samples in long-term storage at the JPL Edwards Test Station.

Extensive tradeoffs were conducted to establish the optimum (or most desirable) subsystem configuration with
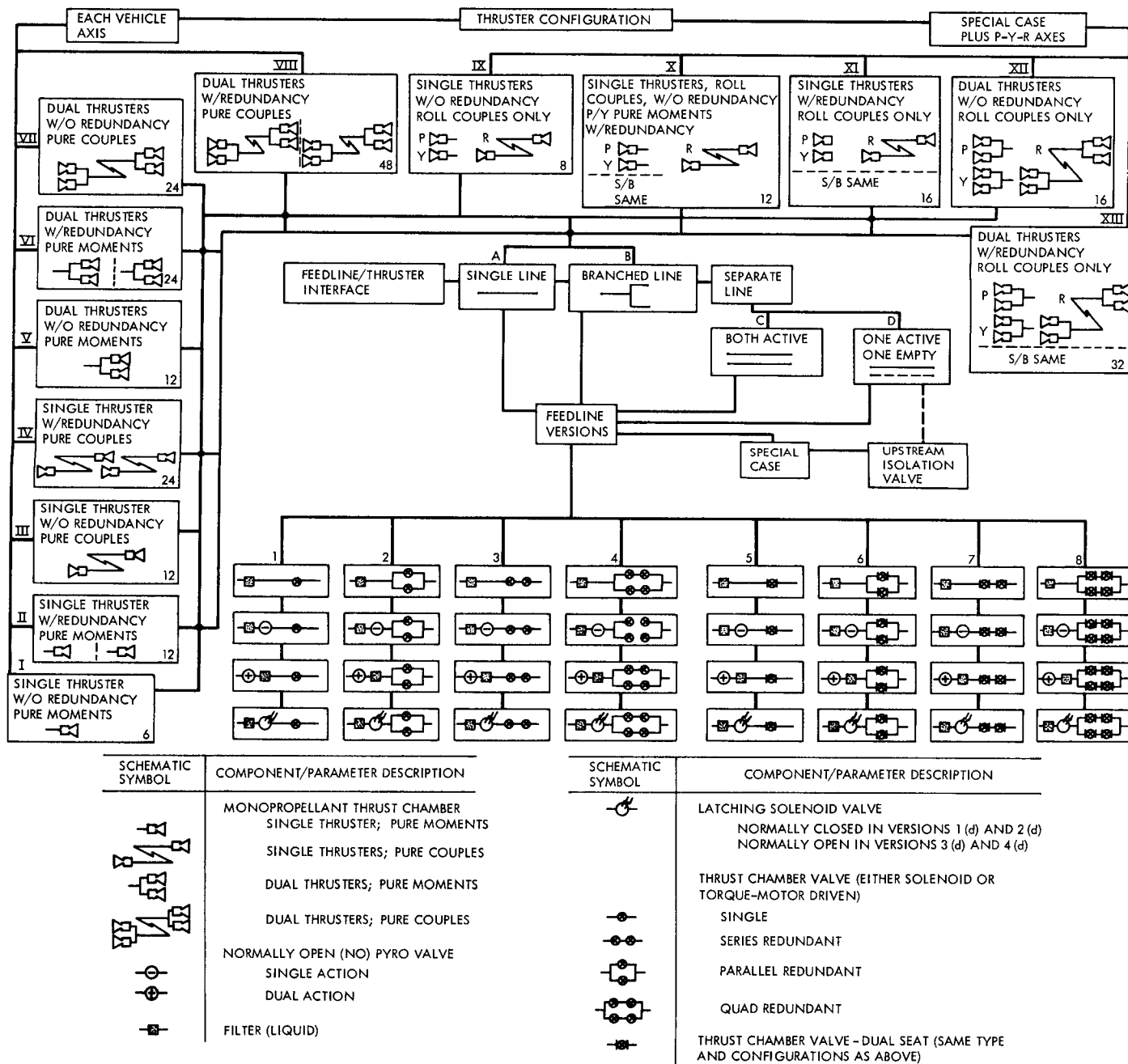
Fig. 6. Thruster redundancy comparison diagram

SCHEMATIC SYMBOL	COMPONENT/PARAMETER DESCRIPTION
	MONOPROPELLANT THRUST CHAMBER
	SINGLE THRUSTER; PURE MOMENTS
	SINGLE THRUSTERS; PURE COUPLES
	DUAL THRUSTERS; PURE MOMENTS
	DUAL THRUSTERS; PURE COUPLES
	NORMALLY OPEN (NO) PYRO VALVE
	SINGLE ACTION
	DUAL ACTION
	FILTER (LIQUID)

SCHEMATIC SYMBOL	COMPONENT/PARAMETER DESCRIPTION
	LATCHING SOLENOID VALVE
	NORMALLY CLOSED IN VERSIONS 1 (d) AND 2 (d)
	NORMALLY OPEN IN VERSIONS 3 (d) AND 4 (d)
	THRUST CHAMBER VALVE (EITHER SOLENOID OR TORQUE-MOTOR DRIVEN)
	SINGLE
	SERIES REDUNDANT
	PARALLEL REDUNDANT
	QUAD REDUNDANT
	THRUST CHAMBER VALVE – DUAL SEAT (SAME TYPE AND CONFIGURATIONS AS ABOVE)

specific reference to reliability and self-repair in the event of a component failure. A reference configuration consisting of a single, noncoupled thruster in the positive and negative direction of each axis was established, from which relative reliabilities could be compared. A comparison diagram of some of the configurations, and combinations of configurations, that were considered is presented in Fig. 6. Table 2 shows a ranking of the relative reliabilities for a sampling of the configurations considered. As would be expected, the reference configuration, a minimum system with no redundancy, has the lowest reliability. The reliability numbers, however, like any reference to reliability of mechanical systems, are only relative and should not be interpreted as absolute values.

Table 2. APS system configuration comparison (series redundant solenoid and latching valves assumed)

Configuration	Relative reliability ranking
Couples in roll, noncouples in pitch and yaw, 16 thrusters: 8 active, 8 standby redundant	0.9982
Noncouples in all axes, 12 thrusters: 6 standby redundant	0.9980
Couples in roll, noncouples in pitch and yaw, 12 thrusters: 8 active, 4 standby redundant for the noncouples only	0.9973
Noncouples, 12 thrusters; all active, parallel redundant (identical to couples with no redundancies)	0.9960
Noncouples, 6 thrusters; all active, single system	0.9570

The configuration proposed as a result of the tradeoff studies was a noncoupled standby redundant system with twelve thrusters (six active and six standby). This configuration was felt to provide a highly reliable system, with the minimum implementation complexity and minimum interference of the exhaust plume with other subsystems. However, the TOPS design team decided on a configuration with couples in roll and noncoupled moments in pitch and yaw; this resulted in sixteen thrusters: eight active and eight standby redundant. Although this is a slightly heavier system because of the addition of four thrusters, it is also more reliable, since a double thruster/valve failure in one roll axis would result in a fallback to the noncoupled configuration. Details of the APS baseline system are covered in the following section.

The first two of the remaining three items of concern, the qualification of valves of the APS size, and the demonstration of the TOPS duty cycle by the 0.44-N (0.1-lb$_f$)

catalytic thrusters, provided the goals of the APS supporting research and development efforts, which are discussed later in this report. The last item was covered in detail during the Celestarium tests, which are described in Section G.

C. TOPS APS Baseline System

The TOPS APS baseline configuration is integral with the trajectory correction propulsion subsystem, thus comprising the TOPS propulsion module. The TCPS and the APS share a common propellant supply of liquid anhydrous hydrazine, which is sized primarily by the TCPS design requirements. The APS propellant lines extend from the supply tank to the thruster/valve assemblies located at the extremities of the propulsion module. Only the thrusters protrude through the spacecraft thermal blanket. The final configuration of the TOPS propulsion module is depicted in Fig. 7. The locations of the roll, pitch, and yaw thruster/valve assemblies, along with the related components, are indicated. This configuration is shown schematically in Fig. 8.

As designed for TOPS, the complete APS consists of sixteen thruster/valve assemblies, of which eight are active and eight are standby redundant. In the event of a single thruster/valve failure, the function of the failed unit is transferred to the standby unit on a one-for-one basis. There are eight active thrusters rather than six, the minimum number required to stabilize the spacecraft, because the roll thrusters are implemented as a couple, while those for pitch and yaw are not coupled. The nominal beginning-of-mission torque level requirements are 0.136 N-m (0.1 ft-lb$_f$) in pitch and 0.27 N-m (0.2 ft-lb$_f$) in roll and yaw (see Table 1). Each thruster is designed for a nominal 0.44-N (0.1-lb$_f$) thrust.

The single propellant tank operates in a blowdown mode (rather than being pressure-regulated) to improve subsystem reliability. The tank pressure blows down from 2.8×10^6 to 1.4×10^6 N/m^2 (400 to 200 psia), as dictated by TCPS requirements. The APS thrusters operate at a lower inlet pressure than does the TCPS thruster, and therefore each APS thruster/valve combination incorporates a pressure-dropping device. The original baseline device was a coiled section of small-diameter tubing (approximately 0.38 m = 15 in. long by 2.54×10^{-4} m = 0.01 in. internal diameter); however, the Lee Company Viscojet, a smaller fluid resistance device that is less susceptible to flow restriction from contamination, was later substituted. The pressure-dropping device also serves as a means of metering the very low liquid flowrates (approximately 2.3×10^{-4} kg/s = 5×10^{-4} lb$_m$/s).
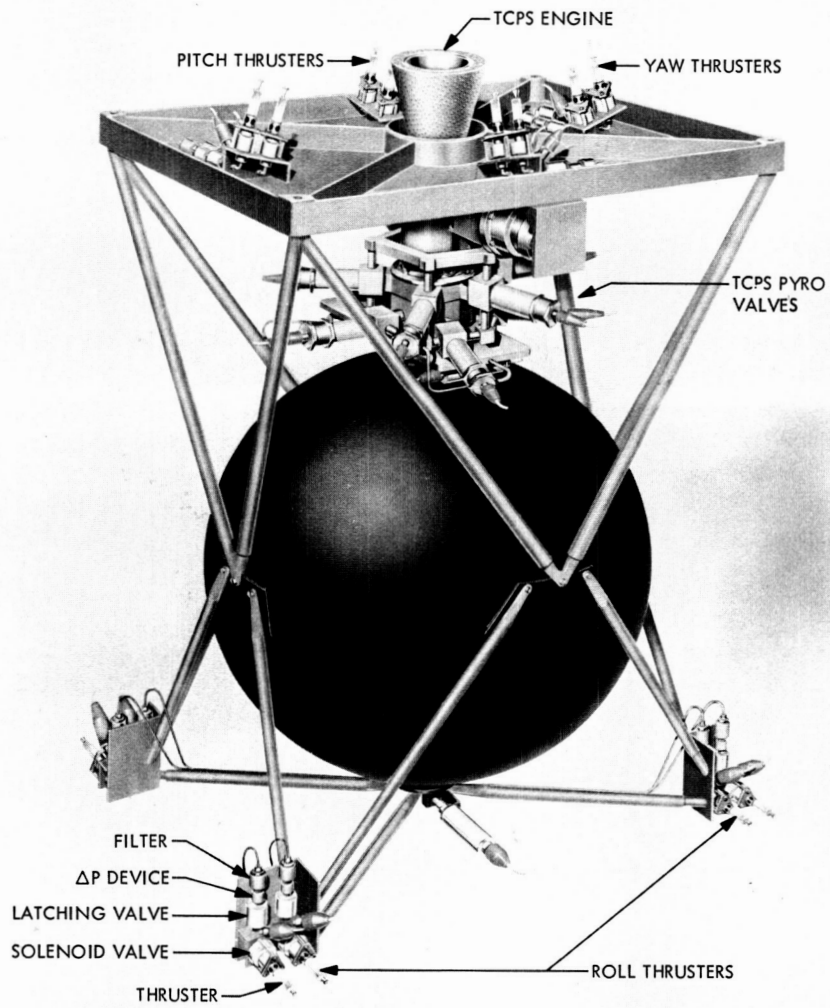
Fig. 7. TOPS propulsion module configuration
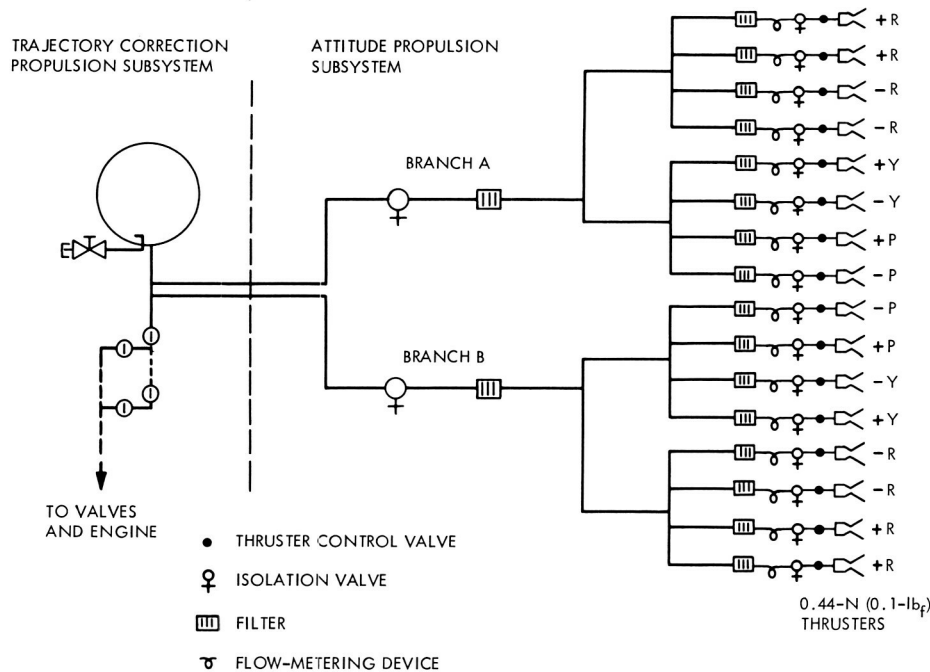
Fig. 8. Attitude propulsion subsystem schematic diagram

Each APS thruster/valve assembly consists of a thruster, a thermal isolation structure and injector tube, a normally-closed solenoid valve, a latching solenoid valve, the pressure-dropping/flow-metering device, and a filter. Each active thruster is injected with liquid anhydrous hydrazine, which is decomposed as it passes through a 20-30-mesh Shell 405 catalyst bed to generate hot gases that are expelled through a high-expansion-ratio nozzle. Each thruster is coupled to its solenoid valve through a thermal isolation structure to minimize heat soakback into the valve seat area.

The baseline filter is a 1-μm (absolute) stacked-disc labyrinth filter. This unit, which incorporates a JPL etched-disc design (Fig. 9), was designed and fabricated by a contractor, who has assembled, acceptance-tested, and delivered five units.

The baseline normally-closed solenoid valve incorporates an internally actuated, in-line poppet to take advantage of the smaller mass and envelope. However, studies of the externally actuated (torque motor) concept were also conducted. The valves incorporate a "soft"-seat sealing configuration. Studies to determine the optimum seat design and material were conducted and are covered in a later section.

The latching solenoid valve is similar to the normally-closed solenoid valve but possesses a bi-stable actuator
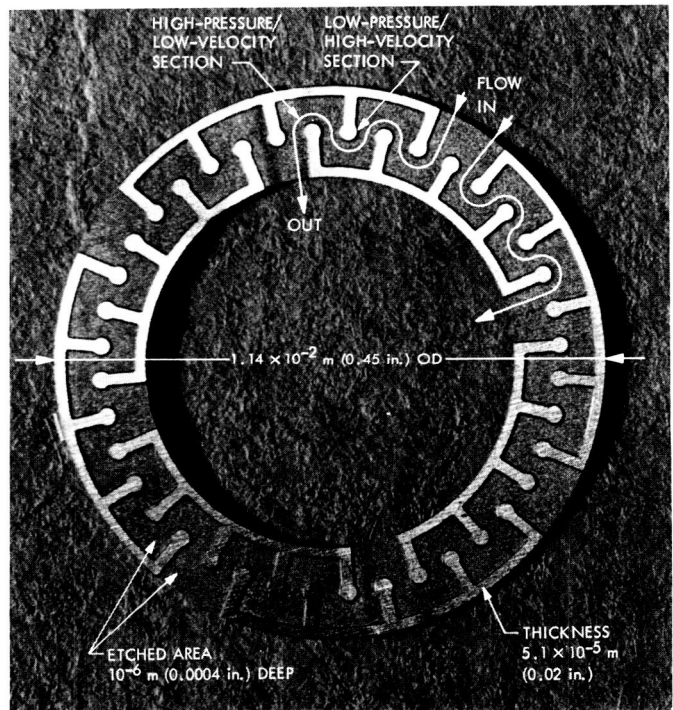
Fig. 9. JPL etched filter disc design

that enables the valve to be positioned in either an open or closed condition. The valve repositioning is executed by a short-duration electrical pulse, after which no further holding power is required.

D. TOPS APS Supporting Research and Development Objectives

With a course of action defined from the results of the tradeoff studies, the TOPS APS supporting research and development (SR/AD) program was initiated. Its primary objectives were:

(1) *Celestarium test (atmospheric system) support.* Build and deliver a portable, "man-rated," self-contained APS module with 0.22-N (0.05-lb$_f$) thrusters in support of the single-axis validation tests in the Celestarium, JPL's stellar simulation facility.

(2) *APS subassembly test in vacuum.* Verify the integrity, functionality, and design concept of an APS subassembly containing all required components.

(3) *Evaluation of valve seat designs.* Analyze, design, test, and evolve a valve seat configuration which will have the greatest sealing capability and survival probability on an outer planet mission.

(4) *Long-term propellant compatibility.* Investigate the capability of and identify the most promising materials for meeting the compatibility requirements of a long-term mission.

(5) *Evaluation of solenoid and latching valves.* Determine design requirements and areas of required improvement for solenoid and latching valves of the APS size.

(6) *Filter design and test.* Design, develop, test, and evaluate a 1-μm absolute, stacked-disc, labyrinth filter assembly.

(7) *Characterization of flow-metering devices.* Evaluate flow characteristics, design requirements, and implementation conditions for several long, small-diameter tubes (3.8×10^{-4} m = <0.015-in. ID) and a series of Lee Company Viscojets.

E. JPL Designs for a 0.22-N (0.05-lb$_f$) Catalytic Engine

As indicated earlier, TOPS APS tradeoff studies showed mass, reliability, and spacecraft integration advantages for a blowdown hydrazine attitude propulsion system utilizing thrusters in the 0.2- to 0.45-N (0.05- to 0.1-lb$_f$) class in common with the TCPS. Early in the TOPS effort, a program was initiated to demonstrate the integrated attitude control interfaces by simulating the pitch axis on an air-bearing table in the JPL Celestarium facility. (Details of the test will be covered in a later section.) The pitch axis torque requirement of 0.135 N-m (0.1 ft-lb$_f$), coupled with a moment arm of 0.61 m (2.0 ft), which was dictated by the

air-bearing table physical constraints, necessitated a nominal maximum thrust of 0.22 N (0.05 lb$_f$) at atmospheric pressure. (The Celestarium has no vacuum capability.)

A survey of the industry revealed that there was no thruster available "off-the-shelf" which could be procured and incorporated directly into the single-axis setup. It was therefore decided to design, fabricate, and test a 0.22-N (0.05-lb$_f$) "sea-level" catalytic hydrazine thruster at JPL for this test series (Ref. 2). It was felt that, in addition, this development would provide valuable experience in problem areas peculiar to small thrusters of this class. Such was indeed the case, and details and problems relating to design, fabrication, joining, assembly, catalyst loading, and instrumentation are treated at more than usual length because of their uniqueness to thrusters of this small size and because of the major role these factors played in this development program.

For purposes of the single-axis simulation test series, high thruster performance, as measured by characteristic velocity (c^*) or specific impulse (I_{sp}), was deemed relatively unimportant. Instead, the primary system design requirements, in addition to the basic nominal thrust criterion, were:

(1) Safe and reliable operation over an accumulated life of at least 5000 s and 30,000 total starts.

(2) Impulse repeatability to electrical pulse widths at least as small as 100 ms.

(3) Repetitive operability in an ordinary air-conditioned building without hazard to personnel or equipment in immediate proximity, and without the need for purges after actuation or other special handling.

(4) Demonstration of the feasibility of employing a high feed pressure for the thrusters (in consonance with the objective of eventual integration into a common feed system which supplies the trajectory correction engine).

Design simplicity, from a fabrication standpoint, was also a paramount consideration.

1. Thruster description. The 0.22-N (0.05-lb$_f$) thruster design is illustrated conceptually in Fig. 10, and one of the delivered thrusters is shown in Fig. 11. A nominal nozzle throat diameter of 0.76 mm (0.030 in.) was selected as a reasonable compromise between the larger throat desired for less stringent fabrication tolerances and the smaller throat desired to permit higher operating chamber pressures. For this nozzle size class, it is known that
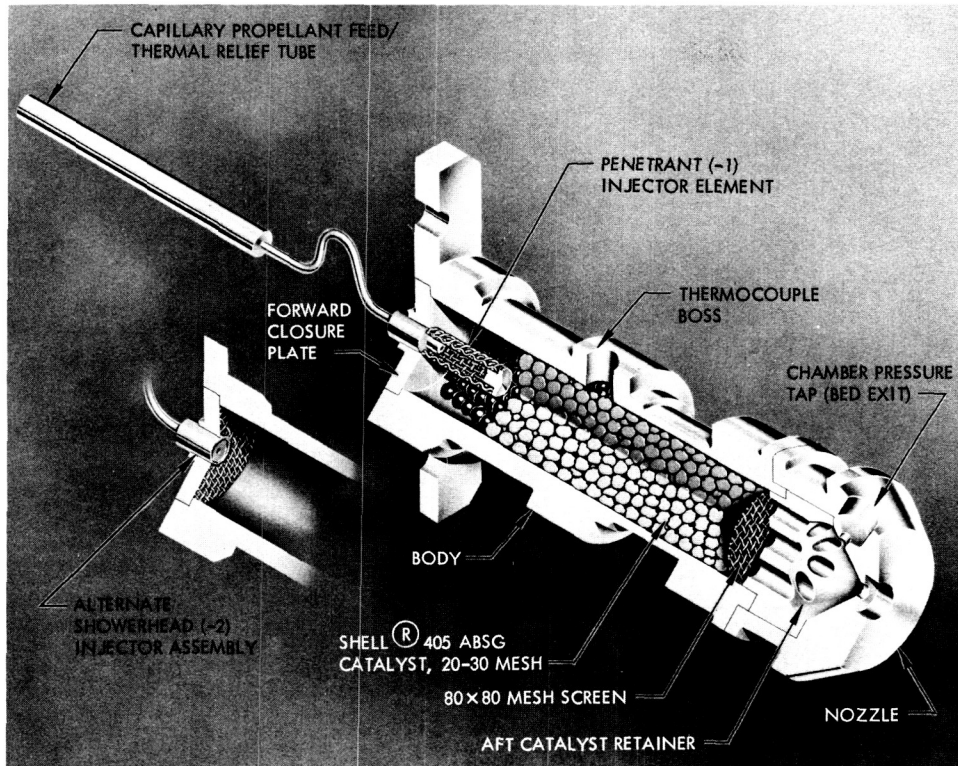
Fig. 10. 0.22-N (0.05-lb$_f$) catalytic hydrazine thruster (conceptual view)

boundary layer effects begin to be significant. Recourse was therefore taken to the methods of Ref. 3, incorporated into a computer program, to predict actual thrust coefficients. A 15-deg half-angle conical nozzle with an expansion-area ratio of 1.5:1 was selected to prevent jet separation and provide effective plume confinement over the anticipated blowdown range at site run conditions. With this geometry, nominal chamber pressure to produce a site thrust of 0.22 N (0.05 lb$_f$) is about 435 kN/m² (63 psia).

2. Catalyst bed configuration. Catalyst bed life was recognized to be a potentially serious problem under the somewhat unrealistic test conditions (atmospheric environment) prevailing in the Celestarium, and an extremely conservative approach was therefore taken to bed design. Nominal bed diameter was set at 0.5 cm (0.2 in.), resulting in a superficial mass flux G of 9.15 kg/m² s (0.013 lb$_m$/in.² s) at nominal thrust. The smallest standard granular Shell 405 ABSG catalyst on hand, 20-30 mesh, was selected for maximum active surface area per unit bed volume. Data from Ref. 4 indicated that a bed length of about 1.25 cm (0.5 in.) would have been adequate for smooth decomposition at an ammonia dissociation level of 50 to 55%. How-

ever, a 2.5-cm (1.0-in.) bed length was selected for the first group of thrusters for two reasons:

(1) Possible gradual deactivation of the lower portion of the bed due to atmospheric cooldown.

(2) Increased ammonia dissociation so as not to exceed maximum allowable concentration levels in the Celestarium.

Accordingly, the predicted ammonia dissociation for this bed length was 72%.

3. Injector configurations. Several injector configurations were considered initially, including single- and multi-element showerheads (flat-face injectors), a porous plug, and a single-element penetrant. Fabrication constraints narrowed the selection to single-element injectors. In the face of little experience with thrusters of this size and lack of definitive analytical criteria, two different injector types were designed and tested: a single partial penetrant element called the "−1" configuration, and a single-orifice showerhead termed the "−2" configuration. It was believed that the showerhead might yield faster response, while the penetrant should offer smoother performance as a result of more uniform propellant distribution.
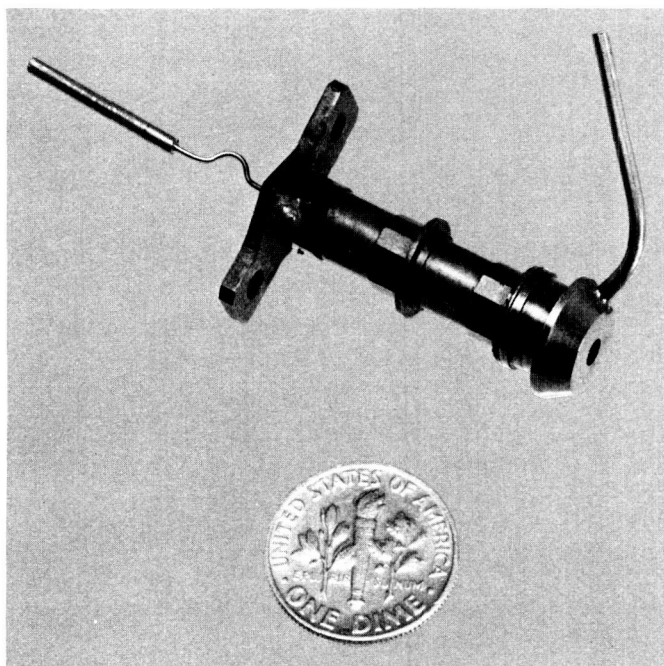
Fig. 11. 0.22-N (0.05-lb$_f$) catalytic hydrazine thruster, delivered configuration (without insulation)

Both injector types consisted of a nominally 1.65-mm OD × 0.2-mm ID × 3.2-cm long (0.065-in. OD × 0.008-in. ID × 1¼-in. long) capillary feed tube with a thermal relief bend, passing through, and welded to, the chamber's forward closure plate. In the penetrant configuration, the feed tube extended through the forward closure plate to a length of 1.0 mm (0.040 in.). The protruding end of the capillary feed tube was machined to a nominal 0.61-mm (0.024-in.) diameter. A 0.63-cm (0.25-in.) length of 80 × 80 mesh L605 screen was rolled and seam-welded to form a cylinder, which was then fitted over and tack-welded to the feed tube. The downstream end of the screen tube was then sealed with a small plug to complete the penetrant element, as shown in Fig. 10 (see also Fig. 13). In the alternative showerhead configuration, the feed tube was cut off flush with the downstream face of the closure plate. A 1.27-mm (0.050-in.) diameter × 0.23-mm (0.009-in.) deep relief was then counterbored back from the downstream face, and the assembly was completed by tacking a disc of 80 × 80 mesh L605 screen over the entire downstream face, as shown in the inset of Fig. 10.

4. Valves and other components. The propellant valve employed was a modified Gemini RCS fuel valve (Rocketdyne P/N 407559). Use of this valve was suggested by the ready availability of several units at JPL. Its electromechanical response characteristics are more than adequate for this application, although it is non-optimum

from the standpoint of size, weight, power requirement, and downstream volume. A low-volume downstream adaptor, fitted with a modified 1.59 × 10^{-3} m (1/16-in.) Swagelok fitting, was designed to accommodate the capillary feed tube.

All metallic parts of the thruster assembly were either 304L CRES or L605 (Haynes 25). The thruster body, forward (upstream) closure, nozzle, and the capillary feed tube were fabricated from the former, and the screens and aft catalyst retainer from the latter.

5. Thruster fabrication and subassembly. Fabrication of detail parts proceeded smoothly and without incident. Figure 12 shows an exploded-view assemblage of piece parts using the showerhead injector.

Welding problems were encountered, however, in subassembly operation. Initially, electron-beam (E-B) welds were called out for all metal-to-metal joints in the thruster. Experimental weldments revealed both poor penetration and a tendency to crack at the critical seal weld between the feed tube and the forward closure plate in the injector subassembly. Porosity was also encountered in the closure plate/body weld. While the E-B welding experiments were proceeding, it was demonstrated that a welder skilled in precision microwelds could, after some practice, make satisfactory and reproducible manual TIG welds at all joints, including even the penetrant injector subassembly (Fig. 13). The E-B welds were therefore abandoned in favor of the manual operations.

Both dye-penetrant inspections and leak checks were performed at the various stages of assembly, occasionally revealing pinhole leaks and requiring reweld. The finished injector/body subassembly was mounted in a jig used for bed packing and final weld. The unit was then delivered to engineering for catalyst loading.

6. Catalyst-loading procedure. As the design of the 0.22-N (0.05-lb$_f$) thruster crystallized, it became apparent that specialized bed loading techniques would be required and that the technicians performing this operation would have to acquire some experience. Consequently, a series of catalyst-loading experiments was contrived and scheduled in parallel with thruster component fabrication. To this end, a catalyst-loading simulator was designed and fabricated, comprising a dead-ended stainless steel tube (of the same internal dimensions as the thruster body assembly) welded to a flat, stainless steel support plate, and a transparent polystyrene cap geometrically similar to the aft
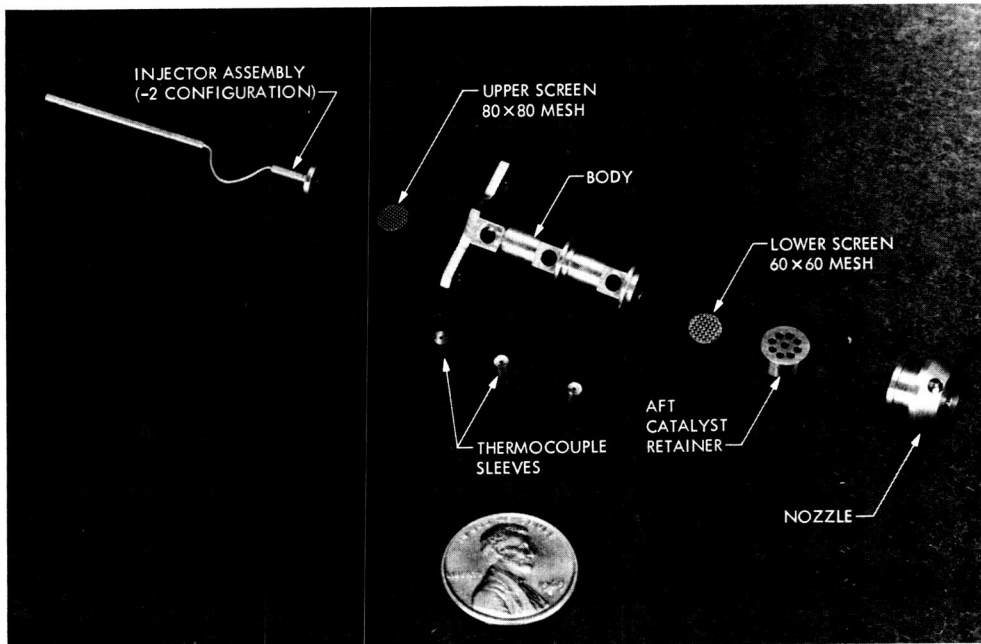
Fig. 12. 0.22-N (0.05-lb_f) catalytic hydrazine thruster components (exploded view)
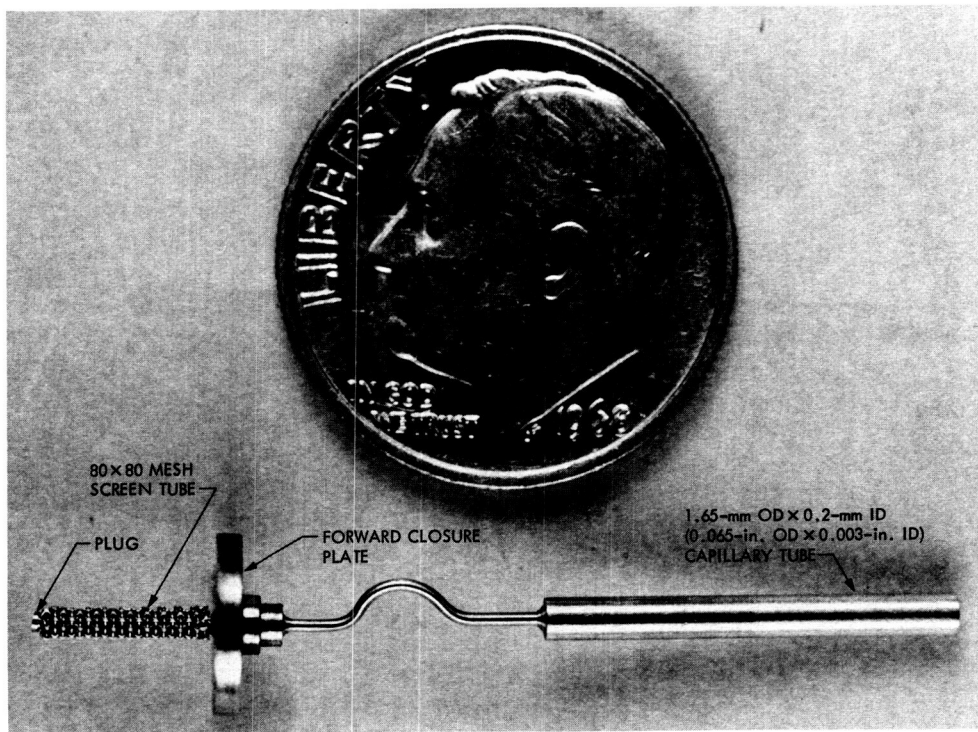
Fig. 13. Penetrant (−1) injector assembly

catalyst retainer (as mounted on the nozzle). Initial experiments were conducted with used catalyst, and the final verification experiments employed fresh catalyst.

The specialized tools and fixtures that evolved in the course of these experiments are illustrated in Fig. 14. An incremental vibratory pack was found most satisfactory and, for the small masses involved, a simple, small, 60-Hz stationary-stacking vibration table (Syntron Model J-1A "Vibrating Jogger") set to minimum amplitude proved to be an adequate driver. The injector/body assembly (or simulator) was clamped to the table, which, in turn, rested upon the base of the tamper support stand. From the vertical rod of this stand, similar to a laboratory ringstand, a tamper guide bracket extended out over the thruster body or simulator. The tamper itself was a 12.7-mm (½-in.) diameter aluminum cylinder enclosed in a low-friction Teflon sleeve and attached to the center of a flat, hexagonal aluminum bearing plate. The latter prevented the tamper from dropping through the guide bracket and also served as a bearing surface for the leaf spring to be discussed presently. A small stainless steel piston was attached to the lower surface of the aluminum cylinder to complete the tamper assembly.

In the initial loading experiments, the tamper piston was simply rested upon the surface of the catalyst and left free to vibrate at will. Amplitude and frequency conditions were such that the tamper travel was excessive and pulverized the upper layer of catalyst. It was therefore found necessary to constrain the tamper to rest against the catalyst with a small positive force of 5.6 ±1 N

(1¼ ±¼ lb$_f$), and a thumbscrew-adjustable beryllium–copper leaf spring was added to the guide bracket to provide this force.

Through repetitive trials, it was determined that the nominal catalyst load weighed about 0.7 g, with an unpacked volume of about 0.5 cm^3. After the sample to be loaded was weighed, loading was accomplished volumetrically. A special metering tube was fabricated from a 2.0-cm^3 laboratory pipette by fusing the lower end shut and flaring the upper end.

The actual injector/body assembly was received from the fabrication shop mounted in a jig to facilitate loading and the final nozzle-to-body weld. The catalyst was loaded in steps. First, approximately 50% by volume was poured into the body from the metering tube and vibration-packed for 60 s, as shown in Fig. 15. Next, an additional 25% was packed for 30 s; then, somewhat less than the 25% residuum was also packed for 30 s. From this point, a series of trial-and-error additions and removals of small quantities of catalyst followed. After each addition/removal, the bed was vibration-packed for 10 to 15 s. The aft retainer was set in place on the catalyst surface through a hole in one of a series of modified feeler gages, as illustrated in Fig. 16. The objective of these operations was to achieve a final compression of 0.38 to 0.43 mm (0.015 to 0.017 in.) when the aft retainer and nozzle were clamped in place, corresponding to a compressive preload of about 1.0 to 1.4 MN/m^2 (150 to 200 lb$_f$/in.^{2}). This level of loading had been shown in the simulation experiments to provide an adequately tight bed.
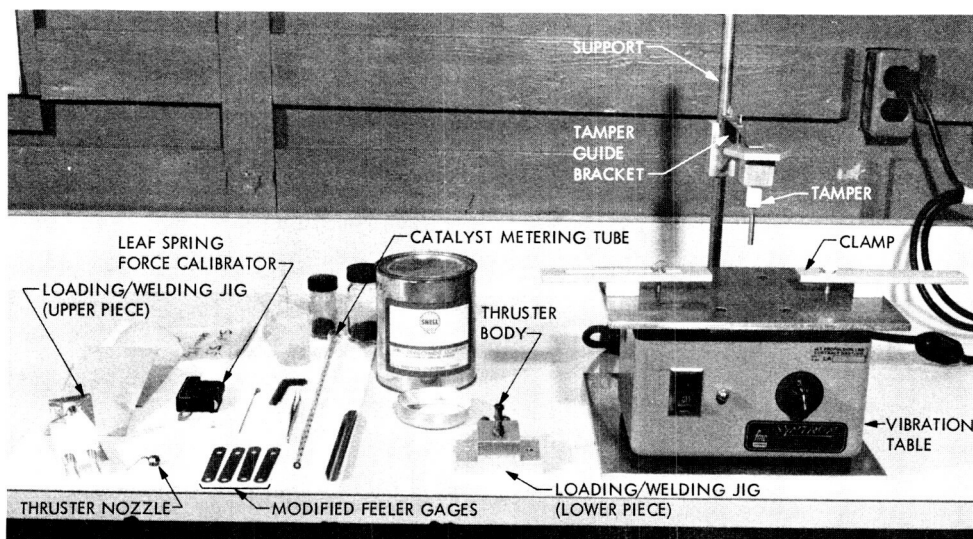
Fig. 14. Catalyst-loading equipment
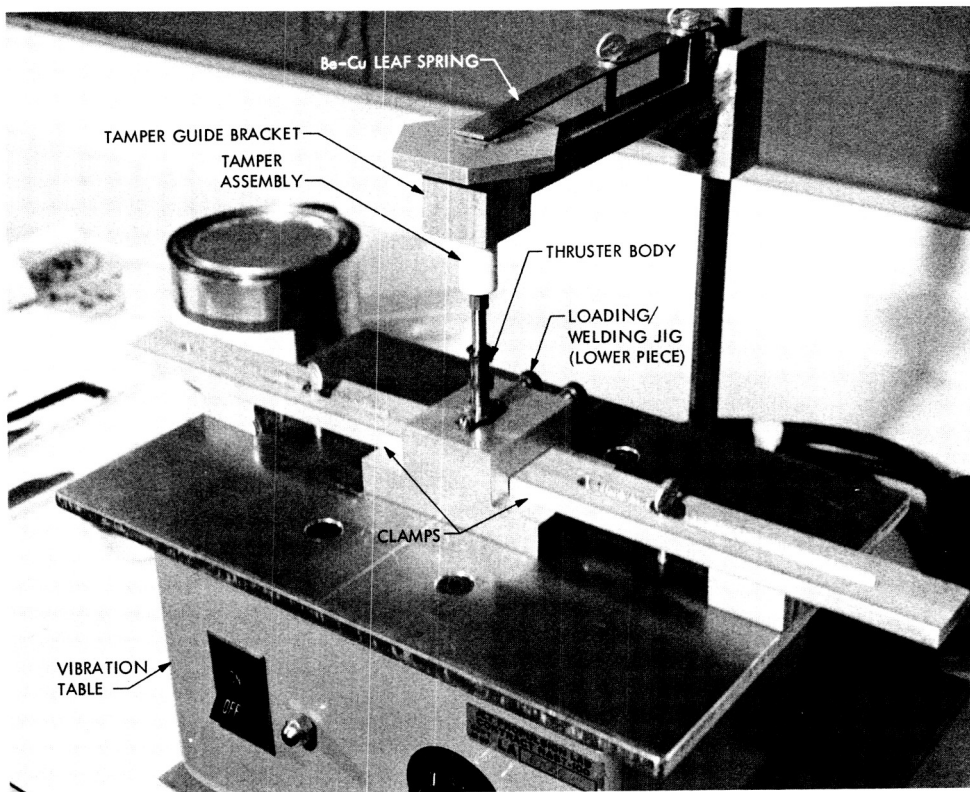
Fig. 15. Vibration packing technique
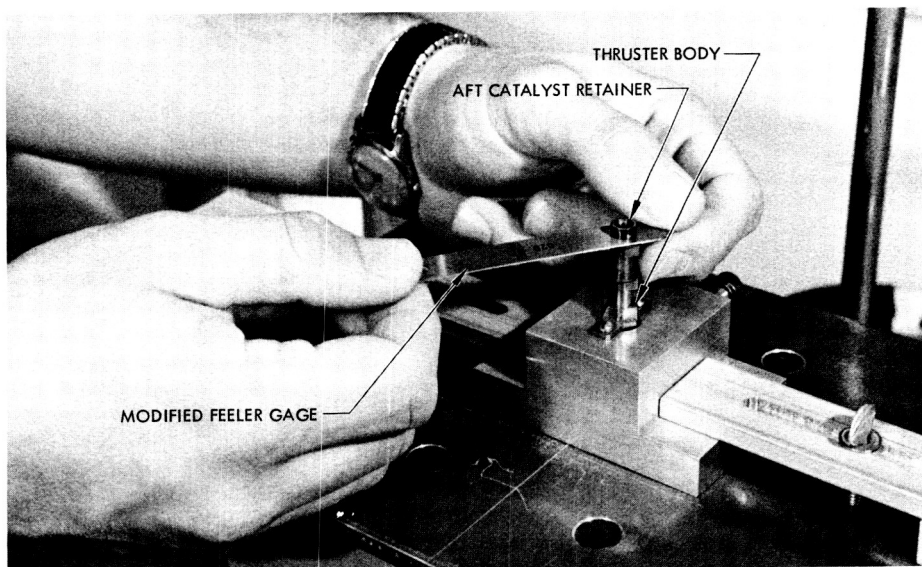
Fig. 16. Setting compressive preload

Once the desired linear compression was achieved, the upstream catalyst retainer and nozzle were clamped in place for the final nozzle-to-body closure weld.

7. Final assembly. After the final weld, the thruster subassembly was purged and leak-checked. It was then installed on the test cell mount plate, and connected to the propellant valve. Upper and lower chamber pressure transducers were also installed on the mount plate and connected to the appropriate sensing lines provided on the thruster subassembly. The completed assembly, ready for firing, is shown in Fig. 17.

The capillary tubing coils and, later in the APS program, the Lee Company Viscojet flow-metering devices (to be discussed in a later section) were calibrated *in situ* with hydrazine. (The Viscojet was not used for the Celestarium tests.) Calibration curves were prepared in the form of nondimensional plots of Reynolds number N_{Re} versus pressure loss modulus N_{PL}, representing a functional dependence of the type

$$N_{Re} = \phi (N_{PL}) \tag{1}$$

where

$$N_{Re} = \frac{4\dot{m}}{\pi d_e \mu}, \qquad N_{PL} = \frac{\rho d_e^3 \Delta P}{\mu^2 \lambda}$$

and the individual parameters are as defined in the Nomenclature. With some care, it was found that extremely reproducible calibrations could be obtained for both the capillary tube coil and Viscojet.

These pressure-dropping devices served the dual purpose of reducing the feed pressure level to that required for nominal thruster operation and of providing a flow measurement capability. The pressure loss was measured with a Statham differential pressure transducer.

It was originally intended to monitor the internal temperature profile of the catalyst bed with three extremely fine 5.1×10^{-4} m (0.020-in.) OD thermocouples sleeved into the bosses provided in the body. These proved too delicate and were abandoned in favor of a single, more rugged 1.58×10^{-3} m (1/16-in.) OD penetrating couple at the midpoint. The other two bosses were welded shut.

8. Test Program. The experimental evaluation of the thrusters was conducted in two phases. Phase I comprised a fairly exhaustive series of preliminary screening tests to evaluate the penetrant and showerhead configuration injector alternates comparatively. From the results of these tests, the more satisfactory configuration was selected and committed to fabrication for the deliverable thrusters. These were then subjected to a brief acceptance and characterization test series, which constituted Phase II.
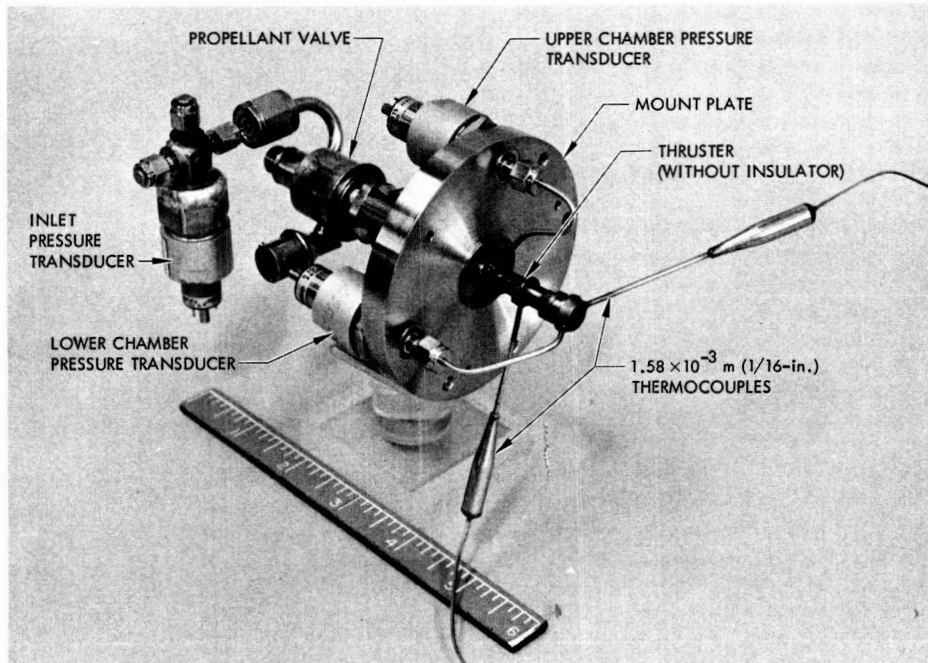
Fig. 17. 0.22-N (0.05-lb$_f$) catalytic hydrazine thruster assembly ready for installation in test cell

Test Plan. A total of five thrusters was planned for the program. The first two, S/N 001 and 002, represented one each of the penetrant and showerhead injector configurations to be subjected to the preliminary screening test series, outlined in Table 3. Thruster S/N 003 was inadvertently damaged in the final stages of assembly and not used. The remaining three units, S/N 004, 005, and 006, were fabricated with the selected (penetrant) injector configuration, subjected to the more abbreviated acceptance/characterization test series of Table 4, and delivered for the single-axis simulation program (two integrated into the propulsion module, one spare). The 100-ms ON/900-ms OFF pulse mode duty cycle (10%) was selected because it is representative of the type of pulse train that would

Table 3. Sequence of 0.22-N (0.05-lb$_f$) preliminary screening tests[a]

Test No.	Thermal condition	Mode	Continuous duration, s	Number of 0.1-s ON/0.9-s OFF pulses	Remarks
1		SS	10	—	Calibration/proof
2		SS	10	—	Calibration
3	U	SS	30	—	Calibration
4	N	SS	420	—	60 s each at 7 feed pressures
5	I	SS	30	—	Performance verification
6	N S	Pulse	—	5	—
7	U	Pulse	—	10	—
8	L A	Pulse	—	20	—
9	T	Pulse	—	100	—
10	E D	SS	30	—	Performance verification
11		Pulse	—	3000	—
12		Pulse	—	2000	—
13		SS	30	—	Performance verification
14		SS	10	—	Recalibration/proof
15		SS	10	—	Recalibration
16		SS	30	—	Performance verification
17		SS	420	—	60 s each at 7 feed pressures
18		Pulse	—	5	—
19		Pulse	—	10	—
20		Pulse	—	20	—
21	I N	Pulse	—	100	—
22	S	SS	30	—	Performance verification
23	U L	SS	420	—	60 s each at 7 feed pressures
24	A	Pulse	—	5000	—
25	T	Pulse	—	5000	—
26	E D	SS	30	—	Performance verification
27		Pulse	—	5000	—
28		SS	30	—	Performance verification
29		Pulse	—	5000	—
30		SS	200	—	Performance verification/gas sample
31		SS	420	—	60 s each at 7 feed pressures
32		Pulse	—	4750	—
33		SS	30	—	Performance verification

[a]Total accumulated duration $\approx$ 5200 s; total number of starts $\approx$ 30,000.

**Table 4. Sequence of 0.22-N (0.05-lb_f) acceptance/
characterization tests[a]**

Test No.	Mode	Continuous duration, s	0.1-s ON/ 0.9-s OFF pulses	Remarks
1	SS	10	—	Calibration/proof
2	SS	60	—	Calibration
3	SS	300	—	50 s each at 6 feed pressures
4	SS	60	—	Basepoint performance
5	SS	300	—	50 s each at 6 feed pressures
6	Pulse/SS	40	1000	Pulse and final performance verification

[a] All testing with thruster insulated; total accumulated duration ≈ 870 s; total number of starts ≈ 1005.

Table 5. Summary of 0.22-N (0.05-lb_f) engine test history

Engine S/N	Injector config- uration	Total number of tests	Accumulated duration, s	Accumulated total starts	Accumulated ambient starts
001	-1	33	7049	30,143	33
002	-2	33	8335	29,400[a]	33
004	-1	9	943	1,019	9
005	-1	8	921	1,018	8
006	-1	17	1720	1,017	17

[a] Estimated number of starts in hydrazine; inadvertent propellant depletion occurred in pulse test.

actually be commanded in reaction wheel unloading, which constitutes the major fraction of APS thruster activity. In the Phase I tests, both thrusters were fired with and without thermal insulation to ascertain the magnitude and significance of heat losses. As a result, it was decided to insulate all of the delivered engines, and all Phase II testing was done in the insulated condition.

Results. The test history of five thrusters involved in the basic program is summarized in Table 5. The first two thrusters, S/N 001 with the penetrant injector and S/N 002 with the showerhead injector, were put through the preliminary screening test series. Data obtained are summarized in Table 6. Both performed reasonably well in the early tests. As anticipated, the relatively high surface-to-volume ratio of these small monopropellant reactors and the high contact conductances provided by the mounting provisions led to significant heat losses when the reactors were run uninsulated in atmosphere. These losses are reflected in the comparative values of c^* obtained. With no thermal insulation, the thrusters exhibited a loss in c^*, ranging from 90 to 150 m/s ($\sim$300-500 ft/s) at the minimum chamber pressure to about 30 to 50 m/s ($\sim$100-165 ft/s) at the maximum chamber pressure, from that obtained in the insulated condition. Insulating the thrusters consisted of replacing titanium mounting washers with equivalent micarta washers and enveloping the thruster body in a 0.95-cm (⅜-in.) layer of castable magnesia/asbestos (Johns-Mansville #301 compound). All three deliverable engines were so insulated from the outset because of the performance improvement thus attained.

Preliminary screening tests. In the preliminary screening tests, it was found that the penetrant injector performed somewhat better under steady-state conditions than its showerhead counterpart: (1) The c^* for S/N 002 was approximately 52 m/s ($\sim$170 ft/s) lower, on the average, than that for S/N 001 (and the other penetrant configuration thrusters, as subsequently demonstrated); (2) the penetrant injector gave a slightly more rapid start transient, as shown in Fig. 18; and (3) the penetrant ran more smoothly than the showerhead under steady-state conditions, the former producing a mean P_c roughness of $\pm 3.3\%$, compared with $\pm 5.6\%$ for the latter. Pulse performance, too, ruled in favor of the penetrant. Since impulse (i.e., thrust) was not measured directly, the "pressure impulse" ($\int P_c d\theta$) was taken as the criterion of pulse reproducibility. Further, since only one sample of each injector type was available, only test-to-test, and not engine-to-engine, reproducibility could be studied. On the basis of a randomly selected sample of equilibrium pulses from pulse tests run in the insulated condition, the 1σ pressure-impulse reproducibility of the penetrant configuration was found to be $\pm 1.3\%$, compared with $\pm 4.9\%$ for the showerhead, at nominal supply pressure and 100 ms ON/900 ms OFF. These considerations alone would have mitigated for selection of the penetrant configuration. The decisive factor, however, was a significant increase in steady-state chamber pressure roughness to about $\pm 26\%$ near the end of the test series on engine S/N 002. No corresponding major change in roughness was noted on engine S/N 001. The penetrant configuration was therefore selected for the three deliverable thrusters.

Acceptance/characterization tests. In several unsuccessful attempts to initiate the acceptance/characterization test series on thruster S/N 003, it was discovered that its capillary feed tube was inadvertently damaged by weld burn-through during assembly, causing blockage of the major fraction of the passage area and excessive flow ΔP.

Table 6. Performance summary of 0.22-N (0.05-lb$_f$) thrusters

Tests		Penetrant configuration S/N 001		Showerhead configuration S/N 002	
A. Preliminary screening					
Steady-state					
Chamber pressure, kN/m² (psia)	min.	234 (34.0)		207 (30.0)	
	nom.	438 (63.5)		438 (63.5)	
	max.	658 (95.5)		655 (95.0)	
Thrust, N (lb$_f$), at	min. P_c	0.093 (0.0208)		0.080 (18.0)	
	nom. P_c	0.222 (0.050)		0.222 (50.0)	
	max. P_c	0.371 (0.0833)		0.370 (93.1)	
Ammonia dissociation, %		72		77	
P_c roughness, ± %, at	nom. P_c	3–4 (early in series) 4–5 (end of series)		5–6 (early in series) 15–26 (end of series)	
		Uninsulated	Insulated	Uninsulated	Insulated
$c*$, m/s (ft/s), at	min. P_c	1059 (3470)	1148 (3770)	935 (3020)	1090 (3580)
	nom. P_c	1169 (3830)	1220 (4000)	1136 (3720)	1174 (3850)
	max. P_c	1195 (3920)	1245 (4080)	1162 (3810)	1194 (3920)
Pulse mode[a]					
Pressure impulse reproducibility, 1σ, ± %		1.3		4.9	
B. Acceptance/characterization (Thrusters S/N 004, 005, 006)					
Steady-state		Mean performance at site standard conditions, $\epsilon = 1.5{:}1$			
Chamber pressure, kN/m² (psia)		438 (63.5)			
Thrust, N (lb$_f$)		0.22 (0.05)			
$c*$, m/s (ft/s)		1223 (4010)			
Specific impulse, N-s/kg (lb$_f$-s/lb$_m$)		1274 (130)			
Pulse mode[a]					
Impulse bit, N-s (lb$_f$-s)		0.44 (0.01)			
Specific impulse, N-s/kg (lb$_f$-s/lb$_m$)		1156 (118)			

[a]For 100-ms ON/900-ms OFF equilibrium pulse.

Consequently, it was removed from the program. Engine S/N 002 was therefore reworked to the penetrant configuration, re-identified as S/N 006, and put back into the program to replace S/N 003.

Engines S/N 004, 005, and 006 were then subjected to the acceptance/characterization test series, without further incident. A coiled capillary tube was formed and "custom" trimmed as the calibrating feed-pressure-reduction device for each of these thrusters, and delivered with them. The Lee Viscojets, evaluated in peripheral tests with thruster S/N 001, would have been preferable because of their existence as standard components, inherent reproducibility, and lesser susceptibility to blockage by particulate contaminants; however, they were not available in time to meet the delivery schedule. Some diffi-

culty was experienced in preparing a capillary pressure-reduction tube for S/N 006, which was ultimately traced to a batch-to-batch diametral variability in the tubing procured; this is the reason for the greater accumulated duration on that unit reported in Table 5.

All three engines performed satisfactorily, once calibrated, and essentially mirrored the performance of S/N 001. The steady-state performance data for the group are summarized in Table 6 for site conditions, reduced to a standard atmospheric pressure of 97.1 kN/m² (14.1 psia), a propellant supply temperature of 298 K (77°F), and at a nozzle expansion-area ratio of 1.5:1. The nominal steady-state thrust of 0.22 N (0.05 lb$_f$) was achieved at an average reactor-exit chamber pressure of about 438 kN/m² (63.5 psia) and a tank pressure of 2165 kN/m² (300 psig).
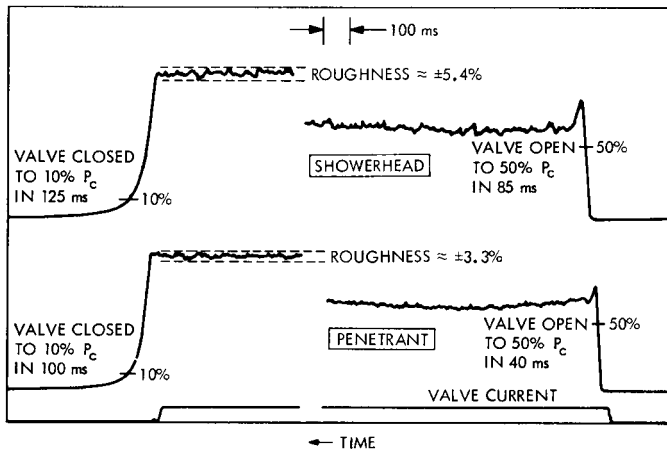
Fig. 18. Comparison of typical chamber pressure start/shutdown transients for penetrant and showerhead injector configurations—0.22-N (0.05-lbf) thruster

In the multiple-feed-pressure-level tests conducted, tank pressure was varied in steps from 2850 to 786 kN/m² (400 to 100 psig) to ascertain the performance variation that would occur in a blowdown mode, although these tests actually oversimulated the nominal 2:1 tank pressure decay expected. The range of site thrust spanned by the tests was from 0.39 to 0.08 N (0.088 to 0.018 lbf).

Actual ammonia dissociation was calculated from the mole fraction ratio of hydrogen to ammonia, as determined by the analysis of reactor-exit gas samples taken in several runs. It averaged about 72% for these penetrant thrusters, compared with approximately 77% for the single showerhead thruster fabricated.

Pulse mode operation, at the nominal tank pressure and 100-ms ON/900-ms OFF duty cycle, is represented by the typical equilibrium pulse of Fig. 19. The mean impulse bit obtained under these conditions was 0.044 N-s (0.01 lbf-s), and the corresponding specific impulse was about 1156 N-s/kg (118 lbf-s/lbm), compared with the 1275 N-s/kg (130 lbf-s/lbm) delivered in steady-state.

Data reduction. It must be pointed out here that the performance data reported are only quasi-empirical, and that their absolute accuracy is less than optimum. Evaluation of the thrusters was hampered somewhat by the unavailability of a thrust stand. Thrust and thrust-derived parameters (total impulse and specific impulse) were calculated, through a data-reduction computer program, from the pressure, temperature, flow, and ammonia dissociation data, together with measured geometry and known material properties. For steady-state computations,
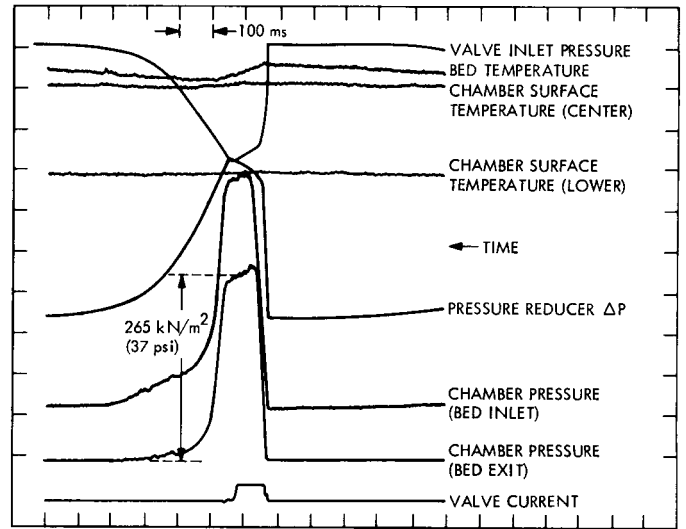
Fig. 19. Typical equilibrium pulse, 100 ms ON/900 ms OFF (penetrant injector, 0.22-N = 0.05-lbf thruster)
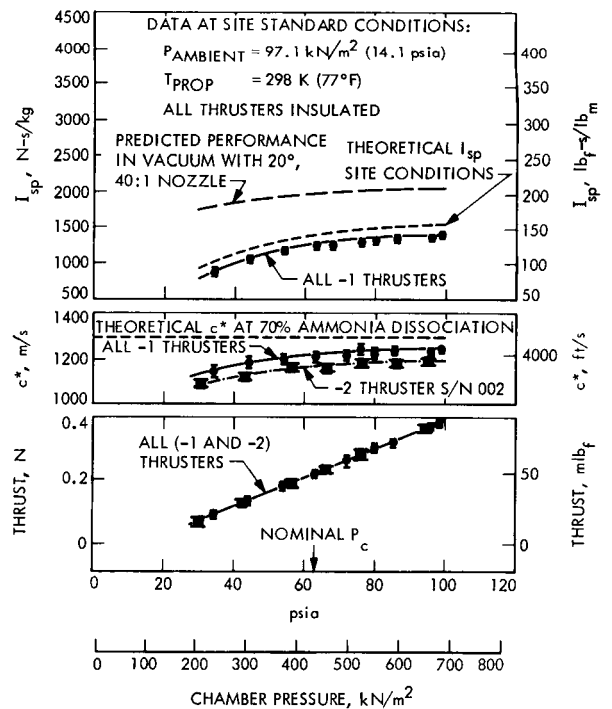
Fig. 20. Steady-state performance of insulated 0.22-N (0.05-lbf) thrusters

the thrust was computed from chamber pressure as a $C_F A_t P_c$ product. The throat area was estimated from the known geometry at ambient conditions and the thermal expansion coefficient of the nozzle material, as

$$A_t \cong (A_t)_{\text{cold}} [1 + 2\alpha \Delta T] \qquad (2)$$

where ΔT is the mean increase in throat temperature above ambient. This admittedly oversimplified correction was used consistently on all thruster tests and does not affect the comparative results, although it does, of course, affect the absolute accuracy. A more sophisticated thermal stress analysis of the nozzle would have given a more accurate throat area correction, but the end use here did not justify the time and expense of the more comprehensive treatment. The thrust coefficient was also calculated, using the conventional equation

$$C_F = \eta_{CF}(C_F)_{VT} - \frac{P_a}{P_c}\epsilon \qquad (3)$$

where $(C_F)_{VT}$ is the vacuum theoretical value for one-dimensional frozen composition, and was interpolated on ϵ and ammonia dissociation from tables built into the program. A separate subroutine, using the method of Ref. 4, computed an η_{CF} accounting for viscous and divergence losses.

The usual equations were then used to calculate c^* and I_{sp}:

$$c^* = \frac{g_c P_c A_t}{\dot{m}} \qquad (4)$$

and

$$I_{sp} = \frac{F}{\dot{m}} \qquad (5)$$

respectively. The flowrate was obtained from flowmeter frequency data (with feed-pressure reducer ΔP as backup) using the empirical calibration curve, measured propellant temperature, and built-in tables of physical properties. The performance data were reduced to site standard conditions by the same program via influence coefficients deduced from the test data. An approximate error analysis indicates a minimum 3σ accuracy of about $\pm 10\%$ in thrust, $\pm 13\%$ in c^*, and $\pm 14\%$ in I_{sp}. (The vertical spread of the data points in Fig. 20 attempts to show their standard uncertainty.)

Pulse performance was calculated by a subroutine of the same program from a digitized input of chamber pressure, temperature, and feed-pressure-reducer ΔP histories, together with point values of the other significant parameters. Considerably greater uncertainties than in the steady-state data are introduced by both the dependence upon the response of the transducers and the simplifying assumptions implicit in the numerical integration. Although a quantitative error analysis was not performed,

it is reasonable to assume that the error in impulse bit is somewhat greater than in steady-state thrust, and the pulse mode specific impulse uncertainty is probably 50 to 100% larger than its steady-state uncertainty.

9. Discussion of results. Despite the comparative lack of precision of the data obtained, the results of this program are more than satisfactory and in consonance with the objective of developing and delivering three reasonably reproducible and reliable 0.22-N (0.05-lb$_f$) thrusters for use in the single-axis simulation program, at minimum expense and within a 7-month schedule.

The preliminary screening tests of Phase I did indeed reveal a marked difference in the behavior of the single-element penetrant and showerhead injector configurations. From these limited test data, however, it would be very difficult to generalize on the comparative merits of showerhead versus penetrant injector configurations. To say that the particular showerhead configuration evaluated here was less satisfactory than the penetrant design is *not* to say that an equivalent or better performing showerhead could not have been achieved, given the opportunity for some development. The physical reasons for the observed performance differences are not thoroughly understood. The increased ammonia dissociation of the showerhead configuration (77%, versus 72% for the penetrant) may account, in part, for its somewhat lower c^*. The increasing P_c roughness with accumulated burn time (and/or number of starts) is also without satisfactory explanation. Perhaps the single orifice, coupled with the comparatively coarse screen, produced inordinately high localized bed loading and flooding, and eventually resulted in a small oscillation-inducing void through a directed fluid stream attrition process. No major void or significant catalyst loss was noted, however, upon disassembly after testing. Whatever the problem, schedule constraints precluded an investigative test program, and the showerhead configuration was not considered further.

In the Phase II tests, the remaining engines, fabricated with the penetrant-type injector, performed as expected on the basis of the performance of S/N 001 in the screening tests. Figure 20 maps the spectrum of steady-state performance data obtained for the insulated penetrant thrusters on plots of thrust, c^*, and specific impulse versus reactor exit chamber pressure. The range of chamber pressures obtained corresponds to a variation in propellant supply (tank) pressure of 2850 to 786 kN/m^2 (414 to 114 psia). By comparison, a typical tank pressure blowdown range during the tests in the Celestarium would be $2070 \rightarrow 1035$ kN/m^2 ($300 \rightarrow 150$ psia), well-bracketed by

the test pressure range. From Fig. 20, it can be seen that the site thrust linearly follows the chamber pressure, even to its lower limit, covering a range from 0.08 to 0.39 N (0.18 to 0.88 lb$_f$). The corresponding variations in c^* and site specific impulse are from 1134 to 1245 m/s (3720 to 4080 ft/s), and from 785 to 1390 N-s/kg (80 to 142 lb$_f$-s/lb$_m$), respectively. At nominal thrust, c^* and site I_{sp} were 1223 m/s (4010 ft/s) and 1274 N-s/kg (130 lb$_f$-s/lb$_m$), corresponding to 94.3 and 90.4%, respectively, of their theoretical values at site conditions and 70% ammonia dissociation. The c^* data for the one showerhead configuration thruster tested are included in the plot for comparison as the lower (broken) curve.

As previously noted, the measured ammonia dissociation of the penetrant configuration averaged 72% for the group. This value agrees exactly with that predicted by Eq. (21) of Ref. 4. This amazing degree of agreement may be coincidental, however, since the showerhead configuration ran 5% higher.

All of these thrusters were, of course, fitted with low-expansion (1.5:1) nozzles for testing at "sea level," in accordance with their end use in the Celestarium. It was of interest, however, to ascertain what their steady-state performance would have been under vacuum conditions with 40:1 expansion nozzles, such as would be employed in a spacecraft APS thruster. Hence, a routine was included in the data reduction program to compute the equivalent specific impulse under these conditions, and the resulting data are presented as the upper I_{sp} curve in Fig. 20. At nominal chamber pressure, the equivalent I_{sp} is 1970 N-s/kg (201 lb$_f$-s/lb$_m$), corresponding to about 87.5% of theoretical at 70% ammonia dissociation.

The pulse performance of the penetrant thrusters is summarized in Fig. 21 as plots of delivered impulse bit and specific impulse versus pulse number in a train of 100-ms ON/900-ms OFF pulses. These data are for nominal supply pressure (2165 kN/m² = 314.1 psia), ambient pressure (97.1 kN/m² = 14.1 psia), and propellant temperature (298 K = 77°F), with the thruster initially at ambient temperature. The upper (dashed) curves again show the estimated equivalent performance in vacuum with a 40:1 expansion nozzle. Both sets of data were computed by the methods outlined earlier, and thus contain an uncertainty, as previously noted. The impulse bits reported are higher than might be expected from the steady-state thrust and electrical pulse width. This is primarily attributable to the comparatively large volume of the chamber pressure sensing lines and transducer chambers, which is of the same order as the free volume of the
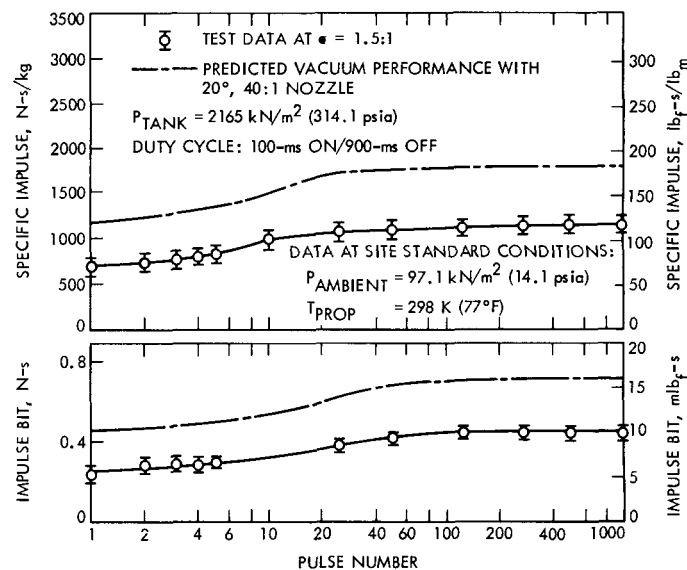
Fig. 21. Pulse performance of insulated 0.22-N (0.05-lb$_f$) thrusters

combustion chamber itself, but is nevertheless representative of what the thruster was actually delivering with the instrumentation attached.

10. Conclusions and recommendations. The success of this effort, and of similar work by some engine contractors, has clearly demonstrated the feasibility of using this class of thruster as attitude propulsion engines for planetary spacecraft. Considerable experience in their characteristics has been accumulated at JPL in the conduct of this program. Within the limited accuracy of the data obtained, it is evident that quite respectable steady-state performance (88 to 90% of vacuum theoretical I_{sp}) can be obtained from thrusters of this class. Pulse mode operation demonstrated reproducible response characteristics with acceptable performance.

Although no general conclusion can be drawn from this brief test program concerning the intrinsic superiority of either a well-designed penetrant or a well-designed showerhead injector, it might tentatively be concluded that the penetrant is the more forgiving configuration because of the uniformity of propellant distribution it affords.

F. Cold-Start Feasibility Demonstration With Modified JPL Thruster

Early in the TOPS APS supporting research and advanced development program, it was determined that for the catalytic hydrazine thrusters to be serious contenders for final spacecraft implementation, they must be able to
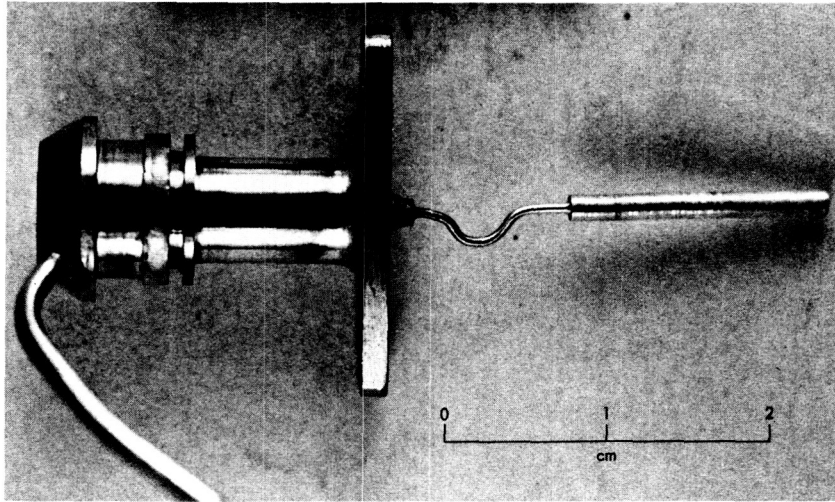
Fig. 22. Short-bed 0.22-N (0.05-lb$_f$) thruster for "cold" start life test

demonstrate the capability of performing the number of cold starts required by the mission. ("Cold" as defined here indicates that the thruster and propellant are below $32°C = 90°F$.) The cold-start requirements, as they were defined early in the program, evolved from the constraints that the propulsion bay of an outer planet mission spacecraft would be thermally controlled between 4 and 32°C (40 and 90°F) at a nominal 20°C (70°F), and that there would be approximately 1100 starts per thruster, with the thruster initially in thermal equilibrium with the propulsion bay. Until that time, only minimal cold starts had ever been attempted, and there was much concern from industry that significant performance degradation would be experienced well before 1100 cold starts were accomplished. With heed to these expressed concerns, a JPL 0.22-N (0.05-lb$_f$) thruster was modified for this feasibility demonstration (see Fig. 22). The thruster was fabricated with a shorter (0.0128-m) catalyst bed for less ammonia dissociation (55 instead of 72%) and loaded with 20-30 mesh, 90% attrited Shell 405 catalyst (nearly spherical granules). The 90% attrited catalyst was chosen on the basis of data suggesting that it may have the highest cold-start survival probability. (However, more recent findings indicate that the lesser attrited granules may be superior.) This thruster was then subjected to a series of 1532 cold starts in a JPL vacuum facility. The steady-state on-time for each cold start was approximately 10 s to allow the catalyst bed temperature to approach thermal equilibrium. The number 1500 was chosen as having sufficient margin above 1100 to demonstrate feasibility.

The results of these tests, as presented in Fig. 23, indicated only a slight initial decrease in c^* and I_{sp} (approximately 5%), along with a nominal P_c roughness of less than
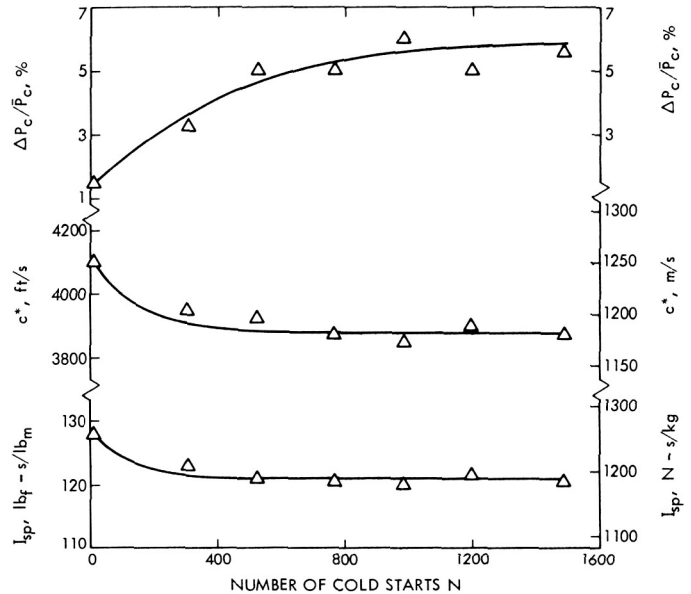
Fig. 23. Cold-start performance of modified JPL 0.22-N (0.05-lb$_f$) thruster (nozzle area ratio 1.5:1)

6%, throughout all 1532 cold starts. (Note that a sea-level nozzle with an area ratio of 1.5 was utilized.) The excessive thermal cycling, however, succeeded in crimping the injector tube at the downstream stress relief point (downstream radius near thruster backface, as seen in Fig. 22), causing a flow impedance and P_c loss. This was felt to be merely a design weakness that is readily correctable. The essence of the results was that a large number of cold starts could be performed by this size engine, and that it would experience negligible performance loss (as determined by I_{sp} and c^*).

G. Single-Axis Attitude Control Integration Tests

As part of the overall TOPS APS program, the single-axis attitude control verification test program was conducted on an air-bearing table in the JPL Celestarium. The purpose of the program was to test a complete, integrated attitude control system (for a single spacecraft axis) on an air-bearing table, using a self-contained, man-rated, liquid hydrazine fueled thrusting system with two 0.22-N (0.05-lb$_f$) thrusters facing in opposite directions. The concept of using a liquid hydrazine fueled system for this type of test program had not been previously considered at JPL and was therefore not generally accepted. Several potential problems were contemplated, primarily from the propellant safety standpoint, which had to be addressed as part of the overall program. Most questions were resolved by education; the rest were answered by proper design considerations of the propulsion module. A summary of the overall effort is presented below.

1. Tests performed. The general procedures followed during the attitude control verification tests in the Celestarium are described in the following paragraphs. For each of these tests, the portable hydrazine propulsion module was installed and active. The air-bearing table with the propulsion system installed is shown in the insert in Fig. 24.

(1) Tipoff rate reduction and sun acquisition: The table was spun up to the desired initial rate (approximately 1 deg/s), with the torque generated by the hydrazine propulsion module. The system then accomplished the reduction of the simulated tipoff rates, acquired the sun (simulated sun source), activated the reaction wheel, and disconnected the gyro output.

(2) Bias sun sensors: A sun sensor bias was inserted during the cruise mode, which caused the system to move to the offset position without activating the thrusters. This test was repeated for sun diameters corresponding to various distances from earth.

(3) Reaction wheel unloading: This phase of the air-bearing table tests was designed to verify the normal reaction wheel unloading characteristics for both the wheel saturated mode and the command-to-unload mode for any wheel speed. The test sequence was approximately as follows:
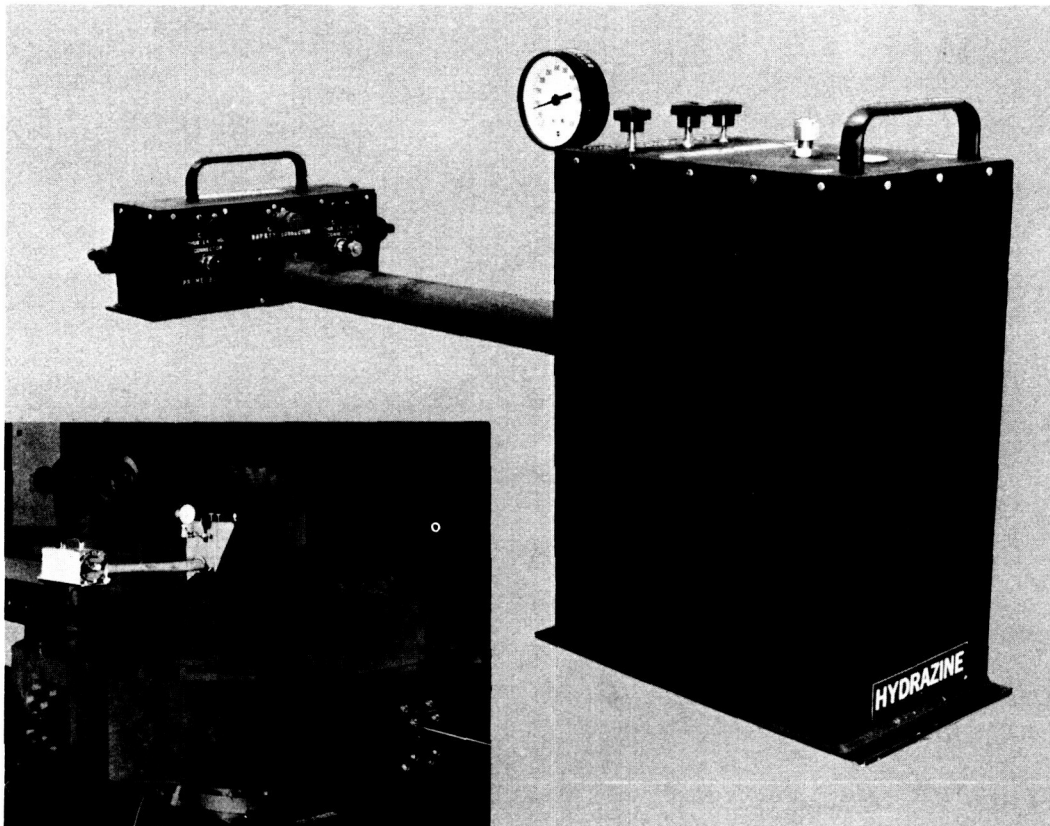
Fig. 24. Portable hydrazine propulsion module

(a) With the attitude control electronics bypassed, the thrusters were actuated until the wheel was saturated. The attitude control system was then re-engaged and the wheel was unloaded.

(b) With the wheel below the saturation speed, an unloading command was input, and the thrusters were activated to unload the wheel.

(4) Commanded turns: With the reaction wheel unloaded, a turn angle requirement was introduced and the turn executed. All commanded turns were performed without activating the thrusters, since this test series had been designed before the commanded turn functions had been assigned to the APS by the TOPS Project.

(5) Cruise mode performance: Limit-cycle performance in the presence of various disturbance torque levels was determined over the range of minimum available to approximately 1000 dyne-cm, the worst-case solar torque at 1 AU. The thrusters were actuated to provide the initial disturbance torque.

(6) Transient disturbances: The table was perturbed (by pulsing the thrusters) to simulate a transient

disturbance large enough to require the thrusters to actuate. Recovery was observed.

Since the air-bearing table was very well balanced, a special test was performed to determine the actual torque output (and hence thrust) of the propulsion module. The results are presented in Figs. 25 and 26. A flow restriction caused by excessive thermal cycling of the downstream bend in the thermal stress relief section of the injector tube was observed at the completion of the program and accounts for the difference in magnitude between the actual and theoretical thrust levels. This reflects a design weakness, so future JPL thrusters in this size range will incorporate a different thermal stress relief concept.

2. Hardware description. The self-contained, completely enclosed, portable propulsion module which was delivered to the Celestarium is shown in Fig. 24. The module was composed of a $0.3 \times 0.15 \times 0.33$ m ($12 \times 6 \times 13$ in.) sheet metal enclosure for the feed system and a $0.23 \times 0.1 \times 0.08$ m ($9 \times 4 \times 3$ in.) container for the solenoid valves, capillary tubes, and thruster supports. These aluminum enclosures were joined by an 0.46×0.04 m ($18 \times 1\frac{1}{2}$ in.) diameter tube which functioned both as a

TABLE ROTATION DIRECTION: CLOCKWISE
INITIAL TANK PRESSURE: 1.84×10^6 N/m^2 (267 psia)
ANGULAR ACCELERATION: 1.935×10^{-4} rad/s^2
RESULTANT TORQUE: 0.102 N-m (0.0745 ft-lb$_f$)
THEORETICAL TORQUE AT 1.84×10^6 N/m^2 (267 psia)
TANK PRESSURE: 0.116 N-m (0.085 ft-lb$_f$)
TABLE MOMENT OF INERTIA: 525 kg m^2 (385 slug-ft^2)
THRUST
    ACTUAL: 0.165 N (0.0372 lb$_f$)
    THEORETICAL: 0.19 N (0.0425 lb$_f$)
DATE OF TEST: 23 JUN 71
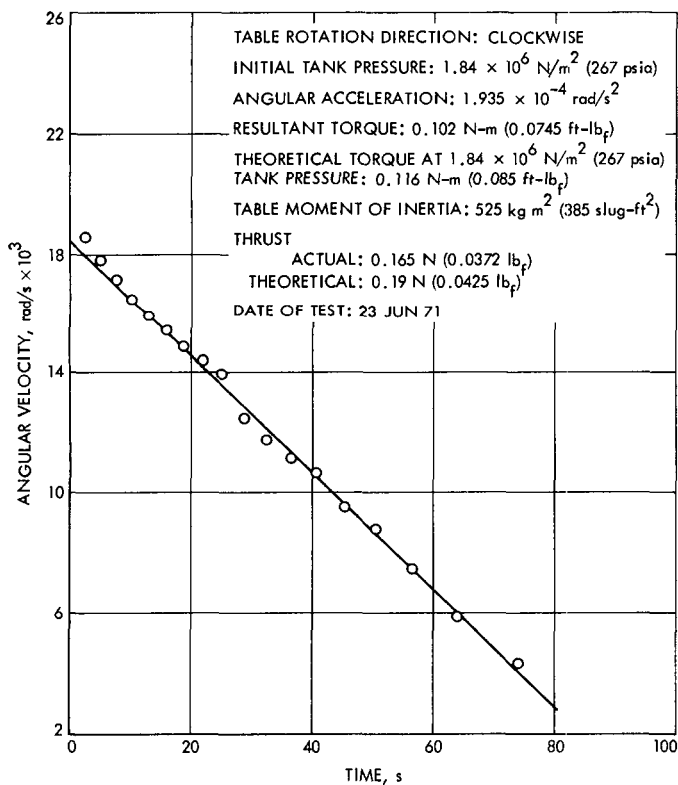
Fig. 25. Celestarium air-bearing table angular velocity reduction rate (thruster S/N 006P)

TABLE ROTATION DIRECTION: COUNTERCLOCKWISE
INITIAL TANK PRESSURE: 1.78×10^6 N/m^2 (258 psia)
ANGULAR ACCELERATION: 1.28×10^{-4} rad/s^2
RESULTANT TORQUE: 0.067 N-m (0.0493 ft-lb$_f$)
THEORETICAL TORQUE AT 1.78×10^6 N/m^2 (258 psia)
TANK PRESSURE: 0.11 N-m (0.0814 ft-lb$_f$)
TABLE MOMENT OF INERTIA: 525 kg m^2 (385 slug-ft^2)
THRUST
    ACTUAL: 0.11 N (0.02465 lb$_f$)
    THEORETICAL: 0.181 N (0.0407 lb$_f$)
DATE OF TEST: 23 JUN 71
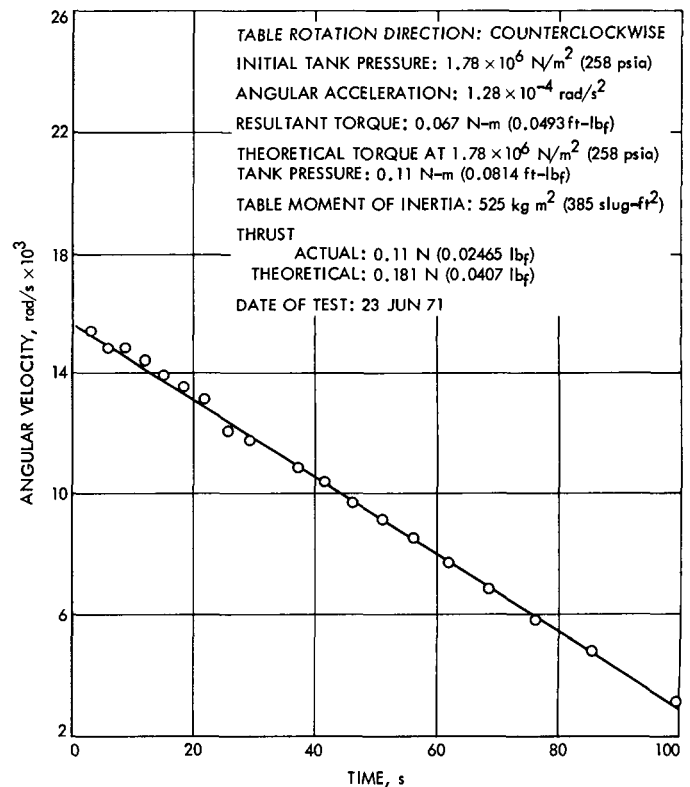
Fig. 26. Celestarium air-bearing table angular velocity reduction rate (thruster S/N 004P)

support member and as an enclosure for the propellant feed tube. All surfaces were black anodized for minimum light reflection during sun sensing operations. The larger section of the module enclosed the feed system (shown in Fig. 27), which consisted of a propellant tank containing less than ½ liter of hydrazine, a 5-μm (absolute) filter, a hand-operated shutoff valve (shown between the liquid and gaseous nitrogen fill valves), and the related tubing. The smaller enclosure contained the two opposing thrusters (shown protruding from each end in Fig. 28), the solenoid valves, and the pressure-dropping/flow-metering capillary tubes. The thrusters were insulated for better performance in the atmosphere. The propulsion module is shown assembled on the air-bearing table in the insert of Fig. 24 and has been photo-retouched (lightened in tone) for clarity.

The feed system was assembled from components designed to sustain very high pressures. The propellant supply tank had been ASME-coded for a 2.76×10^7 N/m^2 (4000-psig) working pressure with a 4:1 safety factor and had been proof-tested to 4.14×10^7 N/m^2 (6000 psig). The maximum pressure experienced during air-bearing table tests was 2.76×10^6 N/m^2 (400 psig). (The other components had larger safety factors.) This ample margin of safety, combined with a history of safe operation and low thruster chamber pressures, was instrumental in obtaining a man rating for the module so that it could be operated in the presence of personnel. This greatly facilitated the checkouts and demonstrations of the air-bearing table.

The deliverable thrusters themselves were identical replicas of a design which has sustained, on a single thruster, in excess of 30,000 starts, with an accumulated on-time on the order of 8000 s. These thrusters were acceptance tested for approximately 1000 starts and less than 1000 s on-time in order to provide a sufficient life margin for the duration of the single-axis tests. The number of starts required of each thruster for the single-axis tests was estimated to be approximately 5000. The actual number, however, exceeded this number by more than a factor of 20 for an accumulated on-time in excess of 4 h. One thruster (S/N 004P) was estimated to have experienced on the order of 180,000 starts, since it had been operational for fifteen tank refuelings. The original mate to this thruster (S/N 005P) was replaced after seven tank refuelings because of what sounded like an excessive "popping" noise. This did not constitute a personnel hazard, but a potential reduction in thruster life was visualized. The thruster was then instrumented and tested at atmospheric conditions in a liquid propulsion test facility. The checkout test consisted of operating at both the 2.75×10^6 and 1.38×10^6 N/m^2 (400 and 200 psig) steady-state inlet pressure limits, and of sweeping through low to high pulse mode duty cycles (percent of time per total cycle time). At no time could the "popping" be repeated, and no anomolous performance behavior was indicated on the oscillograph. One possible explanation for the original occurrence of the sound is that it may have been caused by gas in the
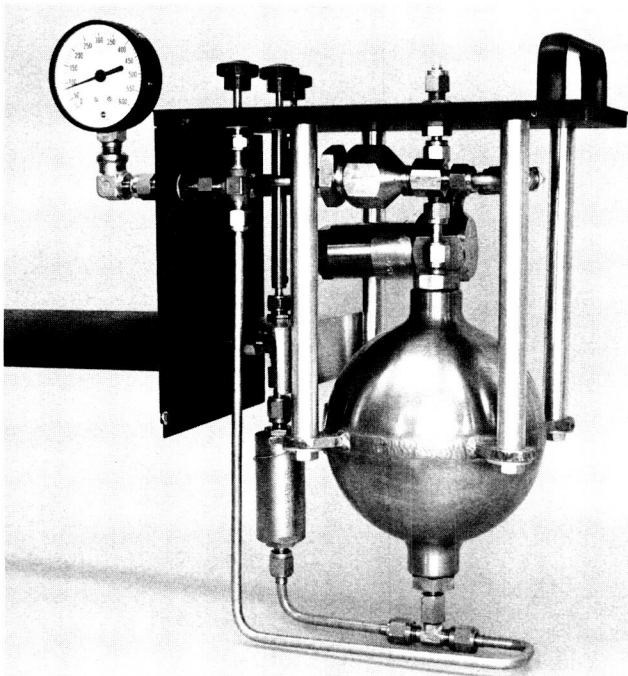
Fig. 27. Hydrazine propulsion module feed system
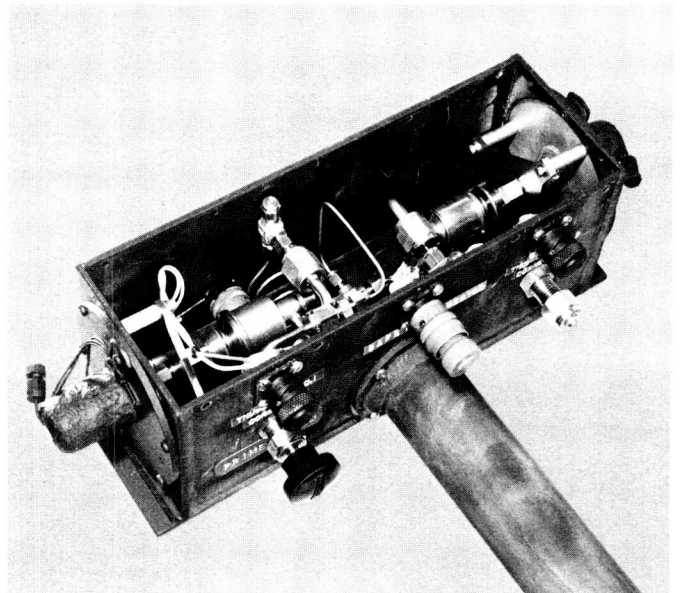
Fig. 28. Hydrazine propulsion module thruster/valve assembly

thruster feed line due to an improper priming. The thruster/valve assembly was set aside as a usable spare.

The propellant tank contained a maximum of 0.85 kg (1.9 lb$_m$) of liquid anhydrous hydrazine (0.425 liter). No propellant transfer was performed in the Celestarium. The module was brought into the Celestarium fully loaded and pressurized, and was removed to a liquid propellant handling area for refueling. During the active phase of this program, a total of fifteen propellant refuelings were required, which was a factor of three more than was originally designed. It is felt that this propulsion module demonstrated ample life margin.

3. Safety considerations. The presence of a liquid hydrazine system in the Celestarium was of concern because of the hazards that exist when hydrazine is transferred, spilled, or open to the atmosphere, or when ammonia concentrations are severe. The system was therefore designed such that the propellant would be completely contained within the feed system and exposed only to the nitrogen pressurant; at no time would propellant itself be handled in the Celestarium. The "splash-shield" outer enclosure was also added to act as a container as a precaution in the unlikely event of any liquid leakage. Evacuation of the entire building during thruster operations was suggested, but was decided against with the concurrence of the JPL Safety Office.

Because of the quantity of ammonia that could be generated by the thrusters during operation in the Celestarium, and its effect on personnel and adjacent electronic components, the Celestarium air-conditioning was modified to provide one complete air change in 8 min.

In the meantime, it was estimated that the maximum quantity of ammonia that would be present within the stellar simulation room of the Celestarium after a 5-min thruster operation without venting would be approximately 16 parts per million. An ammonia environmental test was devised in which representative electronic components and other materials of concern were exposed to an average of 17.4 parts per million of ammonia for 191.5 h, a time estimated to exceed the total accumulated exposure to ammonia throughout the entire single-axis validation test program. The results indicated that there was no danger of corrosion or deterioration of peripheral equipment from ammonia at this concentration. This was later substantiated by the actual air-bearing table tests.

The propellant feed system was continuously exposed to propellant from July 1970 to July 1971, the end of the test program. Throughout the entire Celestarium test program, the system operated successfully and without incident, establishing a JPL precedent for this type of activity involving this class of propulsion system.

H. Results of 0.44-N (0.1-lb$_f$) Thruster Feasibility Demonstration Program

During the latter part of FY'70, JPL purchased 0.44-N (0.1-lb$_f$) thrusters from Hamilton-Standard, Marquardt, and Rocket Research (Fig. 29) for in-house evaluation to demonstrate the feasibility of applying hydrazine catalytic thrusters to an outer planet mission spacecraft. This feasibility demonstration effort was performed in a JPL vacuum facility. The intent of the test program was to accumulate approximately 1000 cold starts on each thruster to verify the capability of any specific design of at least partially meeting the TOPS mission requirements. When this was accomplished on all three designs, one was selected to demonstrate the complete mission, with a total of 2600 cold starts (1000 events is more typical of the pitch- and roll-axis requirements, whereas 2600 represents worst-case yaw-axis demands). These thrusters were evaluated according to the test program outlined below. Table 7 addresses the TOPS duty cycle specifically, and each event indicated represents a required cold start.

It should be noted that the purpose of the feasibility demonstrations was not to compare one contractor or thruster with another but primarily to determine whether there is an existing design that can demonstrate the TOPS requirements and, secondly, to identify design factors which can be classified as either desirable or undesirable. This will aid greatly in the final selection of a generic type of attitude propulsion subsystem for an outer planet mission spacecraft.

A decision was made early in the program to evaluate the thruster designs in sequence of their simplicity, with the Rocket Research thruster being first, followed by Hamilton-Standard's, and finally the most complex one which was manufactured by Marquardt.

1. Test program. The overall effort consisted primarily of five phases. Phase I was designed to verify the contractor data that were delivered with each thruster. Phase II defined the limitations of each thruster through operation at various off-nominal conditions. Phase III was the essence of the test program in that it demonstrated the TOPS duty cycle. In Phase IV, each thruster that had completed life testing to the point where performance degradation was observed was disassembled, inspected, and the probable cause of performance loss analyzed.

Table 7. Phase III—Original test plan for 0.44-N (0.1-lb$_f$) thrusters based on worst-case TOPS APS duty-cycle requirements for a single thruster

| Event	Duty cycle	Number of separate events	Minimum on-time per event, s	Minimum total time per event, s	Minimum number of pulses per event
Rate reduction (54 mr/s)	Steady-state	1	405 (6.75 min)	405 (6.75 min)	1
Turns (3 mr/s)					
9 commanded	Steady-state	9	450 (7.5 min)	450 (7.5 min)	1
60 science rolls	Steady-state	60	22.5	22.5	1
20 acquisitions	Steady-state	20	29	29	1
Solar torques[a] Micrometeoroids[a] Contingencies[a]	0.1 s ON/0.9 s OFF	2520	1.3	12.1	13

[a] Wheel unloadings.
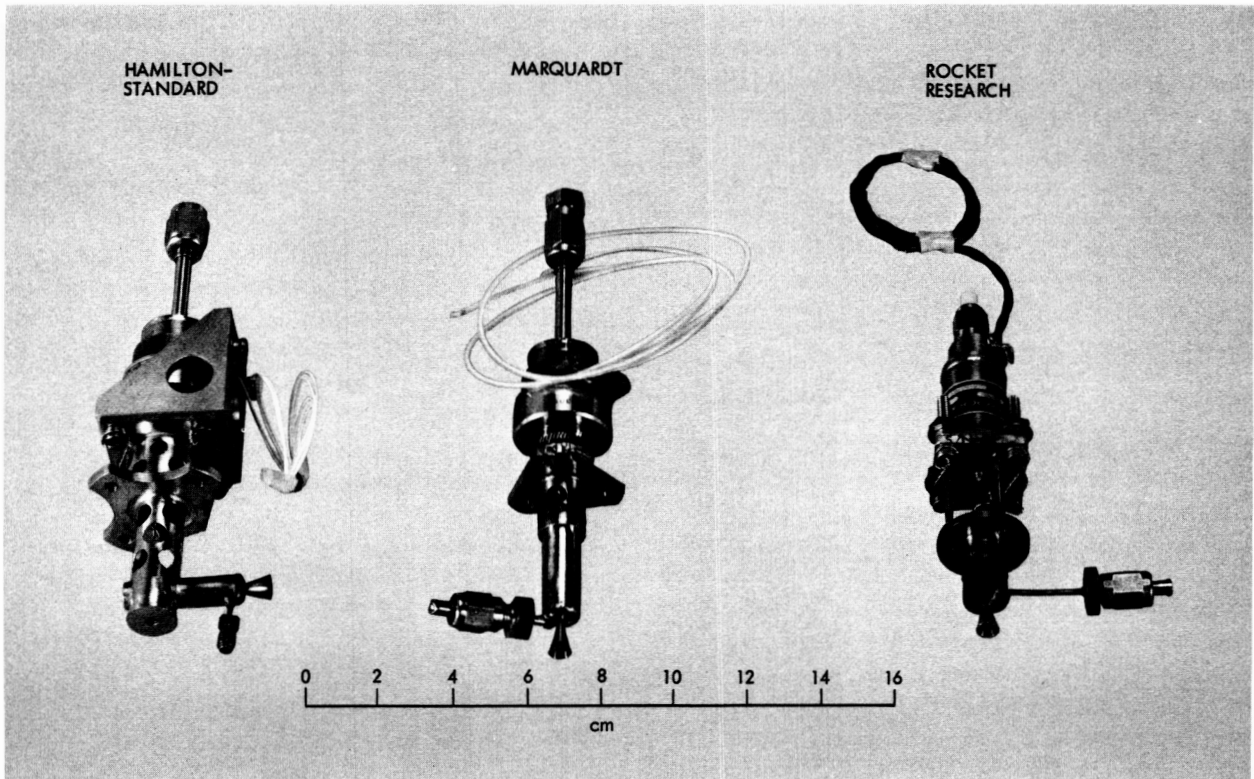
Fig. 29. 0.44-N (0.1-lb$_f$) hydrazine thrusters evaluated

Phase V consisted of the documentation of the results. All thruster testing was conducted in a vacuum.

Phase I—Verification of contractor data

(1) Test each thruster with supply tank pressures increasing from 6.9×10^5 N/m² (100 psig) to 2.75×10^6 N/m² (400 psig) in 3.45×10^5 N/m² (50-psi) increments, dwelling at each pressure for 60 s. (Hereafter, this is referred to as a "multilevel" test.) Establish the tank pressure required for a thrust level of 0.44 N (0.1 lb$_t$).

(2) Test all six thrusters with the following duty cycles and 0.44-N (0.1-lb$_t$) thrust:
    0.07 s ON, 0.7 s OFF for 20 pulses
    0.1 s ON, 0.1 s OFF for 20 pulses
    0.4 s ON, 0.4 s OFF for 20 pulses
    100 seconds of steady state

(3) Compare data with contractor results.

Phase II—Characterization tests

Perform the following tests on all six thrusters at ambient propellant temperature (21°C = 70°F):

(1) Perform the "multilevel" test.

(2) Pulse each thruster for 1000 pulses at a tank pressure selected to give a nominal thrust of 0.44 N (0.1 lb$_t$). Use a duty cycle of 0.4 s ON and 0.4 s OFF.

(3) Reduce duty cycle to 0.2 s ON and 0.2 s OFF and pulse for 1000 pulses.

(4) Reduce duty cycle to 0.15 s ON and 0.15 s OFF and pulse for 1000 pulses.

(5) Reduce duty cycle to 0.1 s ON and 0.9 s OFF and pulse for 1000 pulses.

(6) Reduce duty cycle to 0.07 s ON and 0.7 s OFF and pulse for 1000 pulses.

(7) Reduce duty cycle to 0.05 s ON and 0.5 s OFF and pulse for 1000 pulses.

Phase III—Life tests

Perform the test plan presented in Table 7.

Phase IV—Disassembly and inspection

Remove thrusters from test stand; disassemble each thruster that has experienced steady-state performance decay and analyze for the cause of failure or incipient failure. Use the thruster valves for further testing and analysis.

Phase V—Report of results

Complete the data analysis and write the final report.

2. Rocket Research thruster. The first thruster tested was the Rocket Research Model MR-47, I.D. No. 25917-301-11, S/N 01. The resulting data, presented in Figs. 30, 31, and 32, are separated into two parts. The various performance parameters are displayed first as a function of chamber pressure (obtained by varying tank pressure) and secondly as a function of life (number of cold starts). The parametric variation with upstream pressure (multilevel test) is essentially a "calibration" of the thruster. Comparison of one multilevel test to another is indicative of thruster relative performance variations as a function of life. Figure 31 depicts the thruster performance as a function of number of cold starts (thruster and propellant temperature less than 32°C = 90°F for Phase III and less than 49°C = 120°F for Phases I and II). As can be seen from Figs. 30–32, general performance, with the exception of P_c roughness, is relatively consistent. The greatest variation in P_c roughness occurs with accumulated starts, reaching a peak-to-peak maximum of approximately 20% ($\pm 10\%$).

Flow was determined by two flowmetering techniques: by using a turbine-type device from Flow Technology, Inc. (Omniflow, FTM-30-GJS), and by measuring the ΔP across a Lee Company Viscojet, a multiple-orifice fluid-resistance device. The flow/ΔP characteristics of the both flowmetering devices were determined with hydrazine. The Viscojet is felt to provide the more believable of the two flow indications. The Omniflow flowmeter appears to experience a "friction" drag at the lower flowrates, resulting in lower indicated flowrates and, hence, higher indicated performance parameters. Whether this drag was caused by very slight contamination buildup on the bearings or whether it was due to the coil magnetic field is not known. (This flowmeter has a built-in compensator to overcome the magnetic drag of the pickup coil within the designed flow range. However, the efficiency of the compensator at very low flows is not known.)

The number of cold starts at less than 32°C (90°F) accumulated on this thruster design is 896. An additional 30 starts were accumulated during Phases I and II, with an initial thruster temperature of approximately 49°C (120°F). Although the accumulated number of starts at temperatures below 49°C (120°F) was 926 (short by 74 of the 1000-start goal), because of facility scheduling it was convenient to shut down at that time. During this shutdown, the second thruster was installed for evaluation.
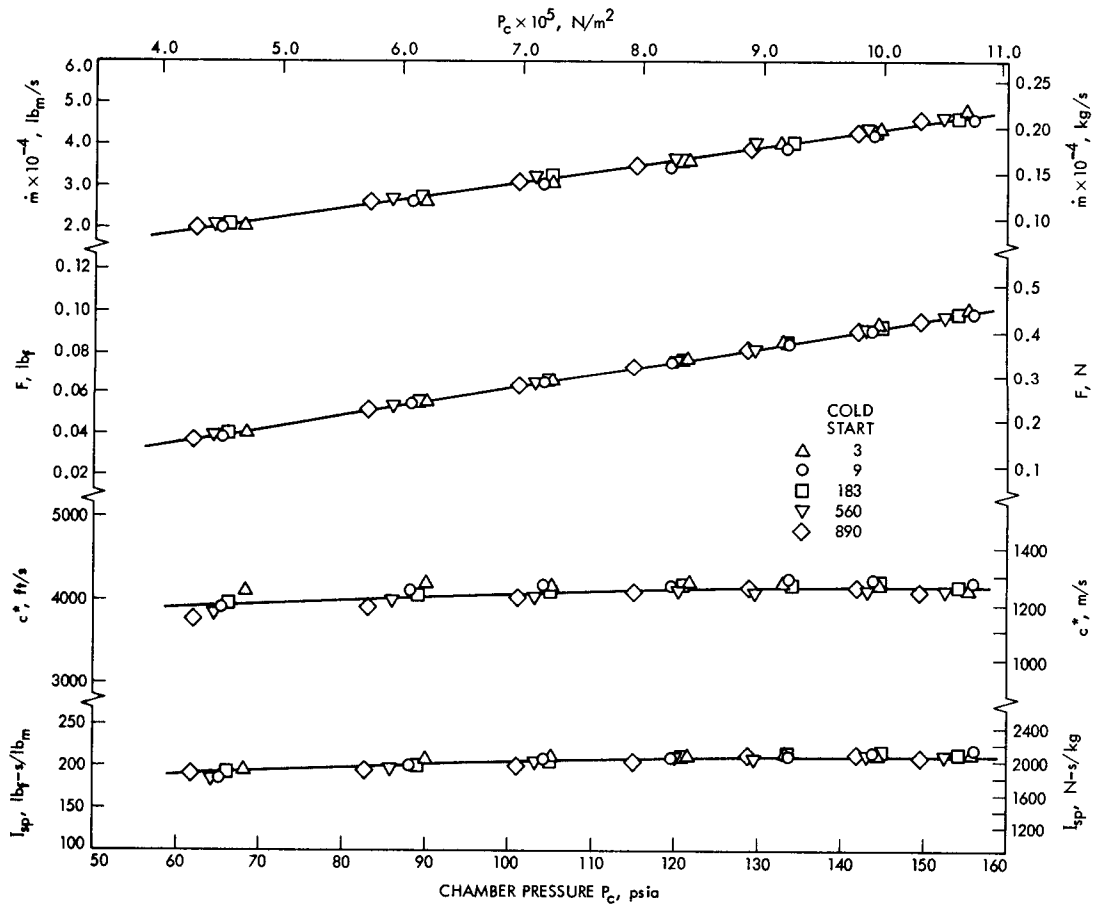
Fig. 30. Thruster performance as a function of chamber pressure and cold-start history (Rocket Research 0.44-N = 0.1-lb$_f$ S/N 01)
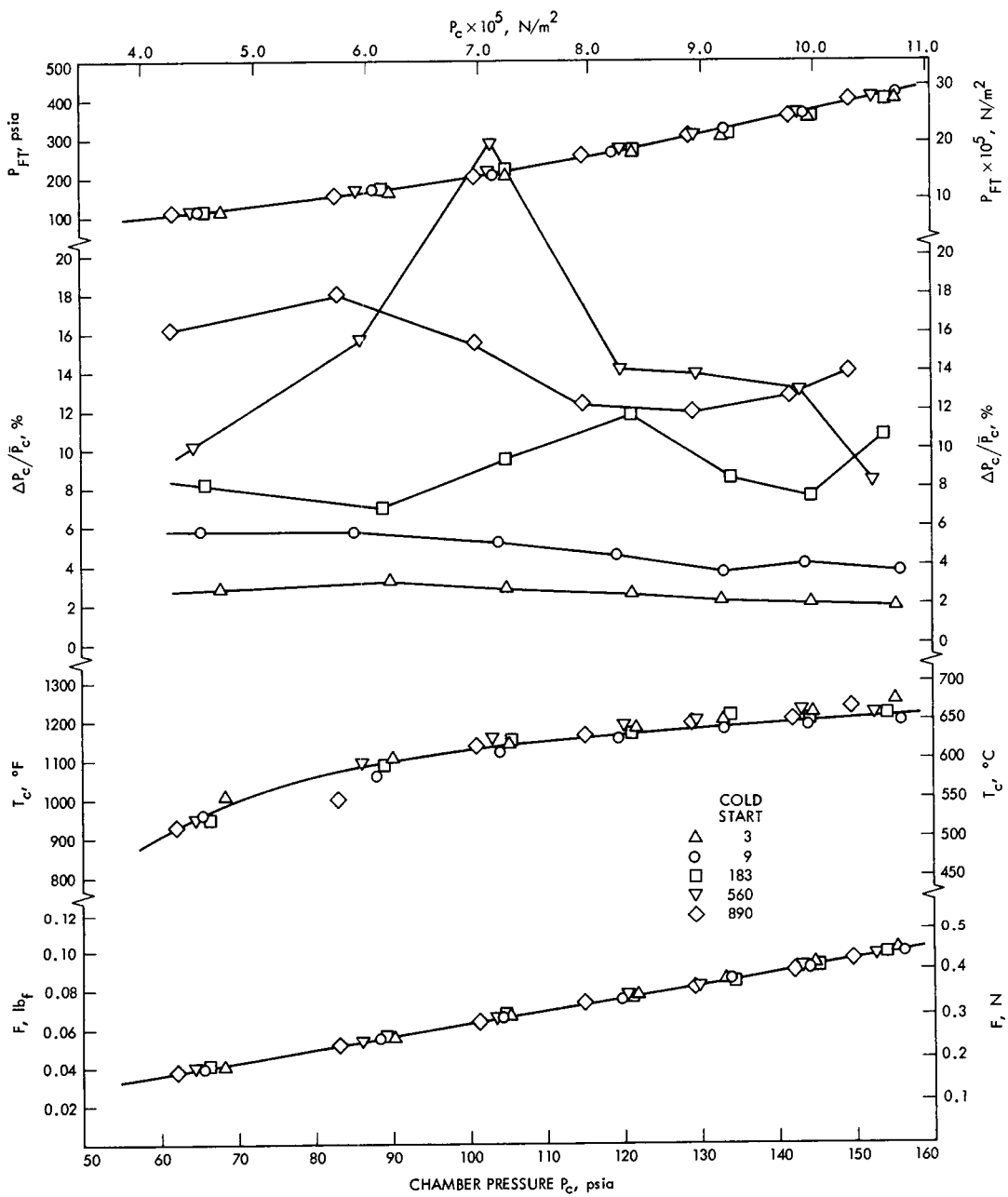
Fig. 31. Tank pressure, roughness, and temperature as a function of chamber pressure and cold-start history (Rocket Research 0.44-N = 0.1-lb_f S/N 01)
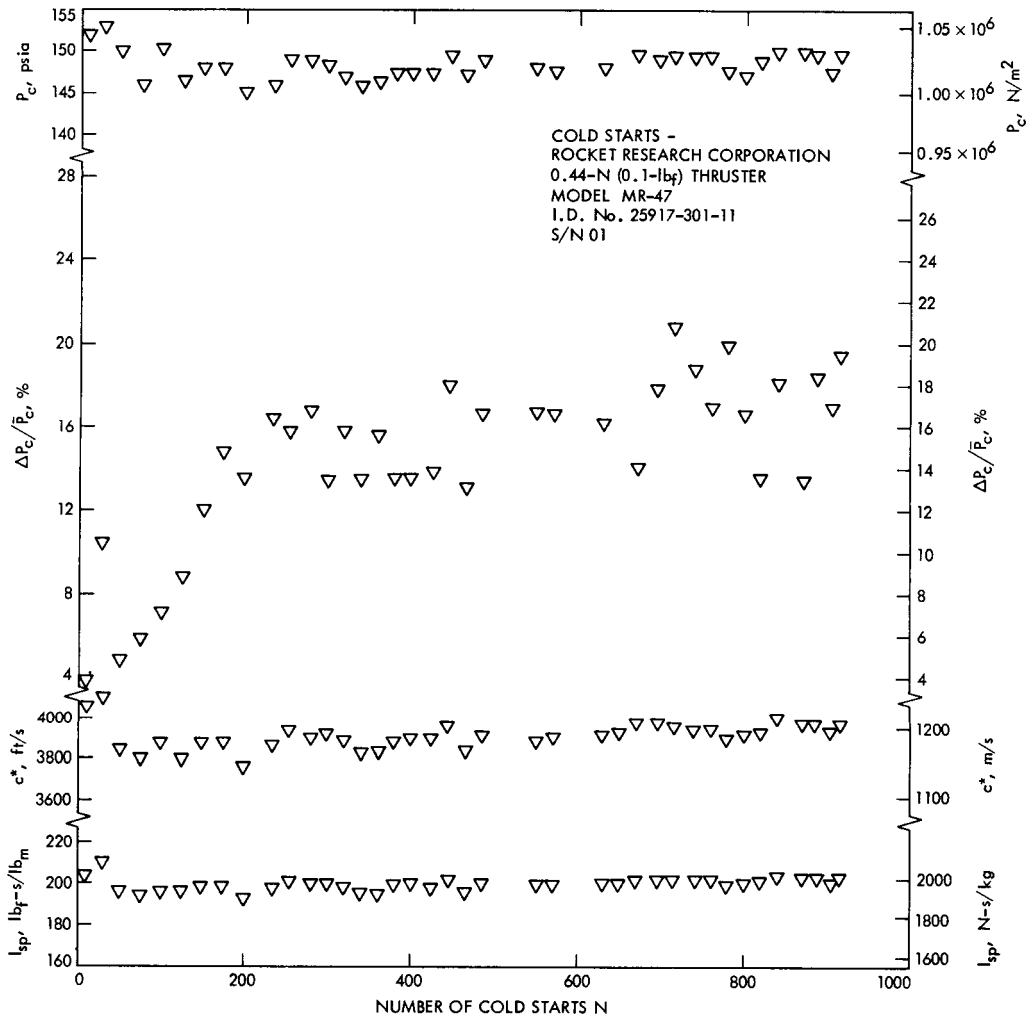
Fig. 32. Thruster performance as a function of cold starts (Rocket Research 0.44-N = 0.1-lb₁ S/N 01)

Since thrust was not measured during this test program, it was necessary to sample the exhaust gas products and analyze the constituents for composition in order to correctly ascertain thruster performance. The ammonia dissociation, which is used in the performance calculations, was determined from the results of these analyses. Hence, engine exhaust gas samples were routinely collected and analyzed for composition to determine the ammonia dissociation history. The samples were extracted through the thrust chamber pressure port near the end of a 60-s steady-state test at 0.44-N (0.1-lb$_t$) thrust. An evacuated 10-cm³ valved stainless steel cylinder was used for the collection. At the nominal 0.44-N (0.1-lb$_t$) steady-state thrust level and near thermal equilibrium conditions, the chamber pressures for the various thrusters ranges between 344 and 1030 kN/m² (50 and 150 psia). The volume of gas collected at standard conditions, therefore, varied

between 50 and 100 cm³. This was sufficient to perform the monometric and mass spectrometric analyses required to determine gas constituency. The results of a "typical" exhaust gas analysis (generalized to be representative of all thrusters) are shown in Table 8. Since some fraction of the pressurant nitrogen dissolves into the propellant and carries over into the exhaust gas, only the mole fraction ratio of hydrogen to ammonia is used in determining the ammonia dissociation. The ammonia dissociation (X) is derived from the relationship:

$$3N_2H_4 \xrightarrow{\text{catalyst}} 4(1 - X)NH_3 + 6XH_2 + (2X + 1)$$
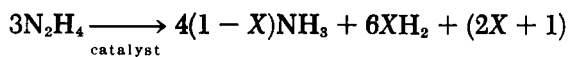
$$N_2 + [144,300 - X(79,200)] \text{ Btu}$$

and is presented in Fig. 33 as a function of the mole fraction ratio of hydrogen to ammonia (% by volume H_2/% by

34

Table 8. Typical analysis of hydrazine decomposition gases

Volume and composition of gases collected

Temperature, °C	Total volume, cm³	Volumetric composition, %				
		N₂	H₂	NH₃	Ar	CH₄
−195	73.82	40.6	59.1	−	0.01	0.35
− 30	20.62	0.93	0.08	99.6	0.01	−

Total volume and volumetric composition

Total volume, cm³	Partial volume, cm³			Composition, %		
	N₂	H₂	NH₃	N₂	H₂	NH₃
94.44	30.05	43.65	20.54	31.8	46.2	21.7

$$\text{Ratio} = \frac{\text{mole fraction } H_2 \text{ (% by volume)}}{\text{mole fraction } NH_3 \text{ (% by volume)}} = \frac{46.2}{21.7} = 2.13$$

NH_3 dissociation = 59.0% (from Fig. 33)

$$3 N_2H_4 \longrightarrow 4(1-X) NH_3 + 6X H_2 + (2X + 1) N_2$$
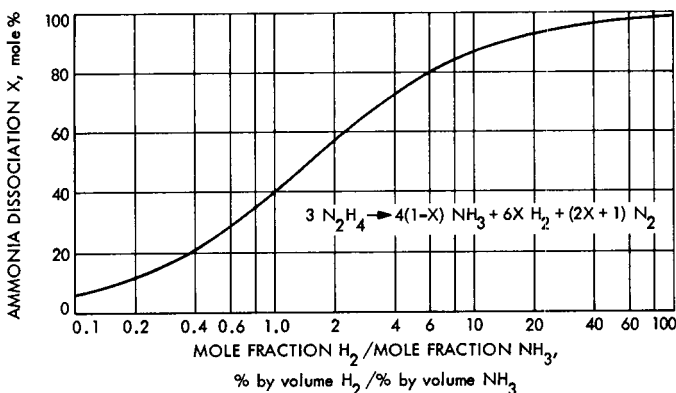
Fig. 33. Ammonia dissociation for hydrazine composition

Table 9. Rocket Research 0.44-N (0.1-lb$_t$) thruster (S/N 01) ammonia dissociation history

Date of sample	Test number	Cold-start number	Ammonia dissociation, %
26 May 1971	729	10	63
9 Jun. 1971	913	184	66.5
21 Jun. 1971	954	561	60.5
27 Jul. 1971	988	891	66
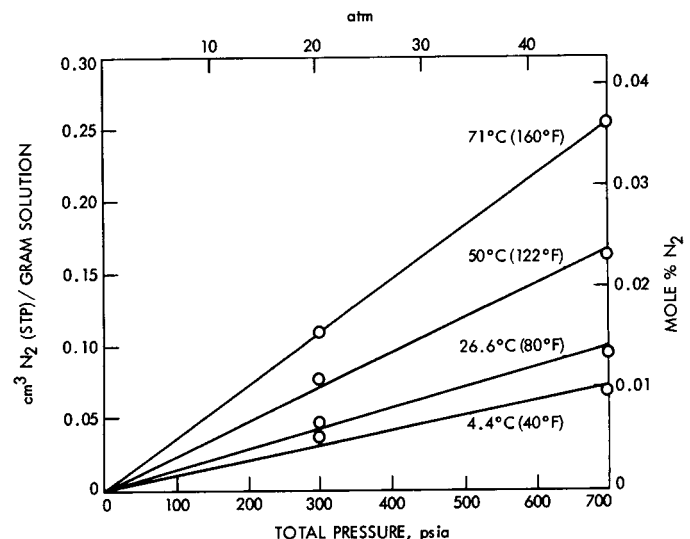
Fig. 34. Quantity of nitrogen in a saturated nitrogen-hydrazine solution as a function of temperature and pressure

volume NH_3). The dissolution of nitrogen in hydrazine as a function of pressure and temperature was extracted from Ref. 6 and is presented as Fig. 34. A history of the ammonia dissociation variations for the Rocket Research thruster is shown in Table 9.

A comparison of the pulse mode P_c profile variation throughout the life tests was made for each thruster. A pulse near the end of a typical pulse train was selected as representative of the condition nearest thermal equilibrium. Figure 35 indicates very little change in pulse mode characteristics throughout the life tests on the Rocket Research thruster.

3. Hamilton-Standard thruster. The second thruster tested was the Hamilton-Standard Model 10-12, I.D.

No. SVSK 77657-1, S/N 002. For this and subsequent test series, the Phase III test sequence was modified from Table 7 in order to ease control console operation. This new test sequence, which was a slightly more severe duty cycle than required by TOPS, is shown in Table 10.

A total of 1083 cold starts (propellant and thruster temperature below 32°C = 90°F) were accumulated on this thruster. Figures 36 and 37 show results of the multilevel performance variations, while Fig. 38 depicts the thruster performance as a function of number of cold starts. The I_{sp} and c^* presented in these figures are based upon flow data determined by the Viscojet. Symbols used in the figures are defined in the Nomenclature. The ammonia dissociation history is presented in Table 11.

Steady-state c^* and I_{sp} were essentially constant throughout the life tests. The P_c roughness parameter ($\Delta P_c/\overline{P}_c$) was nominally 6% (i.e. ±3% of steady-state P_c) and did not exceed 10% during any of the steady-state tests. However,

Table 10. Modified test operations plan for 0.44-N (0.1-lbf) thruster life tests

Test sequence	Nominal thrust level, N (lbf)	Duty cycle	Thruster on-time per pulse, s	Number of pulses	Total number of operation times	Event	Recorded
1	Multilevel[a]	Steady-state	300	1	1	Calibration	Yes
2	0.44 (0.1)	Steady-state	60	1	1	Gas sample	Yes
3	0.44 (0.1)	Steady-state	450	1	1	Commanded turn/acquisition simulation	At three points during the test
4	0.44 (0.1)	Pulse mode	0.1 (1 pulse/s)	30	32	Simulated wheel unloading	One pulse train only
5	0.44 (0.1)	Steady-state	30	1	1	Reference point	Yes
6	Repeat test sequence 4 and 5 eight times						
7	Repeat test sequence 1 through 6 X times[b]						

[a]Tank pressure is varied from 6.9×10^5 to 2.75×10^6 N/m² (100 to 400 psig) in 3.45×10^5 N/m² (50 psid) increments.

[b]$X = 4$ for 1000 cold starts; $X = 10$ for 2600 cold starts.

PULSE 19 IN PULSE TRAIN INITIATED BY COLD START 30

0.1 s

PULSE 19 IN PULSE TRAIN INITIATED BY COLD START 435

PULSE 19 IN PULSE TRAIN INITIATED BY COLD START 813

TIME→

$P_c = 6.9 \times 10^5$ N/m² (100 psia)

VALVE SIGNATURES
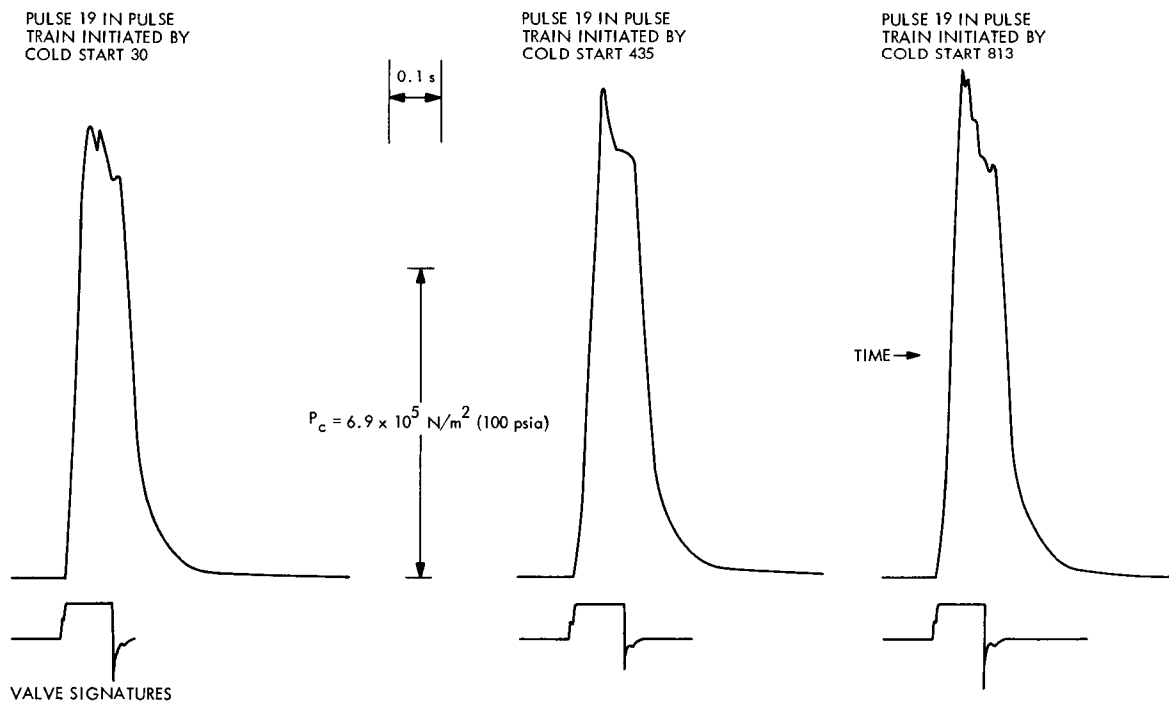
Fig. 35. Thruster pulse mode P_c profile comparison throughout life tests (Rocket Research 0.44-N = 0.1-lbf S/N 01)

a ±15% of P_c resonance characteristic of a suspected gas volume (20 to 30 cps) developed during pulse mode operations around the 290th cold start and remained near this level until approximately two thirds of the way through the test series, where it appeared to increase in amplitude to as high as ±50%. When the resonance was first observed, the feed system was re-primed to eliminate any accumulated gas that may have been trapped there; how-ever, this effort had no effect on the pulse profile. The resonance appeared in subsequent steady-state tests but damped out in less than 0.25 s. Because of the short on-time associated with the pulse mode duty cycle (0.1 s ON/0.9 s OFF), the resonance dwell time was insufficient for complete damping. Figure 38, a pulse mode P_c profile comparison, shows typical pulses before the occurrence of the resonance and after the resonance appeared.

Table 11. Hamilton-Standard 0.44-N (0.1-lb_f) thruster (S/N 002) ammonia dissociation history

Date of sample	Test number	Cold-start number	Ammonia dissociation, %
2 Aug. 1971	1000	5	41.5
4 Aug. 1971	1009	14	47
5 Aug. 1971	1018	23	46
11 Aug. 1971	1040	290	45.5
17 Aug. 1971	1062	552	44.5
20 Aug. 1971	1085	812	45
27 Aug. 1971	1108	1081	47
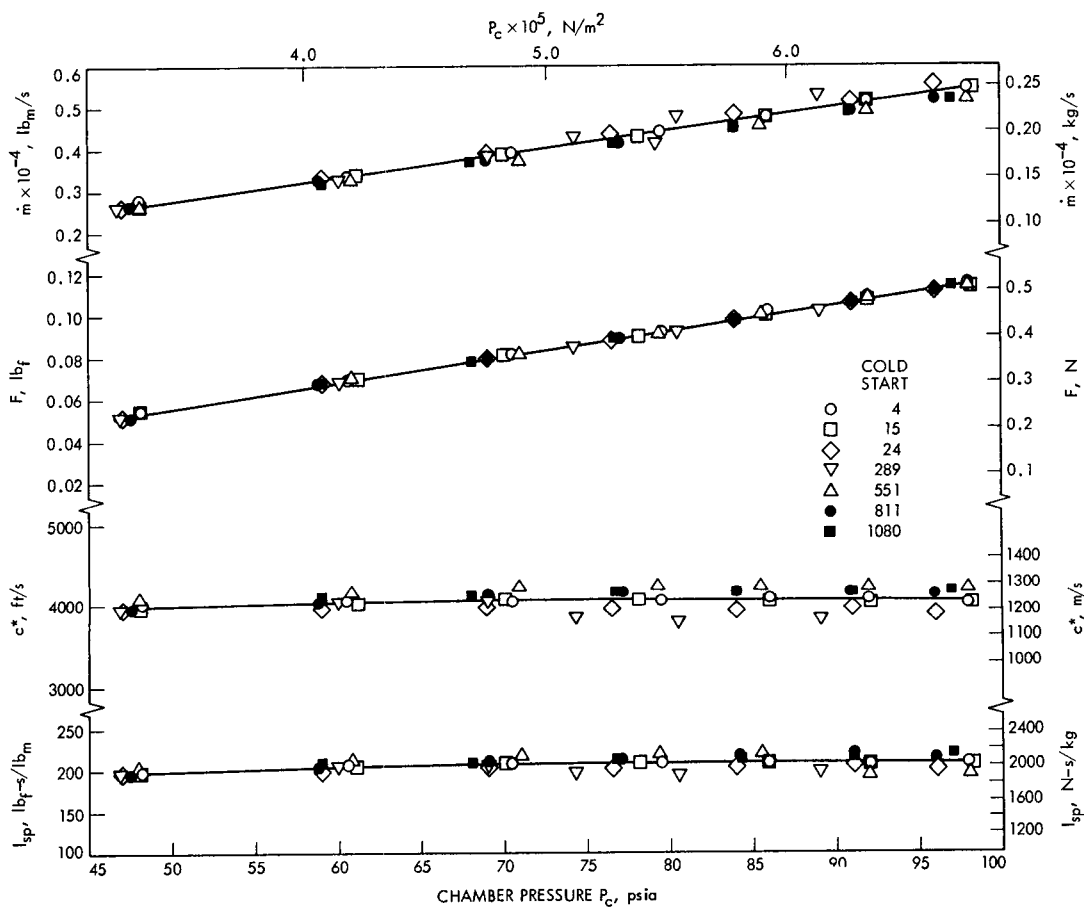
Fig. 36. Thruster performance as a function of chamber pressure and cold-start history (Hamilton-Standard 0.44-N = 0.1-lb_f S/N 002)
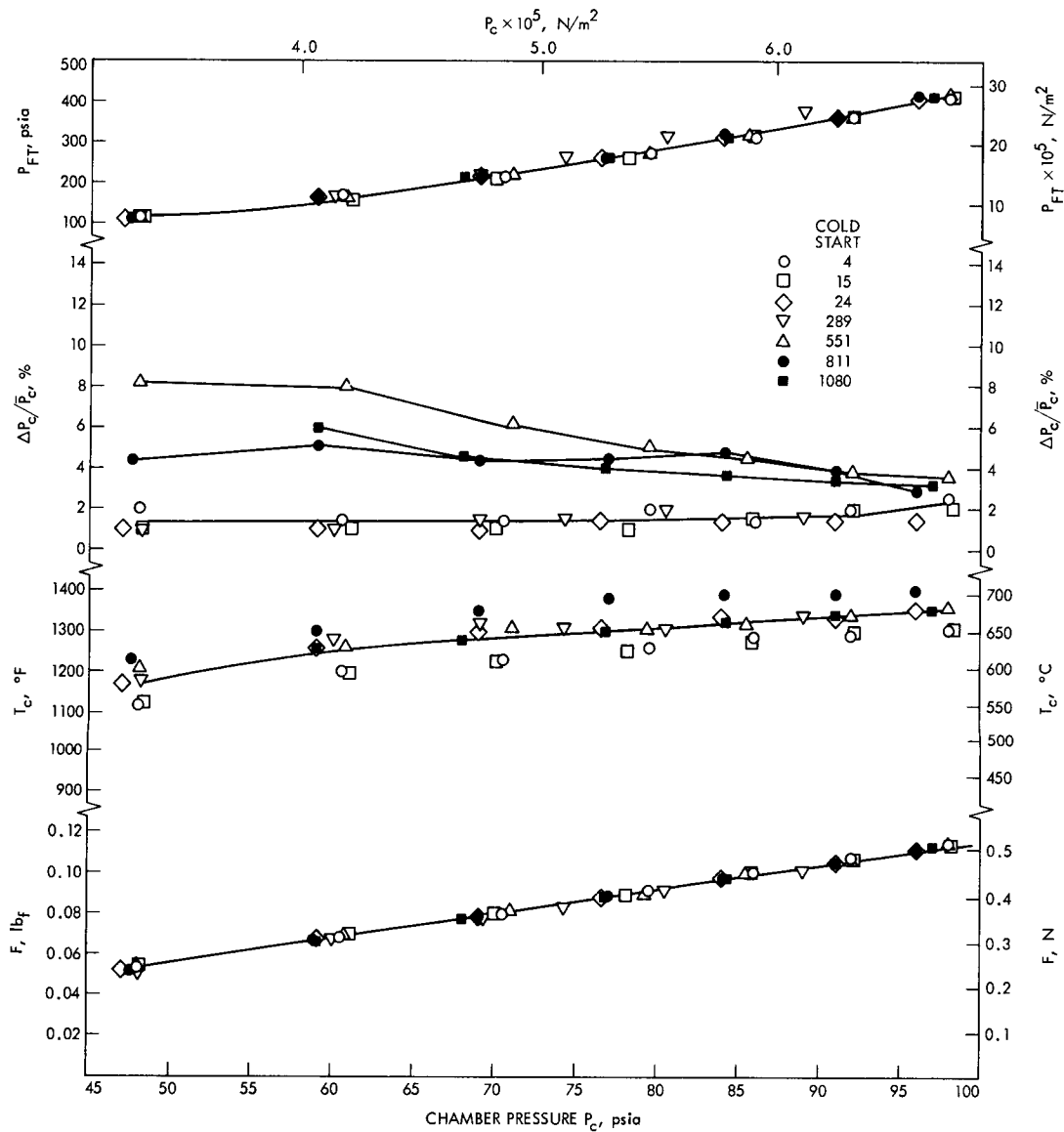
Fig. 37. Tank pressure, roughness and temperature as a function of chamber pressure and cold-start history (Hamilton-Standard 0.44-N = 0.1-lb_f S/N 002)

The most probable cause of the phenomenon (agreed upon during conversations with Hamilton-Standard representatives) was a change in injector characteristics (e.g., the appearance of a void volume in the catalyst bed around the injector). The injector is a short, cone-like penetrant composed of an 85-mesh inner screen and a 200-mesh outer screen. Erosion of the catalyst around the injector could effect a volume change, allowing an increased gas accumulation.

Hamilton-Standard has changed its bed packing procedures since the time these thrusters were purchased by

JPL. Their new technique offers a much higher probability of survival for extended duty cycles.

4. Marquardt thruster. The third and final thruster evaluated was the Marquardt Model R 25 A, I.D. T 17412, S/N 002. Phase III used the modified test sequence shown in Table 10.

A total of 2710 cold starts (propellant and thruster temperature below 32°C = 90°F) were accumulated on this thruster. Figures 40 and 41 present the results of the multi-level performance variations throughout the test effort.
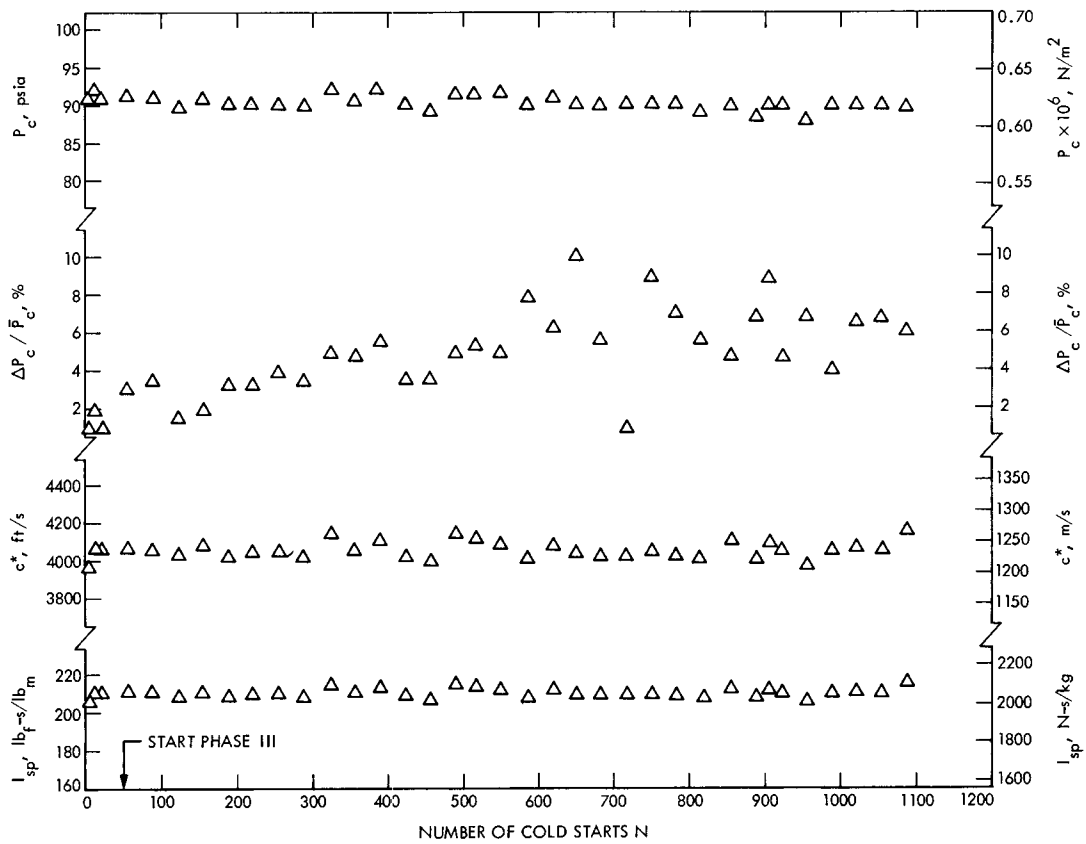
Fig. 38. Thruster performance as a function of cold-starts (Hamilton-Standard 0.44-N = 0.1-lb$_f$ S/N 002)
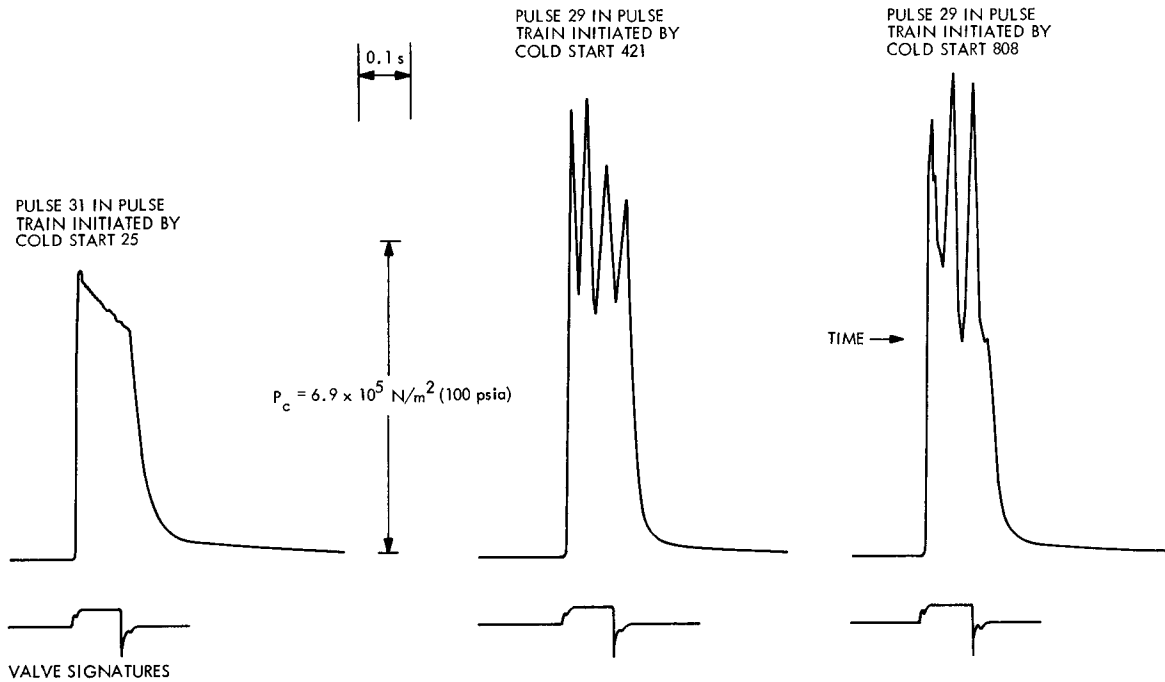
Fig. 39. Thruster pulse mode P_c profile comparison throughout life tests (Hamilton-Standard 0.44-N = 0.1-lb$_f$ S/N 002)
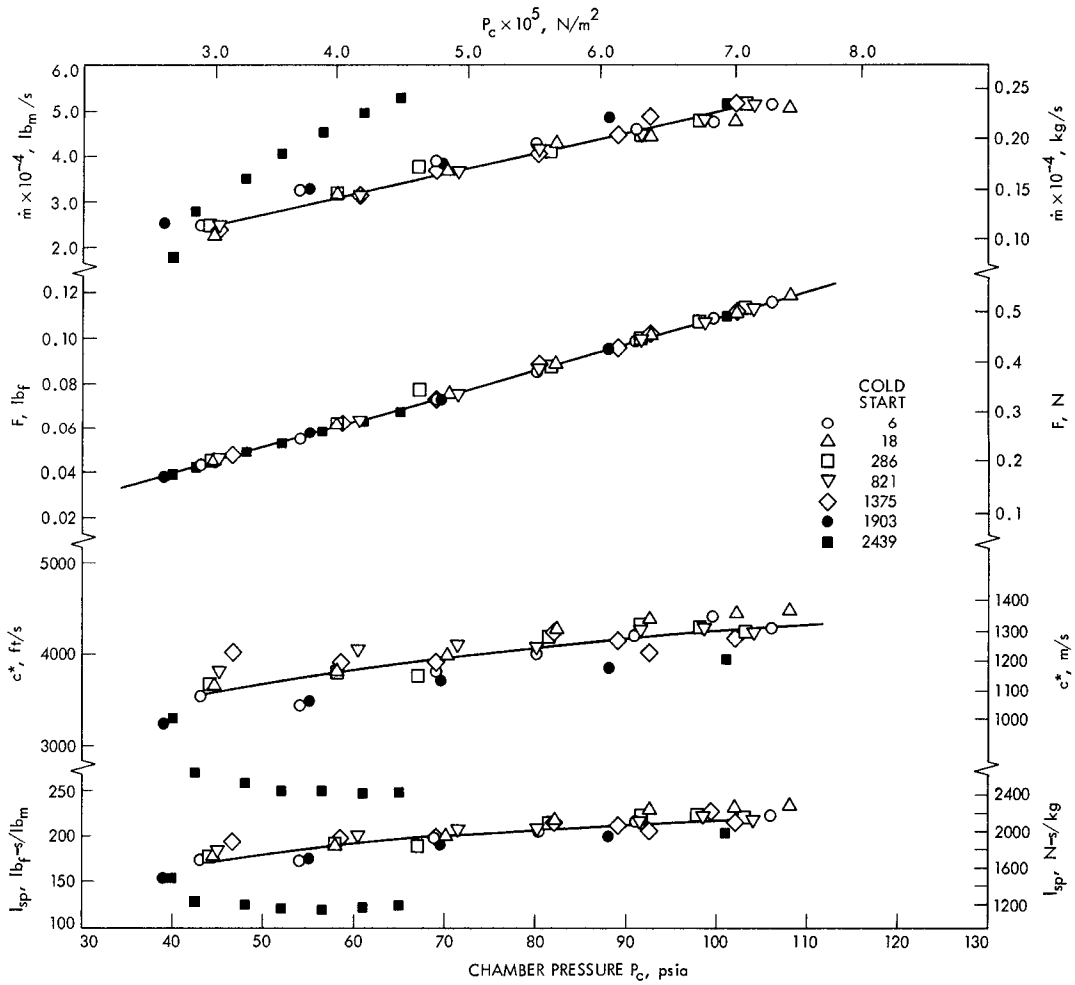
Fig. 40. Thruster performance as a function of chamber pressure and cold-start history
(Marquardt 0.44-N = 0.1-lb$_f$ S/N 002)
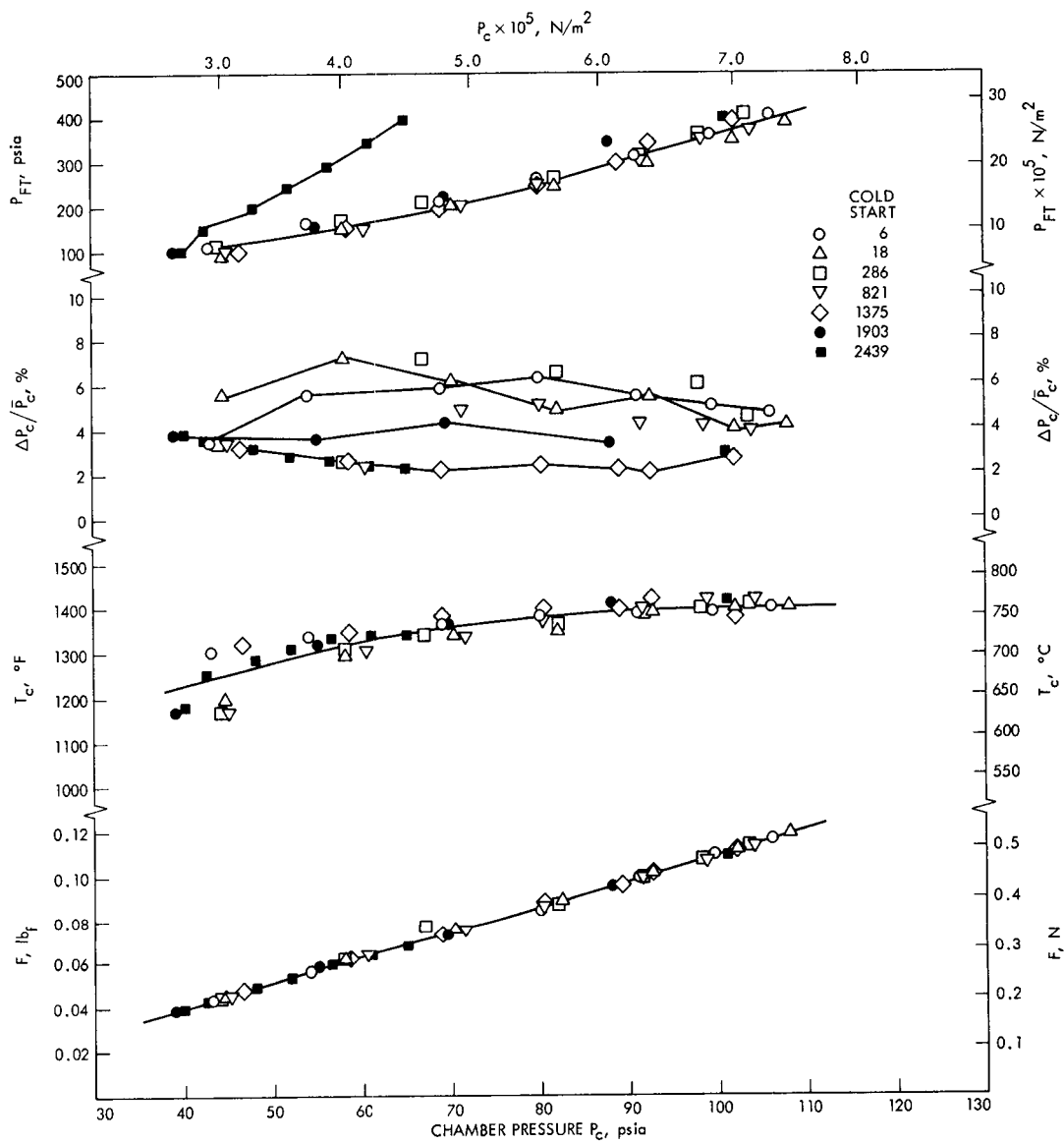
Fig. 41. Tank pressure, roughness, and temperature as a function of chamber pressure and cold-start history (Marquardt 0.44-N = 0.01-lb$_f$ S/N 002)

The definitions for the symbols are identified in the Nomenclature. Figure 42 depicts the thruster performance as a function of number of cold starts. As for the previous two thrusters, the I_{sp} and c^* presented in these figures are based upon Viscojet (ΔP device) flow data only. Figure 43 shows the chamber pressure and roughness parameter as a function of number of cold starts.

As can be seen in Fig. 42, the steady-state c^* and I_{sp} were essentially constant until about cold start 1700, after which they steadily decayed to approximately 57% of the original performance. At cold start 1700, the thruster had already experienced more than 50,000 total starts. The P_c roughness parameter ($\Delta P_c/\overline{P_c}$) was nominally less than 6% (i.e., ±3% of steady-state P_c) throughout the test series, making this the smoothest operating of the three commercial thrusters evaluated. In all, the thruster experienced 83,023 total starts for an accumulated on-time of 5.88 h.

Although this thruster was not specifically designed for pulse mode operation, there was very little observed change in pulse profile throughout the entire test series. Figure 44 compares three typical pulse profiles that were demonstrated during the evaluation of this thruster.

Table 12, which presents the ammonia dissociation history for this thruster, indicates that an apparent decrease in ammonia dissociation was observed at approximately the same time that the decrease in performance occurred. A decrease in ammonia dissociation usually implies an increase in performance. However, random traces of raw hydrazine (from 3 to 200 μg) were observed during the gas sample analyses. It is suspected that, in reality, quantities of raw hydrazine greater than these trace amounts were passing through the catalyst bed undecomposed. When the gas samples were taken, these quantities of hydrazine autodecomposed between the time the sample was taken and the time it was analyzed. This would result in a generation of ammonia which, when analyzed, would give the appearance of a smaller amount of ammonia dissociation.
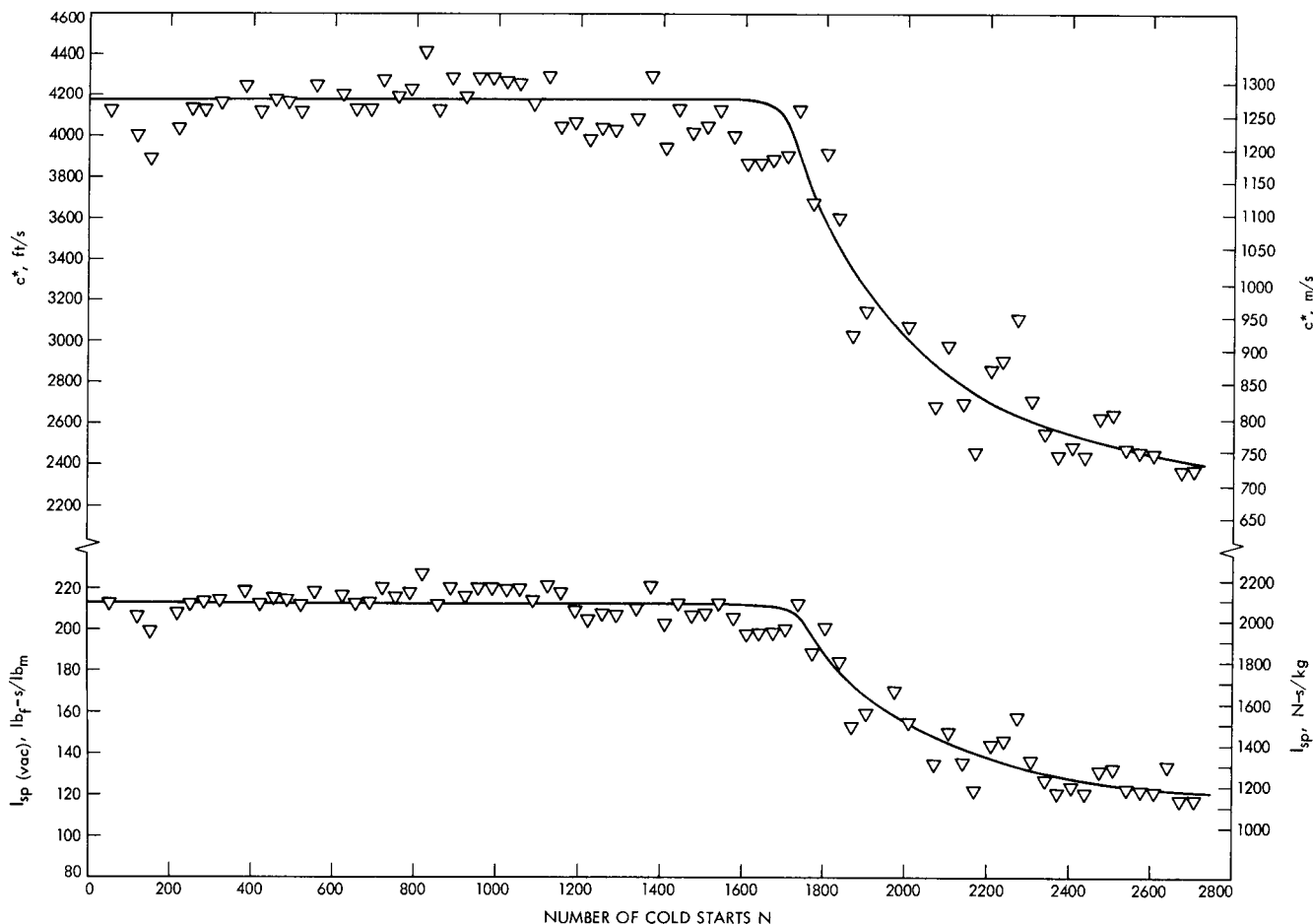
Fig. 42. Thruster performance as a function of number of cold starts (Marquardt 0.44-N = 0.1-lb$_f$ S/N 002)
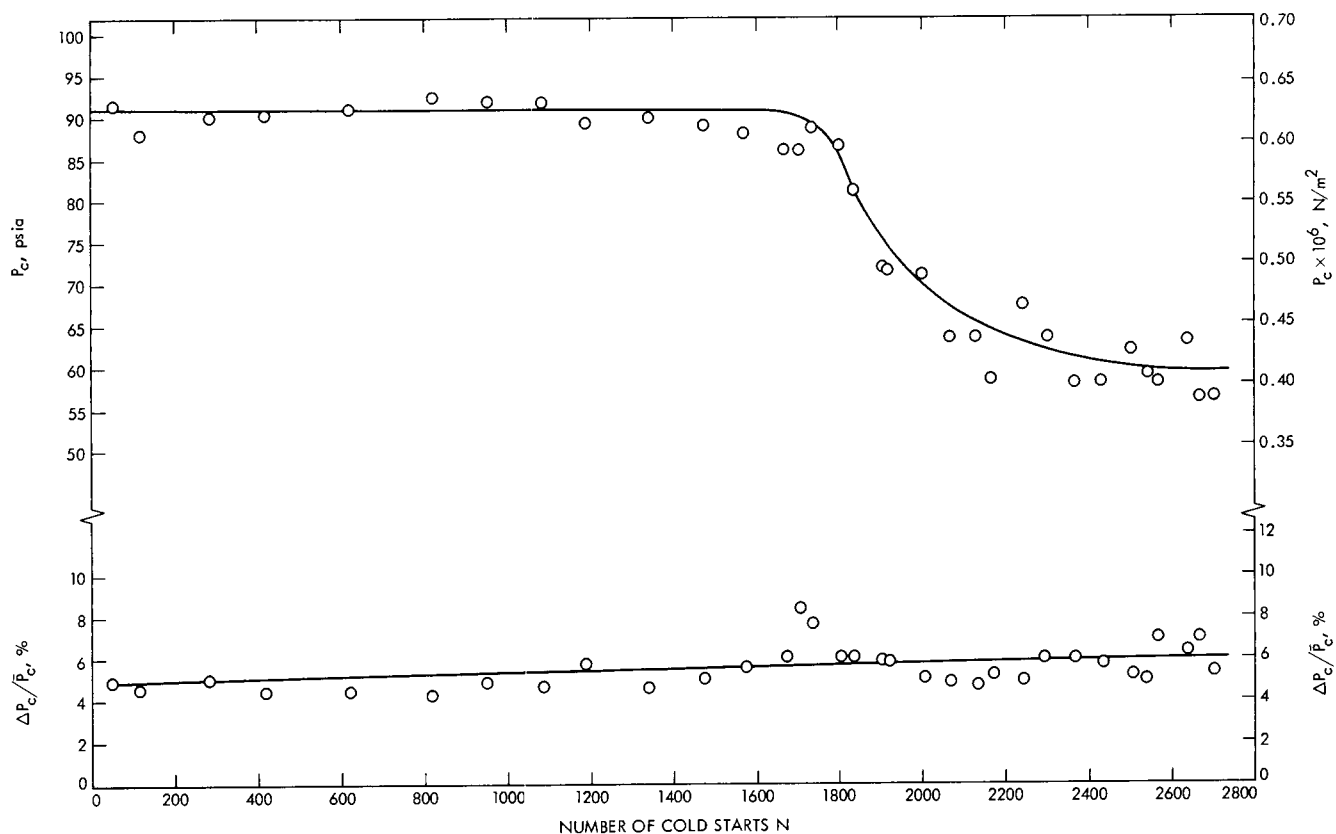
Fig. 43. Thruster chamber pressure and chamber pressure roughness as a function of
number of cold starts (Marquardt 0.44-N = 0.1-lb$_f$ S/N 002)
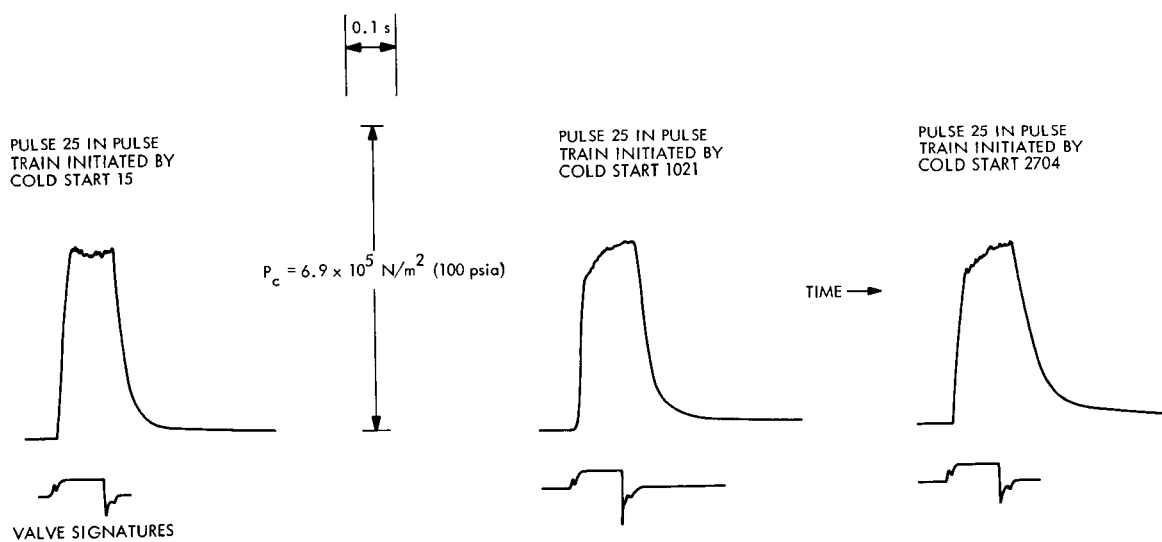
Fig. 44. Thruster pulse mode P$_c$ profile comparison throughout life tests (Marquardt 0.44-N = 0.1-lb$_f$ S/N 002)

Table 12. Marquardt 0.44-N (0.1-lb$_f$) thruster (S/N 002) ammonia dissociation history

Date of sample	Test number	Cold-start number	Ammonia dissociation, %
13 Aug. 1971	1114	4	42
1 Sep. 1971	1117	7	39.5
9 Sep. 1971	1129	19	43.5
20 Sep. 1971	1150	287	34
24 Sep. 1971	1172	556	34
30 Sep. 1971	1193	823	35.5
5 Oct. 1971	1214	1099	35.4
11 Oct. 1971	1237	1362	34.5
14 Oct. 1971	1258	1629	34.5
28 Oct. 1971	1286	1909	29.5[a]
4 Nov. 1971	1307	2176	25[a]
9 Nov. 1971	1327	2063	24[a]
15 Nov. 1971	1349	2706	23[a]

[a] Data may be invalid for reasons stated in the text.

The most probable time for this autodecomposition to have occurred would be when the gas sample was removed from the sampling tube in the chemistry laboratory. The standard procedure of ensuring that any ammonia which may be adsorbed to the metal walls of the sampling tube is removed is to drive it off by heat. This is accomplished by passing a torch over the tube until it becomes hot to touch. Since the tube is heated immediately prior to analyzing the gas for traces of hydrazine, any hydrazine that may have condensed on the tube walls could be dissociated, especially if there were catalyst fines present, as may be the case for a thruster experiencing performance degradation. Although this additional hydrazine decomposition could have occurred in any of the earlier gas sample analyses, the quantities of hydrazine present were apparently insufficient to condense on the tube surface in any significant amount as they did not perturb the ammonia dissociation results. There is later evidence tending to indicate that some performance degradation could also be caused by a temporary "poisoning" of the active sites of the catalyst bed by a cumulative adsorption of the exhaust gas products during the long-term exposure of these gases to the catalyst. This phenomenon was under investigation at the time of this writing.

This test program satisfied two primary evaluation objectives. First, it determined the point at which a performance decay was observed (i.e., the "knee" in the curve, which was around 1700 cold starts in this case), indicating what could be expected from this type of thruster with these start conditions. Secondly, it identified a probable

Table 13. Summary of inspection records and post-test analysis results of disassembled Marquardt thruster

Item	Value at time of original engine assembly	Value at time of teardown
Catalyst lot number	7-MEM-406	—
Catalyst properties		
Specific surface area	111 m²/g	79 m²/g
Hydrogen chemisorption	418 μmoles/g	223 μmoles/g
Catalyst retention spring deflection	1.24 × 10⁻³ m (0.049 in.)	8.1 × 10⁻⁴ m (0.032 in.)
Catalyst weight	0.73 g[a]	0.77 g[a]
Catalyst mesh size (U.S. Series)		
25 to 30 mesh, by weight %	99%	93.5%
30 to 60 mesh, by weight %	1%	6.5%
< 60 mesh, by weight %	≈0%	≈0%
Nitrided depth through 1.9 × 10⁻⁴ m (0.0075-in.) diameter screen wire	—	3.3 × 10⁻⁵ m (0.0013 in.)
Spring deflection at a 13.2-N (3-lb$_f$) load	9 × 10⁻⁴ m (3.55 × 10⁻² in.)	8.7 × 10⁻⁴ m (3.43 × 10⁻² in.)
Injector pressure drop at 2.45 × 10⁻⁴ kg/s (5.4 × 10⁻⁴ lb$_m$/s) flowrate	1.05 × 10⁶ N/m² (152 psid)	1.04 × 10⁶ N/m² (151 psid)

[a] Apparent catalyst weight gain is within ±0.05 g instrumentation uncertainty.

manner in which the performance would decay, such that total propellant loading for extended missions could be anticipated.

Since this thruster had experienced a much more severe test duty cycle than its two predecessors, it was disassembled and inspected (Phase IV of the test program). The thruster was returned to the contractor, who performed the analysis. The results, which are detailed in Ref. 6, are summarized in Table 13.

According to the report of the engine disassembly (Ref. 5), a reduction of 50% in both specific surface area and hydrogen chemisorption is considered neither abnormal nor a factor that may contribute to severe engine performance loss. The 43% performance decay observed might be related to the relatively long penetrant injector element (the longest of the three thrusters tested) and the relatively high injection velocities from the capillary inlet tube (ID approximately 1.34 × 10⁻⁴ m = 0.0053 in.). It could be rationalized that the propellant may have traveled almost to the end of the penetrant element prior to diffusing into the catalyst bed. This would result in a

preferential section of downstream catalyst being utilized, with a lesser amount of upstream catalyst participating in the reaction. Since the final hydrogen chemisorption and specific surface area analyses are for the entire catalyst bed, they represent only an average value. These catalyst activity tests, if performed only on the downstream catalyst volume, might have shown a considerably higher reduction in specific surface area and hydrogen chemisorption for that section of the bed, which in turn would reflect a further reduced performance efficiency. It is felt that this performance degradation could be significantly reduced with a shortened penetrant element and a larger-diameter injector tube.

I. Test Facilities

All of the TOPS APS thruster tests were conducted at the Jet Propulsion Laboratory. The initial exploratory tests with the 0.44-N (0.1-lb$_f$) "workhorse" thruster (an early experimental unit) and the later development tests for the 0.22-N (0.05-lb$_f$) Celestarium thrusters were conducted in Test Cell G. The later tests, including the cold start test program and the characterization and evaluation of the 0.44-N (0.1-lb$_f$) thrusters, were performed in the propulsion vacuum test facility. All of the engine support assembly stands and propellant feed system assemblies were designed and fabricated for this program; and all vacuum pumping systems, which were available as surplus items, were installed specifically for these tests. For the most part, existing instrumentation and recording systems within the JPL test areas were utilized.

1. Test Cell G. Rocket engine Test Cell G is a totally enclosed laboratory facility, normally used for low-thrust liquid propellant engine firings. The reinforced concrete test bay has an adjacent control room with double armor-plate windows that allow full view of the test operations. The small horizontally mounted vacuum test chamber shown in Fig. 45 was installed adjacent to the windowed wall. This 0.61-m-diameter × 0.92-m-long (2-ft-diameter × 3-ft-long) stainless steel chamber was mounted on a Consolidated Vacuum Corporation (CVC) Model PS60A pumping station, with an ultimate vacuum capability of 10^{-7} torr using the 0.213-m (6-in.) diameter oil diffusion pump and 0.007-m^3/s (15-ft^3/min) mechanical roughing pump. An auxiliary vacuum pump, Nash Model CL203, a water-sealed blower-type capable of maintaining 10 torr (0.2 psia) at 0.035 m^3/s (75 ft^3/min), was used for continuous engine operation. The vacuum chamber contains a copper tube wall shroud, which can be used for temperature conditioning of the engine test section.

The hydrazine feed system shown in Fig. 46 was mounted on the side of the vacuum chamber facing the observation windows. It was a regulated, gaseous nitrogen pressurized feed system with a total liquid capacity of 5 × 10^{-4} m^3 (30.5 in.^{3}). The flow system schematic diagram is presented in Fig. 47. All components, lines, and fittings were made of 300-series stainless steel. Normal test operations used remotely controlled 28-V dc electrical solenoid valves. System cleanliness was maintained by using 10-μm (nominal) gas filters and 5-μm (nominal) liquid filters.

Propellant flowrate determination, which was probably one of the more difficult instrumentation problems encountered, was accomplished with tank pressure regulation (0–2750 kN/m^2 = 0–400 psia) and either a coiled length of capillary tubing or a Lee Company Viscojet for the pressure-dropping element. Two types of flowmetering devices were used. For steady-state operation, a turbine flowmeter designed specifically for low flows, Omniflow (Flow Technology, Inc.) Model FTM-04-LJS,
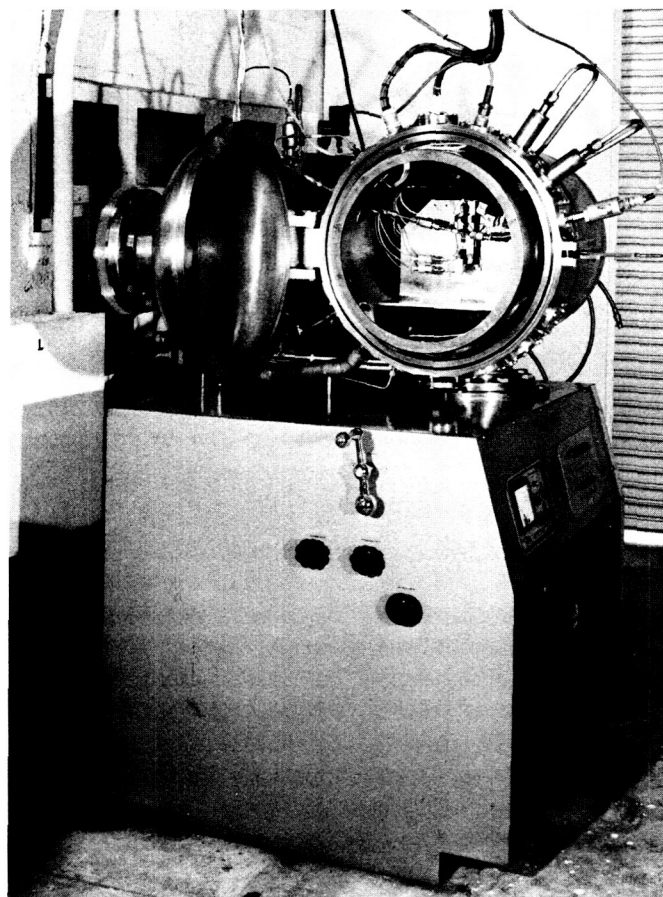
Fig. 45. Small vacuum test chamber, Test Cell G
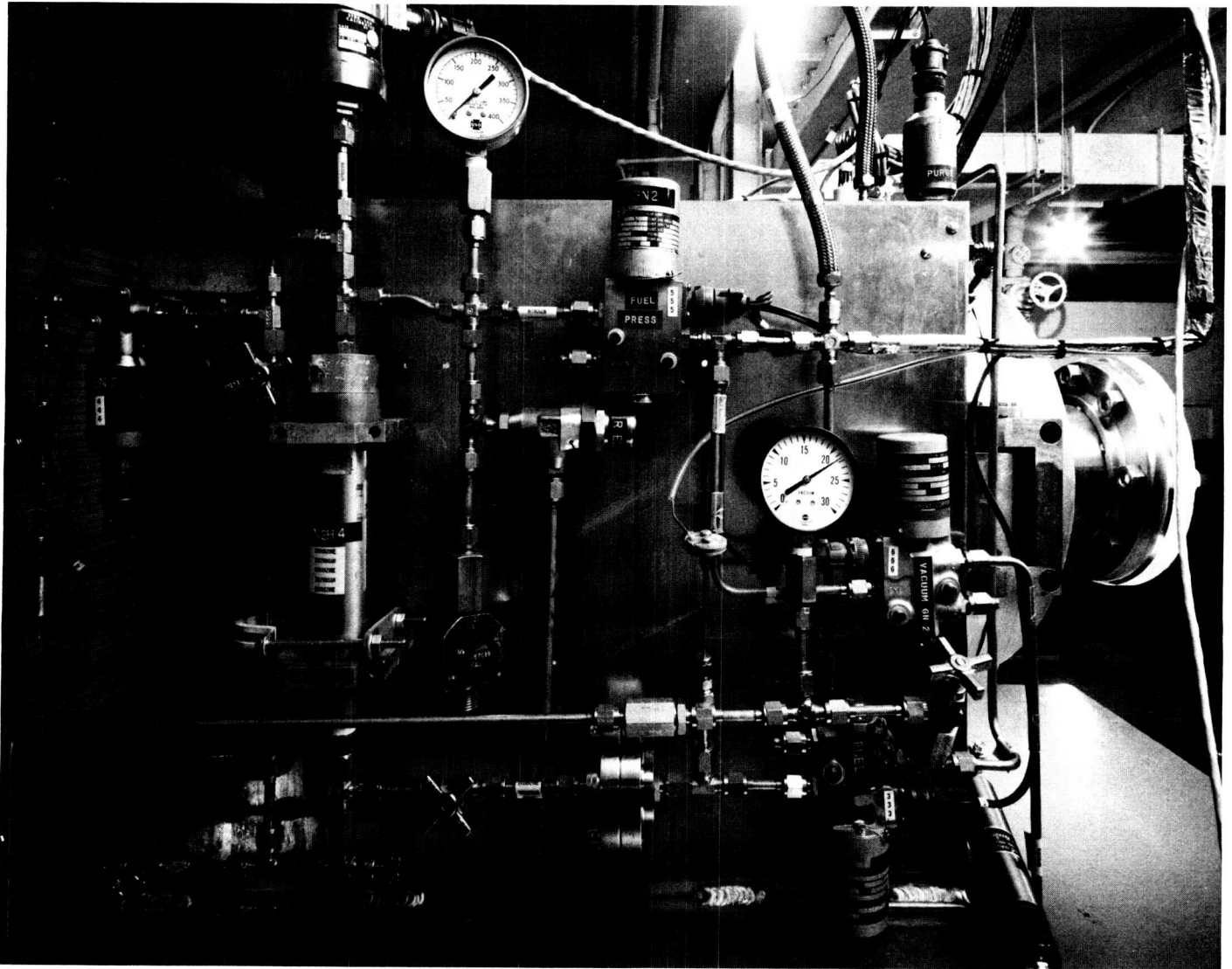
Fig. 46. Hydrazine propellant feed system, Test Cell G

was employed. Differential pressure across a calibrated pressure-dropping device was also used to determine steady-state flowrates and was the only means employed to determine total flow during a pulse. After experience had been gained with both methods of flowmetering, it was felt that the differential pressure technique was also a more precise steady-state flow indication. The pressure-dropping devices used were of two types: (1) a coiled length of capillary tubing (the same tubing used in the fabrication of the 0.22-N (0.05-lb$_f$) thruster propellant feed/thermal standoff tube), and (2) a Lee Company Viscojet Model 38VL5-CM. (For later tests, a Model 38VL3-CM was used.) The latter is a patented fluid-resistance device comprising a stack of discs with chemically etched passages configured to generate large ex-

pansion and vorticity losses. Details of the Viscojet device are given in a later section.

2. Vacuum Test Facility. Test operations for the TOPS APS were relocated from Test Cell G to the Vacuum Test Facility in January 1970, where a larger test chamber and higher-capacity vacuum pumping system had been installed for this program. With a test chamber volume of 2.8 m^3 (100 ft^3) and a pumping capacity of 2.42 m^3/s (5100 ft^3/min) at 10 torr, it easily met the requirements of the small 0.44-N (0.1-lb$_f$) monopropellant thrusters. The test cell on the West side of the facility was selected as the relocation site. The vacuum test chamber as installed in the reinforced concrete test bay is shown in Fig. 48. It is a double-walled, cylindrical steel chamber 1.22 m (4 ft) in

Fig. 47. Schematic diagram of thruster test assembly, Test Cell G

diameter by 2.44 m (8 ft) in length. Mounted horizontally, the chamber vacuum exhaust is at one end, and a full-size entry door mounted on a rail carriage is located at the other. Two additional large access ports with viewing windows are located on each side of the chamber.

The vacuum pumping system, shown in Fig. 49, consists of two 1.09-m³/s (2310-ft³/min) positive displacement, lobe-type, rotary booster pumps with two 0.4-m³/s (850-ft³/min) rotary piston, high-vacuum second-stage pumps. These pumps, connected in a series-parallel arrangement, have an ultimate vacuum of 2 × 10⁻³ torr. Either side of the pumping system has sufficient capacity to maintain a vacuum level of 0.4 torr, with an 0.44-N (0.1-lb$_f$) thruster operating in a steady-state mode and about 0.02 torr operating in a 0.1-s ON and 0.9-s OFF pulsed mode duty cycle. A curve of pumping speed as a function of pump inlet pressure for the vacuum pumping system is shown in Fig. 50.

The complete vacuum pumping system is controlled remotely from the operation console in the control room. All vacuum valves are electrically controlled and shop-air operated. There are automatic interlocks on pump controls which sequence the pump motors and vacuum valves during normal startup and shutdown. Safety interlocks protect the pumps in normal operation against failures of the lubricating system, the water cooling system, the air control system, and excess temperature. There are also safety interlocks between the vacuum pumping system, the test chamber, and the test propellant system. The vacuum test

chamber can be filled up to atmospheric pressure using either ambient air or gaseous nitrogen.

The hydrazine feed system used in the Vacuum Test Facility is similar to the one used in Test Cell G, as shown in Fig. 51. The propellant tank is twice as large, having a nominal volume of 1000 cm³ (1 liter or 61 in.³). The Viscojet ΔP flowmeter and the Omniflow turbine flowmeter were still used as the primary and secondary means of measuring propellant flowrate. Two additional methods of metering flow attempted were a positive-displacement piston flowmeter and a remote indicating rotometer. The piston flowmeter, which was made at JPL, proved to have excessive frictional drag with either ethylene propylene rubber or teflon O-rings, and was therefore not reliable. Alternate sealing techniques are being investigated, including Omni-Seals and Ball-Seals. The rotometer was a Mark X flowmeter manufactured by Ramapo. There were some initial difficulties in obtaining an output signal in the lower 20% of the 1.165×10^{-6} m³/s (0-70 cm³/min) flow range, so the meter was rebuilt. The primary concern with this float-type meter is that a small perturbation in flow stability sets up oscillations (bobbing motion) in the float level which damp out very slowly. However, calibration in stabilized flow with hydrazine has shown the flowmeter to be reasonably accurate.

A major improvement in this propellant system has been the incorporation of latching solenoid valves (V_2 and V_3 in Fig. 51) in place of standard 28-V dc solenoid valves to serve as isolation and safety backup valves in the primary feed line. At the low flowrates encountered in 0.22 to 0.44 N (0.05 to 0.1 lb$_f$) thruster testing, the standard normally-closed (energize to open and hold open) solenoid valves continuously heated the propellant. Measured temperatures up to 49°C (120°F) were not unusual for long steady-state runs. The latching solenoid valves, which require only a momentary pulse of electrical energy to change position (no external power to hold position), do not add heat to the propellant in the lines.

Propellant temperature conditioning is accomplished in this system by circulating a preconditioned mixture of water and ethylene glycol through an enclosure surrounding the 5-μm (absolute) stacked-disc line filter and Viscojet element. Both of these standard system components have a large surface area in contact with the propellant and serve readily as heat exchangers. The heat exchanger fluid is temperature-conditioned in a small, portable environmental chamber to the level required to provide the thruster with propellant ranging from 4.5 to 49°C (40 to 120°F). A small circulating pump and reservoir complete this system, as shown in Fig. 51.

Fig. 48. Vacuum test chamber, Vacuum Test Facility

Fig. 49. Vacuum pumping system, Vacuum Test Facility

Fig. 50. Typical pumping capacity curves for vacuum pumping system

Priming of the propellant system to remove trapped gases is one of the more difficult tasks of these small thruster systems. In addition to the water ejector pump on the vacuum purging manifold in Fig. 51, it was necessary to include a small mechanical pump with a liquid nitrogen cold trap for complete removal of initial system gas. Also, for a system pressurized by gas, where the pressure level is changed frequently to satisfy varying test conditions, the gas dissolved in the saturated propellant comes out of solution whenever the pressure is reduced and becomes trapped in any pockets or high points in the system (see Fig. 34). Frequent bleeding of the high points through valves succeeded in eliminating most of this gas. However, there are always some dead-ended pockets, such as pressure transducer cavities, which can not be bled and must be oriented within the system for self-purging. The most difficult component to purge in this system proved to be the differential pressure transducer across the Viscojet, which is used as the primary flow-measuring instrument. As gas builds up, its response becomes noticeably sluggish with time, especially during pulse mode tests, and occasional repriming was required. A specially modified Statham Model PM280 transducer with pressure taps located at the top edge of both diaphragm cavities has been purchased but did not arrive in time for this test program. It is believed that this change

will provide a simple self-purging capability and reduce the response problem.

The on-site storage and transfer of hydrazine for the test system was simplified through the incorporation of a small (0.0056-m³ = 1.5-gal), portable tank system, eliminating the repeated handling required for the larger (0.208-m³ = 55-gal) shipping drum. Mounted on casters, the dual-sided system with the tank, sight glass, and gas pressurization system on one side and a recirculating pump, filtration, and sampling system on the other, is shown in Figs. 52 and 53. All components, tubing, and fittings are made of 300-series stainless steel. The recirculating pump, driven by an air motor, provides a closed-loop filtering capability through one or both of the 10-μm (absolute) stacked-disc-type filters mounted in parallel, as shown in Fig. 54. The hydrazine can be transferred using either the nitrogen gas pressurization of the holding tank or by using the recirculating pump. Liquid samples can be drawn off as required for analysis. The pump discharge pressure has a maximum capability of 92.05 × 10⁵ N/m² (30 psid), and the discharge temperature is arbitrarily redlined at 49°C (120°F) for safety.

3. Instrumentation. The instrumentation systems used in both Test Cell G and the Vacuum Test Facility were

Fig. 51. Propellant system schematic diagram for small thruster tests
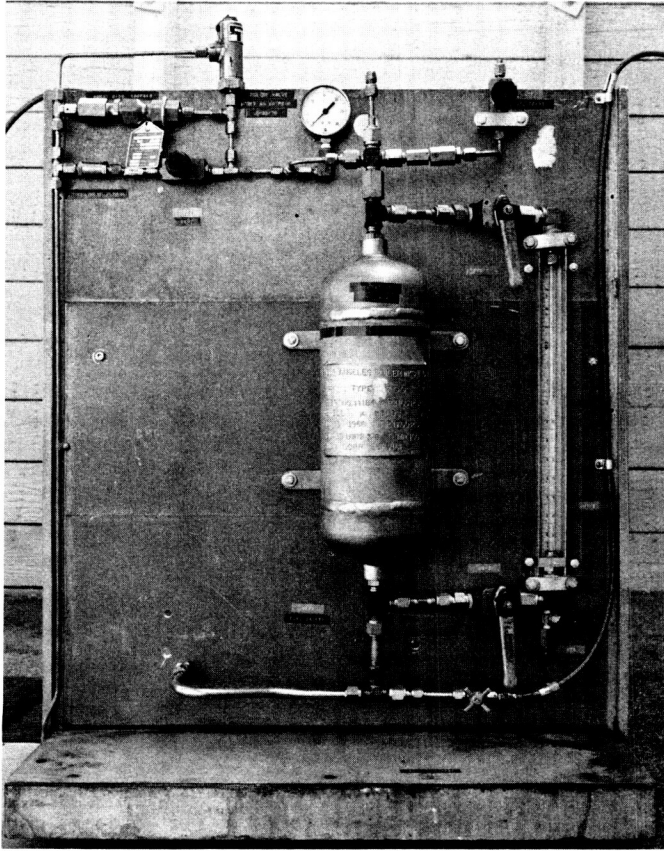
Fig. 52. Portable fuel storage and transfer system,
propellant supply tank

Fig. 53. Portable fuel storage and transfer system,
air-driven turbine/fuel pump and filters

basically similar. They consisted of the test item and facility equipment transducers, the related signal-conditioning system, and the recording equipment, along with the required cabling and patching network for system integration. Both the test instrumentation and the recording equipment were maintained in a controlled environment to minimize instrumentation drift and signal noise interference.

Transducers for the test propellant system were selected on the basis of proven reliability, compatibility, and cleanability so as to prevent contamination of the hydrazine. The pressure transducers used are listed below:

(1) Stathan PA-208-TC, 0 to 3.45×10^6 N/m² (0–500 psia)

(2) Statham PL-280-TC, 1.73×10^6 N/m² (± 250 psid)

(3) Taber 176, 0 to 3.45×10^6 N/m² (0–500 psig)

(4) Taber 217, 0 to 1.38×10^6 N/m² (0–200 psia)

(5) CVC Magnavac, 0–500 torr

The volumetric flowrate transducers were:

(1) Flow Technology Omniflow FTM-0.4-LJS

(2) Ramapo Mark X

(3) Lee Company Viscojet 38VL3CM (used in conjunction with the Statham PL-280-TC differential pressure transducer)

The type-K (chromel–alumel) thermocouples were used for immersion into the propellant and heat-transfer fluids and were spot-welded to the outer surfaces of the thruster chamber body and nozzle.

The pressure transducers were calibrated in the JPL Calibration Laboratory, whose procedures are traceable to the National Bureau of Standards. The flowrate transducers were calibrated both with water and with hydrazine. (The hydrazine calibration was performed in the test system.) Thermocouples were not calibrated, but were made of wire obtained from spools certified by the JPL Calibration Laboratory.
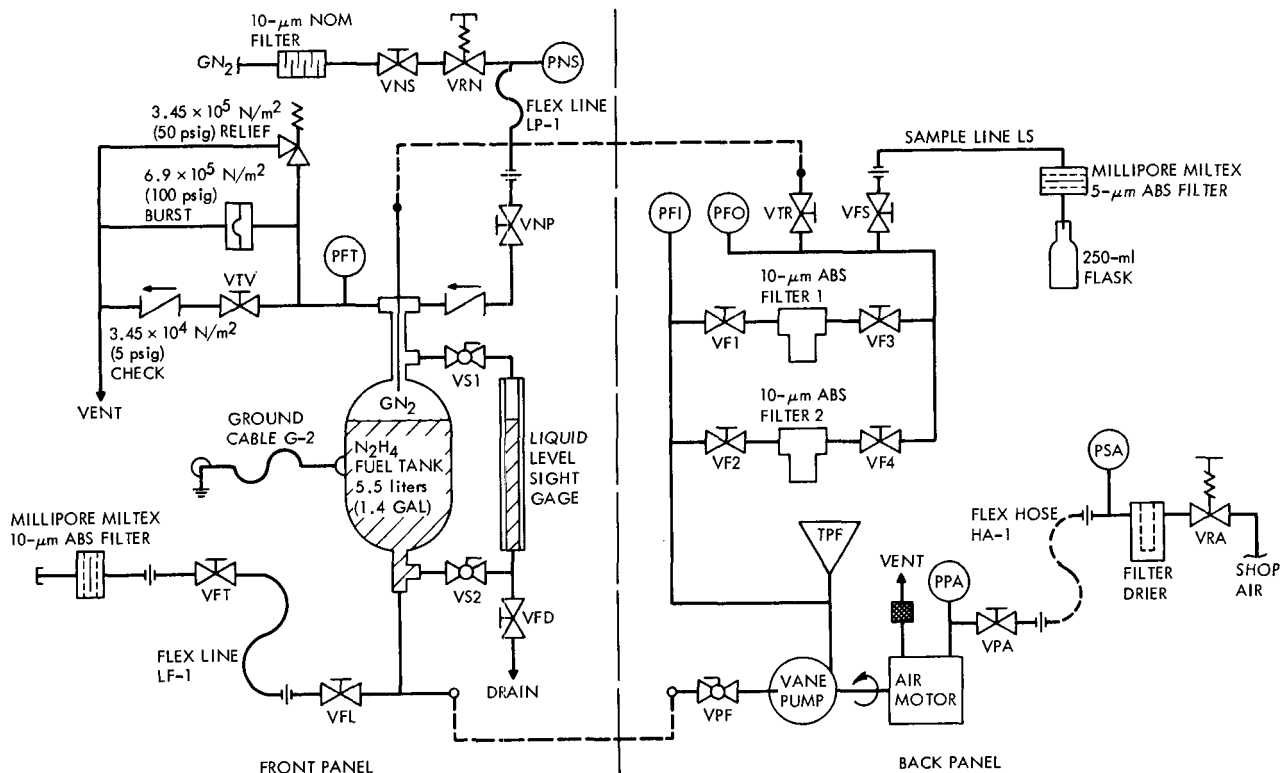
Fig. 54. Portable fuel storage and transfer system schematic flow diagram

The signal-conditioning equipment included the following units:

(1) Dynamics 6496 amplifier

(2) Dynamics 7506 amplifier

(3) Dynamics 6343 A bridge supply

The recording instruments were divided between the low-speed type for slow transients or steady-state data and the high-speed type for transient data. Critical parameters were recorded on both types for redundancy. The low-speed recorders were the Leeds and Northrup Type G strip charts and the Mosely 680 strip charts. The high-speed recorder was a 12-channel Honeywell Model 1912 oscillograph.

Data accuracy was improved by recording critical parameters used in performance calculations on the low-speed recorders. The reported thruster performance was obtained at steady-state operating condition. A listing of instrumentation test parameters, recording instruments, and the results of an error analysis calculated using the root-sum-square (RSS) method are presented in Table 14.

4. Propellant sampling. Liquid hydrazine samples were obtained from each shipping drum before the storage

and transfer system was filled. Other samples were taken from the storage and transfer system both after the propellant had been recirculated through the system filters for several hours and after long periods of storage. These samples were then analyzed. As a minimum requirement, the hydrazine had to conform to the Military Specification, MIL-P-26536C. In addition, ash samples of the hydrazine were analyzed for metallic ions present in solution. A Millipore Mitex (Teflon) filter was used to collect suspended particles. The samples were then read for particulate count and occasionally reduced to an ash for mass spectrometer analysis for metallic elements in suspension. An example of a hydrazine propellant analysis is presented in Table 15.

The hydrazine decomposition products were sampled from each thruster by the method described in Section II-H.

J. TOPS APS Feed-System Component Evaluations

When the system tradeoffs indicated that TOPS would use small liquid hydrazine catalytic thrusters for attitude propulsion, the solenoid-actuated valves, the propellant-metering device, and the filter were designated as critical components because of deficiencies known to exist in

Table 14. Summary of APS test instrumentation parameters

Symbol	Parameter description	Units	Full scale	Recorder	Maximum error
P_{ft}	Pressure, fuel tank	N/m² (psia)	3.448×10^6 (500)	Strip-chart, O-graph	19.3×10^3 (2.8)
P_{fc}	Pressure, fuel capillary or Viscojet inlet	N/m² (psia)	2.758×10^6 (400)	O-graph	79.9×10^3 (11.6)
ΔP_c	Differential pressure, capillary or Viscojet	N/m² (psid)	2.069×10^6 (300)	Strip-chart, O-graph	25.5×10^3 (3.7) 61.4×10^3 (8.9)
P_{fi}	Pressure, fuel injector inlet	N/m² (psia)	2.758×10^6 (400)	O-graph	79.9×10^3 (11.6)
P_{c1}	Pressure, thrust chamber (Statham)	N/m² (psia)	3.448×10^6 (500)	O-graph	101.4×10^3 (14.7)
P_{c2}	Pressure, thrust chamber (Taber)	N/m² (psia)	1.379×10^6 (200)	Strip-chart, O-graph	8.9×10^3 (1.3) 39.4×10^3 (5.7)
P_{vc}	Pressure, vacuum test chamber	N/m² (psia)	186 (0.027)	O-graph	0.006 (0.001)
T_{fl}	Temperature, fuel line	°C (°F)	94 (200)	Strip-chart, O-graph	7.6 (4.2) 16.5 (9.0)
T_{fc}	Temperature, fuel capillary or Viscojet inlet	°C (°F)	94 (200)	Strip-chart, O-graph	7.6 (4.2) 16.5 (9.0)
T_{cl}	Temperature, thrust chamber lower wall	°C (°F)	1094 (2000)	Strip-chart, O-graph	12.3 (18.0) 40.1 (58.5)
T_{ns}	Temperature, nozzle throat surface	°C (°F)	1094 (2000)	Strip-chart, O-graph	12.3 (18.0) 40.1 (58.5)
m_O	Mass flowrate, Omniflow turbine meter	g/s (mlbₘ/s)	0.395 (0.870)	O-graph	0.0015 (0.0034)
m_V	Mass flowrate, Viscojet or capillary tube device	g/s (mlbₘ/s)	0.395 (0.870)	Strip-chart, O-graph	0.0022 (0.0048) 0.0053 (0.0116)
m_R	Mass flowrate, Ramapo float meter	g/s (mlbₘ/s)	0.395 (0.870)	O-graph	0.0109 (0.024)

the state of the art. The performance criteria and operating conditions which generated the most concern were

(1) Material/propellant compatibility on long-duration missions.

(2) Magnetic interference from solenoids.

(3) Physical size, mass, and power required.

(4) Reliability and consistency.

The solenoid-actuated valves were selected for the primary effort since the performance of these components is essential to thruster operation and the balance of the propellant feed system design is influenced by valve characteristics.

1. Solenoid-actuated valves. Two valves are utilized to control the propellant flow to each APS thruster: a normally-closed valve for normal thruster operation and

a bi-stable (latching) valve for redundant propellant shutoff. When thruster operation is required, the latching valve is opened to provide pressurized propellant to the inlet of the normally-closed valve. Thruster operation is initiated when electrical power is supplied to the normally-closed valve and terminated when the power is removed. During periods when thruster operation is not required, the latching valve can be closed to provide a redundant seal. General design criteria for the APS solenoid-actuated valves are:

(1) Construction materials must be compatible with hydrazine, especially materials in the flow path (wetted surfaces). Titanium and aluminum are the most desirable materials. Stainless steel (CRES) is satisfactory for corrosion resistance, and tests are being conducted to establish hydrazine decomposition rates with various CRES materials. Final flight mission definition and propulsion subsystem configurations will determine whether the hydrazine

Table 15. Example of hydrazine propellant analysis

Liquid sample			
Gas chromatograph		Mass spectrometer	
Chemical	Mass percent	Element	Mass percent[a]
N_2H_4	98.73	Fe	27.8
NH_3	0.43	Cr	2.2
H_2O	0.46	Ni	1.3
Aniline	0.28	Cu	0.9
Ash	0.10		

Filter sample			
Particulate count		Mass spectrometer	
Micron size	Number	Element	Mass percent[b]
6–10	53 (11)[c]	Fe	46
11–25	121 (46)	Mn	21
26–50	47 (30)	Cr	16
51–100	11 (9)	Cd	5
101–150	1 (3)	Al	5
> 150	— (1)	Ni	5

[a] Based on an 0.80-g ash residue from a 78.37-g liquid sample.
[b] Based on an 0.00010-g ash residue from a Mitex filter pad and corrected for baseline element in a control filter pad sample ash.
[c] Numbers in parentheses are typical of propellant that had been recirculated by the storage and transfer system prior to use.

decomposition rates from contact with CRES components can be tolerated.

Construction materials must provide satisfactory performance during and after exposure to the radiation environments imposed by the radioisotope thermoelectric generators, as well as radiation encountered in space and during planetary flybys.

(2) A "soft" seat using an elastomeric seal is desirable to minimize the probability of internal leakage, but materials must be selected with care to avoid using a polymer sensitive to radiation damage. A "hard," all-metal seat for the normally-closed valves would be desirable from a durability standpoint, but sensitivity to particulate contamination makes this design concept less reliable. A compromise with a soft seat in the latching valve and a hard seat in the normally-closed valve may represent an optimum configuration.

Satisfactory seats using TFE Teflon for the seal material are available, but these seals are very diffi-

cult to fabricate in the smaller sizes, where allowable tolerances in seat dimensions are so small that verification of seat integrity by inspection is questionable. Use of recently discovered elastomers which are more resilient than TFE Teflon may be the solution to this seat-seal fabrication difficulty. Materials that are currently being evaluated are AF-E-102 (HYSTL-filled ethylene propylene terpolymer) and a copolymer of TFE Teflon and perfluorovinylmethyl ether ("new" Teflon). Both of these compounds can be molded and are compatible with hydrazine. (Details are covered in a later section.)

(3) The interior must be cleanable after assembly. Cavities which could entrap propellant and flushing fluid must be minimized. Particle generation by abrasion due to relative motion between surfaces in the propellant flow path must be avoided.

(4) Generated magnetic fields must be kept to the lowest level commensurate with required valve performance. Required permanent fields must remain constant or be predictable throughout valve operational life. The quantity of magnetic materials must be minimized.

(5) The electrical power required for valve operation must be minimized.

(6) The Envelope for all valves and volume downstream of the seat seal ("dribble" volume) for the normally-closed valves must be minimized.

(7) All external leak paths and coil cavities must be sealed by welding.

(8) A position (opened or closed) indicator must be incorporated on all latching valves.

Using these criteria to establish valve requirements, an industry search was conducted to determine the availability of suitable solenoid-actuated valves for the TOPS APS.

Normally-closed valve survey. A source information request was sent to 89 valve manufacturers to assess the capability of existing solenoid-actuated valve designs. While the industry response was being evaluated, contacts were made with five additional vendors who had previously provided valves for aerospace programs. The following is a brief summary of the results:

(1) Evaluation of the responses from the 19 vendors who responded disclosed only eight valve designs

that were suitable for TOPS APS, and only five of the eight were readily available for initial feasibility studies.

(2) None of the valve designs, as proposed, were suitable for flight. The proposed valve configurations were categorized by their consideration as flight candidates.

(3) "Off-the-shelf" valves were rated for use during initial feasibility demonstrations.

(4) A recommendation for a design study to optimize the APS normally-closed valve configuration was made. Areas to be emphasized were materials, fabrication techniques, size, power, and seat design.

As APS requirements became more specific, detailed requirements for the normally-closed valve were generated. The performance and design criteria shown in Table 16 illustrate the current status of normally-closed valve requirements.

Bi-stable (latching) valve survey. A source information request was sent to 33 valve manufacturers to assess the capability of existing solenoid-actuated latching-valve designs. A latching-valve design which was used on the Intelsat IV program was also included in the evaluation. A brief summary of the results follows:

(1) Evaluation of the submittals from the nine vendors who responded disclosed only three designs that

Table 16. TOPS APS propellant control valve performance and design criteria

Characteristic	Dimension	Requirement
Pressure, operating	N/m² (psig)	2.758×10^6 (400) (maximum)
proof	N/m² (psig)	5.516×10^6 (800) (minimum)
burst	N/m² (psig)	1.1032×10^7 (1600) (minimum)
Leakage, external, He[a]	scc/s	10^{-7} (maximum) from 0 to 2.758×10^6 N/m² (0 to 400 psig)
internal, GN_2	scc/s	2.8×10^{-4} (maximum) from 0 to 2.758×10^6 N/m² (0 to 400 psig)
Flowrate, N_2H_4	kg/s (lb_m/s)	4.54×10^{-4} (1×10^{-3})
Differential pressure	N/m² (psid)	3.4×10^4 (5) (maximum)
Temperature, operating	°C (°F)	4.4 to 71 (+40 to +160)
Voltage, operating	V dc	20 to 32
pull-in	V dc	15 (maximum) with 2.758×10^6 N/m² and 71°C (400 psig and +160°F)
drop-out	V dc	5 (minimum) at ambient pressure and 4.4°C (+40°F)
Power	W	4 (maximum) at 30 V dc and 21°C (+70°F)
Response, opening with 20 V dc	ms	15 (maximum) with 2.758×10^6 N/m² and 71°C (400 psig and +160°F)
closing from 30 V dc	ms	10 (maximum) with rated flow at 4.4°C (+40°F)
Life	cycles	10^6 (minimum)
Port, inlet	m (in.)	3.18×10^{-3} dia $\times$ 3.2×10^{-4} wall (1/8-dia $\times$ 0.015 wall)
outlet	m (in.)	1.59×10^{-3} dia Swagelok $\times$ 1.6×10^{-4} (1/16-dia Swagelok 0.010 ID)
Electric connector	pin	To be determined
Mounting	—	Optional
Material, construction	—	Ti-6Al-4V in flow path
seat (hard)	—	Tungsten carbide
seat (soft)	—	AF-E-102 (EPT)
Weight	N (lb_f)	1.8 (0.4) (maximum)
Dielectric strength	μA	100 (maximum) at 600 V ac RMS (60 cycles)
Insulation resistance	MΩ	100 (minimum) at 500 V dc
Envelope	—	To be determined
Flow media	—	Hydrazine, isopropyl alcohol, water, helium, and nitrogen

[a]Leakage to be measured with a mass spectrometer-type leakage detector, and the recorded value to be the largest rate indicated during a test period of at least 30 min.

were suitable for TOPS APS, and only two of the designs were readily available. A fourth design was satisfactory for initial feasibility demonstrations but was too large for APS application.

(2) None of the valve designs, as proposed, were suitable for flight. The proposed configurations were categorized by their consideration as flight candidates.

(3) "Off-the-shelf" valves were rated for use during initial feasibility demonstrations.

(4) A recommendation for a design study to optimize the APS latching-valve configuration was made. Areas to be emphasized were materials, fabrication techniques, size, power, and seat design.

As APS requirements became more specific, detailed requirements for the latching valve were generated. The performance and design criteria shown in Table 17 illustrate the current status of latching-valve requirements.

Valve test program. The valve test program was structured to identify deficiencies and evaluate promising design concepts. The program was divided into four basic categories:

(1) Valve testing with thrusters.

(2) Short-term (1 to 9 months) exposure to hydrazine, coupled with cycle-life tests to evaluate endurance to repeated actuations.

(3) Long-term (greater than 1 year and continuing) exposure to hydrazine with intermittent actuation to evaluate performance after periods of inactivity.

(4) Separate seat-seal studies using "work-horse" valves for seat endurance testing.

Table 17. TOPS APS propellant shutoff valve performance and design criteria

Characteristic	Dimension	Requirement
Pressure, operating	N/m² (psig)	2.758×10^6 (400) (maximum)
proof	N/m² (psig)	5.516×10^6 (800) (minimum)
burst	N/m² (psig)	1.1032×10^7 (1600) (minimum)
Leakage, external, He[a]	scc/s	10^{-7} (maximum) from 0 to 2.758×10^6 N/m² (0 to 400 psig)
internal, GN_2	scc/s	2.8×10^{-4} (maximum) from 0 to 2.758×10^6 N/m² (0 to 400 psig)
Flowrate, N_2H_4	kg/s (lb$_m$/s)	4.54×10^{-4} (1×10^{-3})
Differential pressure	N/m² (psid)	3.4×10^4 (5) (maximum)
Temperature, operating	°C (°F)	4.4 to 49 (+40 to +120)
Voltage, operating	V dc	20 to 32
pull-in	V dc	15 (maximum with 2.758×10^6 N/m² and 49°C (400 psig and +120°F)
drop-out	V dc	15 (maximum) at ambient pressure and 49°C (+120°F)
Power	W	4 (maximum) at 30 V dc and 21°C (+70°F)
Response, opening with 20 V dc	ms	15 (maximum) with 2.758×10^6 N/m² and 49°C (400 psig and +120°F)
closing with 20 V dc	ms	15 (maximum) with rated flow at 4.4°C (+40°F)
Life	cycles	5000 (minimum)
Port, inlet and outlet	m (in.)	3.18×10^{-3} dia $\times$ 3.2×10^{-4} wall (1/8-dia $\times$ 0.015 wall)
Electric connector	pin	To be determined
Mounting	—	Optional
Material, construction	—	Ti-6Al-4V in flow path
seat (soft)	—	AF-E-102 (EPT)
Weight	N (lb$_f$)	1.8 (0.4) (maximum)
Dielectric strength	μA	100 (maximum) at 600 V ac RMS (60 cycles)
Insulation resistance	MΩ	100 (minimum) at 500 V dc
Envelope	—	To be determined
Flow media	—	Hydrazine, isopropyl alcohol, water, helium, and nitrogen

[a]Leakage to be measured with a mass spectrometer-type leakage detector, and the recorded value to be the largest rate indicated during a test period of at least 30 min.

Most of the overall TOPS valve evaluation centered around valves in the APS size range. The problems associated with solenoid-actuated valves are common to valves of all sizes, but the solutions to the problems are more difficult in the smaller sizes. With this philosophy guiding the choice of test specimens, any existing small valve which showed promise was integrated into some phase of the test program. JPL experience with comparable valves during other programs was evaluated and utilized where applicable to supplement test results and point out existing deficiencies in available data.

A listing of valves tested is presented in Table 18. The individual valve tests are described below.

Allen P/N 13940-02. This soft-seat valve is a normally-closed, coaxial solenoid, poppet type. The valve was designed for larger flowrates than necessary for the APS. Several of these valves had been purchased for another JPL program and were modified for use as thruster test facility valves by replacing the original seat with a design using ethylene propylene rubber (EPR). Valve performance was satisfactory, but usage was limited because of excessive heating of the propellant at the very low APS flowrate.

Hydraulic Research P/N 48000360. This hard-seat valve is a normally-closed, external-torque-motor, flapper type.

Table 18. Valves evaluated in valve test program

Vendor	Part number
Normally-closed valves	
Allen	13940-02
Hydraulic Research	48000360
	39006000
Marquardt	228511, 228683, 228684
	X24572
MOOG	010-58176-1
	010-58723-1
	010-49325-2
Parker	5696050
Rocketdyne	407559
	409402
Wright	15548
Bi-stable (latching) valves	
Carleton	2217-07-2-1
Consolidated Controls	71814-1
Marquardt	T-8700
	X28051

The valve was designed for the transtage 110-N (25-lb$_f$) thruster and as such was larger than necessary for the APS. However, Hydraulic Research loaned the valve to JPL for evaluation of the hard (tungsten carbide) seat design. The valve was used for the TOPS TCPS feasibility demonstration module (Ref. 7) to control thruster operation. Performance was satisfactory, with no indication of hydrazine leakage past the hard seat, as determined by catalyst bed warming for the period between engine firings during the evaluation program.

Hydraulic Research P/N 39006000. This hard-seat valve is a smaller version of the external-torque-motor-type valve. The valve was designed for low-pressure (1.72 × 10^5 N/m^2 = 25 psig) GN$_2$ service and has a larger seat than necessary for the APS flowrate. The valve was loaned to this program after it had accrued approximately 60,000 cycles during an evaluation program of gaseous nitrogen thruster control valves. Valve performance was satisfactory during and after the accumulation of 250,000 cycles over a 10-month exposure period in the hydrazine flow test setup. The test conditions represented an extreme overtest since the valve design operating pressure was only 1.72 × 10^5 N/m^2 (25 psig) and all testing was performed at 2.06 × 10^6 N/m^2 (300 psig). The valve was proof-pressure-tested to 4.12 × 10^6 N/m^2 (600 psig) and leak-tested as high as 2.75 × 10^6 N/m^2 (400 psig). Prior to the exposure/cycle test, the valve leaked 1.67 scc of GN$_2$ per second at an inlet pressure of 2.75 × 10^6 N/m^2 (400 psig). During the test, there was no evidence of hydrazine leakage, and after the test, the valve was "bubble-tight" when tested with GN$_2$. Whatever caused the pretest leakage was either flushed from the seat contact area or dissolved by the hydrazine during the exposure test. The valve is scheduled for disassembly and inspection, and the seat condition will be carefully evaluated.

Marquardt P/N 228683 (Apollo). This soft-seat valve is a normally-closed, coaxial solenoid, poppet type which uses TFE Teflon for the seat seal. The valve was designed for larger flowrates than required for the APS, but the seat design was suitable for seat-seal studies and the valve could also have been used for TCPS feasibility demonstrations. These valves gave satisfactory performance during all testing, which consisted of

(1) TCPS thruster evaluations (one valve).

(2) TCPS feasibility demonstrations (one valve).

(3) Mariner Venus-Mercury thruster evaluations (two valves).

(4) Long-term (greater than 1 year and continuing) storage at the JPL Edwards Test Station (ETS) (one valve).

(5) Seat-seal studies (four valves).

Previous experience with these valves during the Apollo program provided a high degree of confidence in the thruster performance evaluations, as well as being an excellent baseline for assessing the merits of design modifications. One valve was installed as a hydrazine sampling valve in a propellant tank test setup. This valve has been in "test" for approximately 1 year and is periodically actuated to draw a hydrazine sample from the tank. The valve is exposed to uncontrolled ambient temperatures ranging from near $-18°C$ ($0°F$) during the winter nights to above $49°C$ ($+120°F$) during the summer days. This "test" will continue until the tank test is terminated or the valve fails.

Several seat modifications were tested in four of these valves for seat material evaluations. Detailed results of this study are presented in Section K.

Marquardt P/N X24572. This hard-seat valve is a normally-closed, external solenoid, magnetically linked, dual-poppet type that was designed for bipropellant thrusters. The valve was modified by Marquardt for use as the test item for elastomeric seal material evaluations. Performance of the valve during the seal tests was satisfactory for many millions of cycles. Use of the magnetically linked poppets allowed two seat-seal samples to be evaluated simultaneously, making possible a comparison of different materials under identical test conditions and doubling the number of samples that could be evaluated in a given test. The design of the flexures which support the poppets in this valve was also used in Marquardt's bi-stable (latching) valves, P/N X28051. Details of the test results are presented in Section K.

MOOG P/N 010-58176-1. This soft-seat valve is a normally-closed, external-torque-motor, mechanically linked, dual-flapper type that is used on the Mariner Mars 1971 (MM'71) bipropellant thruster. The valve has provided satisfactory performance during the MM'71 program, which includes the flight of Mariner 9. A similar valve was used in the Minuteman PBPS program. The data from these programs were utilized to supplement data obtained from similar valves during TOPS evaluations. The valve uses TFE Teflon for the seat seal.

MOOG P/N 010-58723-1. This soft-seat valve is a normally-closed, coaxial solenoid, poppet type which uses

TFE Teflon for the seat seal. The poppet is constrained radially by flexures that eliminate abrasion due to sliding surfaces. This valve was specifically designed for monopropellant thrusters in the APS range and could, with minor modifications, be used for flight if the catalytic effects of corrosion-resistant steel (CRES) can be tolerated. The valves were installed on Rocket Research thrusters purchased for APS thruster evaluations. Testing of this valve was programmed after completion of the thruster tests. This limited the total hydrazine exposure time. The valve was installed in the hydrazine flow test setup in December 1971. Valve performance was satisfactory during and after the thruster testing, and throughout 250,000 subsequent cycles over a 5-week period of hydrazine exposure.

MOOG P/N 010-49325-2. This soft-seat valve is a normally-closed, external-torque-motor, flapper type which uses TFE Teflon for the seat seal. Two of these valves were used in series on the transtage 110-N (25-lb$_t$) monopropellant hydrazine thrusters evaluated for the TOPS TCPS (Ref. 7). Valve performance was satisfactory during evaluation of the transtage thruster performance capability.

Parker P/N 5696050. This soft-seat valve is a normally-closed, coaxial solenoid, "clapper" type which uses TFE Teflon for the seat seal. The clapper is supported radially by a Belleville spring that provides the return force when the solenoid is de-energized. The valve was specifically designed for monopropellant thrusters in the APS range and could, with minor modifications, be used for flight if the catalytic effects of CRES in contact with hydrazine can be tolerated. These valves were installed on the Hamilton Standard thrusters that were procured for APS thruster evaluation. Testing of the valve was programmed subsequent to completion of the thruster tests, which limited the hydrazine exposure time. The valve was installed in the hydrazine flow test setup in December 1971. Valve performance was satisfactory during and after the thruster testing and throughout 250,000 subsequent cycles over a 5-week period of hydrazine exposure.

Rocketdyne P/N 407559. This soft-seat valve is a normally-closed, coaxial solenoid, poppet type which uses an FEP Teflon seat seal. The valves were built for the NASA Gemini program and were used to control propellant flow to 110-N (25-lb$_t$) bipropellant thrusters. The valve envelope is small, but power requirements are high to provide the fast response that was required for pulsing operation of the Gemini thrusters. The valves were used during testing of the JPL-designed, 0.22-N (0.05-lb$_t$) thrusters and for operation of these thrusters during the

Celestarium tests. Special precautions were taken to ensure that the small-capacity, 2-μm (nominal) integral filter was not overloaded with particulate contamination. Valve performance was satisfactory during all truster testing.

Rocketdyne P/N 409402. This valve is virtually identical to the P/N 407559 valve. The primary differences are in the mounting provisions and an increase in the integral filter capacity, which has a rating of 10 μm (nominal). This valve was used on a later version of the Gemini 110-N (25-lb$_t$) bipropellant thruster, which was also produced for the Manned Orbiting Laboratory program. The valve was tested for 250,000 cycles over a 10-week period of hydrazine exposure, and valve performance was satisfactory.

Wright P/N 15548. This soft-seat valve is a normally-closed, coaxial solenoid, poppet type which uses EPR (Parker Compound E-515-8) for the seat seal. The valve design was not satisfactory for long-duration exposure to hydrazine because of swelling of the seat material and the use of electroless nickel (which is not compatible with hydrazine) on surfaces exposed to hydrazine. The EPR seal swelled sufficiently during one test to completely close the outlet on the S/N 024 valve, thus preventing flow when the valve was actuated. The failure was detected when the valve was actuated after 15 weeks of hydrazine exposure. Performance of another valve (S/N 022) appeared to be satisfactory while accruing 250,000 cycles over a 10-month period of hydrazine exposure; however, water-flow tests after this exposure indicated that the flow, with a pressure drop of 6.9 $\times$ 10^4 N/m^2 (10 psid), had decreased from 1.77 $\times$ 10^{-3} to 4.04 $\times$ 10^{-4} kg/s (3.9 $\times$ 10^{-3} to 8.9 $\times$ 10^{-4} lb$_m$/s) or, conversely, the pressure drop at 1.77 $\times$ 10^{-3} kg/s (3.9 $\times$ 10^{-3} lb$_m$/s) flowrate had increased from 6.9 $\times$ 10^4 to 3.65 $\times$ 10^5 N/m^2 (10 to 53 psig). When it was disassembled after the water-flow tests, the seat-seal appearance was found to be almost identical to that of the seal from valve S/N 024, which had failed by swelling. This evidenced change in flow area due to seal swell during long-term exposure to hydrazine tends to render EPR undesirable as a sealing material for hydrazine valves that would meter flow across the valve seat.

Two Wright valves were modified during the valve evaluation program. For valve S/N 023, which was modified prior to hydrazine exposure, the EPR seat seal was removed and replaced with a seal cut from "new" Teflon (Dupont Fluorelastomer LRU-448). The performance of this valve was satisfactory during and after the accumulation of 250,000 cycles over a 10-month period of hydrazine exposure. The flowrate after this hydrazine exposure was the same as it was before (1.77 $\times$ 10^{-3} kg/s = 3.9 $\times$ 10^{-3}

lb$_m$/s). Valve S/N 024 was modified by replacing the EPR seal with a seal cut from HYSTL-filled EPT (AF-E-102) and was reinstalled in the original test setup. The performance of the valve appears to be satisfactory after approximately 4 months of hydrazine exposure.

Carleton P/N 2217-07-2-1. This soft-seat valve is a mechanically latched, external solenoid, poppet type which uses TFE Teflon for the seat seal. The poppet is balanced by a CRES bellows, which also isolates the solenoid and prevents external leakage. A microswitch, actuated by the armature shaft, provides position indication. This valve was used for propellant (hydrazine) shutoff in the Intelsat IV feed system. Two of the valves were tested during the evaluation program—one at JPL, Pasadena, and the other during the TCPS feasibility demonstration at ETS (Ref. 7).

The performance of one valve during and after accumulation of 3100 cycles over a 26-week period of hydrazine exposure was satisfactory. An increase from 9 to 10.5 ms in opening response after 2700 cycles may be indicative of slight binding on the poppet shaft. The valve had exceeded the original endurance goal of 2000 cycles, and a decision was made after 3100 cycles to remove it from the endurance test and use it for the remainder of its life as a test facility shutoff valve. This shift in function will provide lengthy exposure to hydrazine, with intermittent actuation. Performance will be monitored for additional evidence of degradation.

Consolidated Controls P/N 71814-1. This soft-seat valve is a magnetically latched, external solenoid, poppet type which uses TFE Teflon for the seat seal. The poppet is balanced by CRES bellows, which also isolates the space actuator and prevents external leakage. A microswitch, actuated by the armature shaft, provides position indication. This valve was used for propellant (MMH and NTO) shutoff in the Apollo feed system. Several valves were tested at JPL during engineering evaluation of potential Viking Orbiter components. Data from this program are considered directly applicable to TCPS decisions (Ref. 7).

Marquardt P/N T-8700. This soft-seat valve is a magnetically latched, coaxial solenoid, poppet type which uses TFE Teflon for the seat seal. The valve was designed for interchange with the normally-closed valves which control the propellants (MMH and NTO) to the Apollo R4D 440-N (100-lb$_t$) thruster. The valve provides fast response and adequate flow for the TCPS within a small envelope. Although physically too large for direct APS application, it is believed that its design can be scaled down. This

valve uses the seat concept from the R4D valve, but experience with the rest of the design has been limited. The valve was built to demonstrate improved response for the R4D engine with associated power savings during steady-state operation. The design did not reach production status, and testing was limited to performance demonstration.

Marquardt P/N X28051. This soft-seat valve is a magnetically latched, coaxial solenoid, supported poppet type which uses AF-E-102 (HYSTL-filled ethylene propylene terpolymer) for the seat seal. The valve was designed for use as a shutoff valve in a hydrazine system. A similar valve was used to control the operating fluid (e.g., ammonia, nitrogen) to a resistojet thruster. Considerable test data have been accumulated, but the valve has not completed formal qualification for APS applications.

Three valves were procured by JPL to provide an appropriate latching valve for the APS. The valves were tested as follows:

S/N 001—hydrazine exposure and cycle test

S/N 002—hydrazine exposure test

S/N 003—vibration and H_2O leakage hydrazine feed system test

The performance of the S/N 001 valve was satisfactory throughout 250,000 cycles over a 10-week period of hydrazine exposure; however, valve poppet instability oscillation occurred during the final flow test, with 2.75×10^6 N/m^2 (400 psid) across the valve. The valve armature translated to the closed state, and subsequent attempts to open the valve were unsuccessful. The oscillation was attributed to excessive pressure drop across the armature at a flowrate of approximately 30 times the design flowrate of 4.54×10^{-4} kg/s (1×10^{-3} lb_m/s). The cause of the failure to open has been attributed to a fracture of the bobbin around which the armature coil is wound. The fracture permitted hydrazine to leak into the winding and cause a short. This appears to be a design weakness which is readily correctable.

Valve S/N 002 was installed in a tank-test setup as a sampling valve for hydrazine. The opening solenoid coil failed during a hydrazine sampling attempt. An investigation of the failure indicated a bobbin fracture similar to that of S/N 001.

Valve S/N 003 was subjected to a flight-type vibration test, and post-test performance was satisfactory. There was no evidence of leakage when the valve was vibrated

according to TOPS requirements. This valve has been successfully used in the APS Vacuum Test facility.

2. Flow-metering devices. Since the APS thrusters utilize the same propellant supply as the TCPS, they are required to operate over the same feed-pressure range (6.9×10^5 to 2.75×10^6 N/m^2 = 100 to 400 psia). The normal supply pressure for the APS thrusters is lower than the required supply pressure for the TCPS thruster. Whereas propellant flow to the TCPS thruster is metered by in-line feed-system components and a trim orifice, the nominal flow rate for the APS thrusters is so low (nominally 2.5×10^{-4} kg/s = 5.5×10^{-4} lb_m/s) that the feed-system components do not provide a sufficient pressure drop to maintain thrust at the desired level (0.22 to 0.44 N = 0.05 to 0.1 lb_f). An orifice would be so small that clogging would probably be a serious problem. Therefore, viscous metering was used.

Initial efforts to meet the propellant-metering requirement involved the use of small-diameter stainless steel capillary tubes. These tubes, with internal diameters ranging from 1.52×10^{-4} to 4.8×10^{-4} m (0.006 to 0.019 in.) were cut to length and coiled into a helix with a coil diameter of approximately 2.54×10^{-2} m (1 in.). The results of thruster testing using the capillary tubes for flow-metering were satisfactory, but the unit-to-unit attempts to predict flow characteristics and to trim for thruster performance variations were somewhat disappointing. This was primarily because at these very small internal diameters, slight perturbations in manufacturing tolerances have marked effects on flow and ΔP ($\Delta P \sim 1/D^4$). A coiled capillary with an ID of 2.02×10^{-4} m (0.008 in.) and approximately 0.304 m (12 in.) long (see Fig. 54) was the
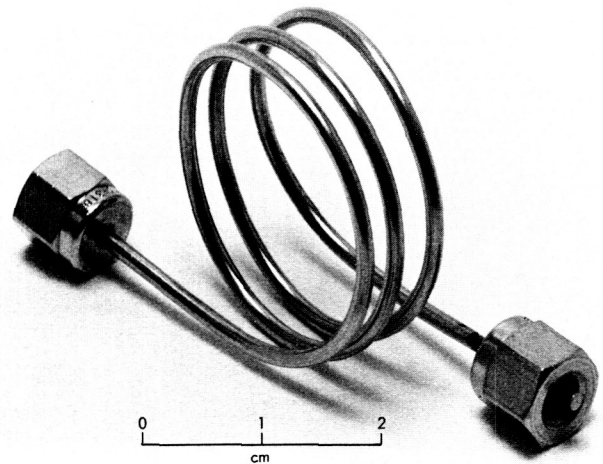

Fig. 55. Coiled capillary tubing

final selection for metering flow to the thrusters used during the Celestarium tests. Threaded fittings (Swagelok) were used to install the capillary tubes into the feed system.

As indicated, the problems in working with these small flow passages were associated primarily with the manufacturing tolerances of capillary diameters. Inspection of the tubing ID is limited to short distances from each end before coiling and even less thereafter. Capillary tubing with the smaller diameters is generally used to provide desired metering with a minimum tube length. However, as would be expected, the smaller diameters are the most sensitive to contamination, since a single particle can restrict or plug the passageway. After fabricating and measuring the pressure drop of the capillary tube, care must be taken to ensure that the metering properties do not change as a result of careless handling or contamination. The coiled tubing is bulky and delicate, and installation with other than threaded fittings is difficult.

CRES tubing in the sizes used for flow-metering is readily available; however, a requirement for capillary tubing from other feed system materials would present problems. Aluminum metering tubes are easily damaged, difficult to clean, and will corrode from moisture and pollutants in the atmosphere. Titanium metering tubes have not been fabricated, and forming titanium into small tubes may be an extremely difficult task. Use of CRES tubing in aluminum or titanium systems may present problems with galvanic corrosion (due to dissimilar metals) and will certainly require mechanical joints or transition tubes, since CRES cannot be joined to aluminum or titanium by conventional welding or brazing methods.

A flow-metering device which eliminates many of the adversities associated with a capillary tube is the Lee Company Viscojet (Fig. 56). This device consists of from one to five metering stages, with each stage having 19 orifices in series. Each stage consists of three discs—a center disc with the metering orifices and the two outer discs with communicating passageways between orifices and swirl chambers around each orifice (Fig. 57). A fourth plate closes the open sides of the communicating passageways and the swirl chambers. A fifth plate acts as a screen to prevent large particles from entering the metering orifices.

The Viscojet design provides several desirable features:

(1) All parts can be individually inspected and cleaned prior to assembly. The dimensions of the metering orifices can be verified by visual inspection.
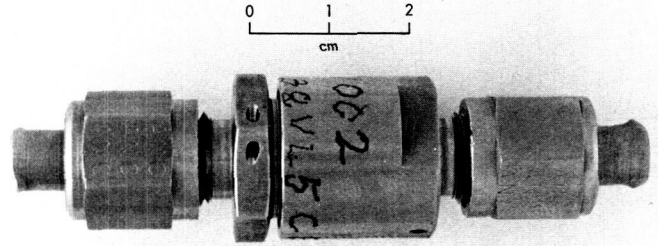
Fig. 56. Lee Company Viscojet housing
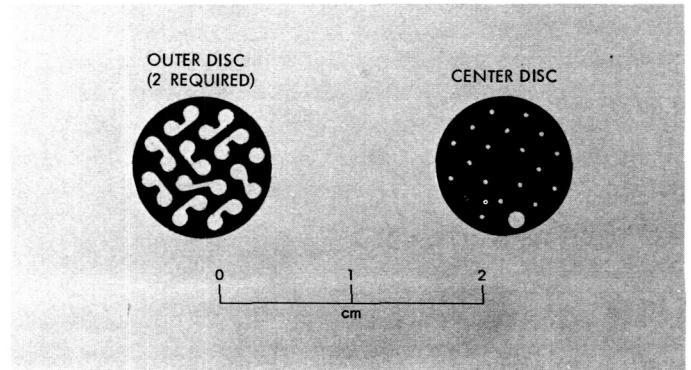
Fig. 57. Viscojet center and outer discs

(2) The minimum metering orifice diameter is 3.8×10^{-4} m (0.015 in.), and the screen hole diameter is 2.54×10^{-4} m (0.010 in.). Several of the screen holes communicate with each disc stage.

(3) Discs and housings can be manufactured from most materials. (An all-titanium unit has been demonstrated.)

(4) The Viscojet cartridge is compact and insensitive to handling damage during installation and usage. The cartridge can be sealed in an installation boss by welding.

Metered flow through the Viscojet has been shown to be consistent and relatively independent of temperature effects (Fig. 58) within the anticipated TOPS propellant temperature range of 4 to 32°C (40 to 90°F). Comparisons of hydrazine and water calibrations indicate that a water calibration is adequate to predict hydrazine metering characteristics (Fig. 59). Steady-state flow is consistent enough to provide the best source of flowrate data during small thruster operation with accuracy dependent only on the ability to measure the pressure drop across the Viscojet.
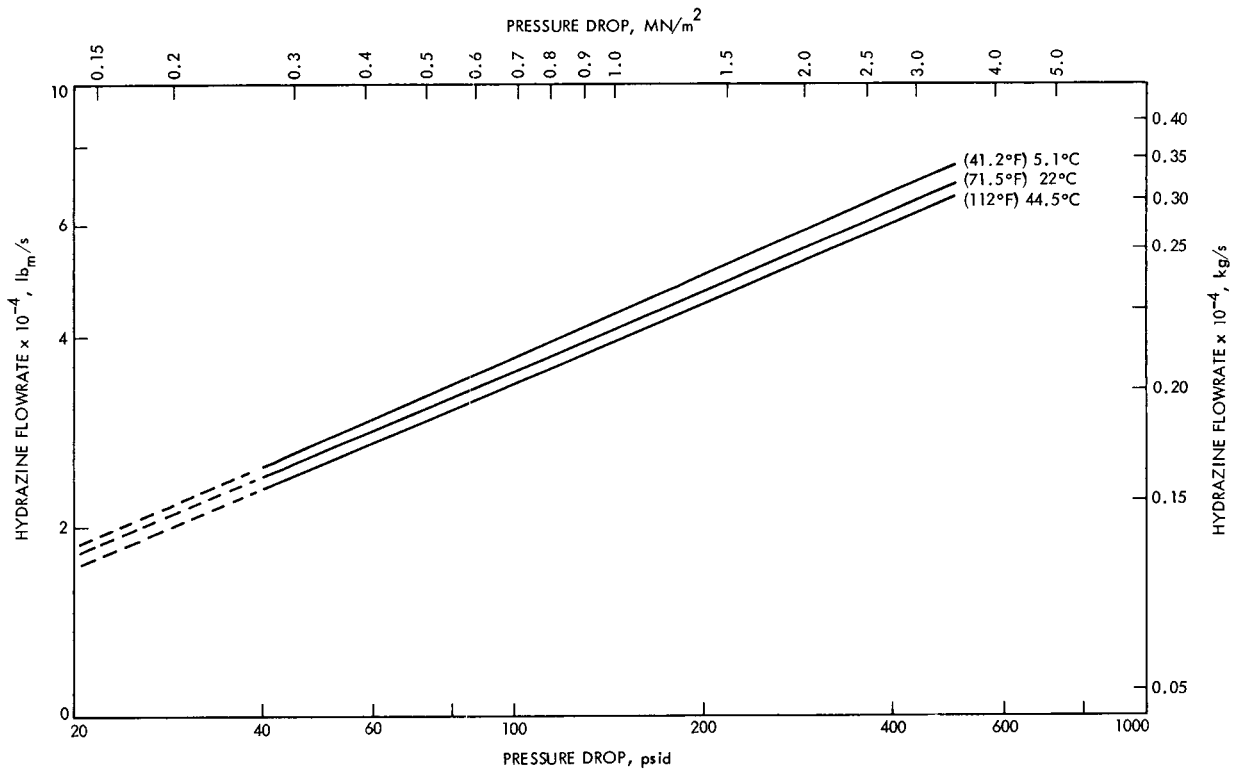
PRESSURE DROP, MN/m^2

Fig. 58. Viscojet calibration curve
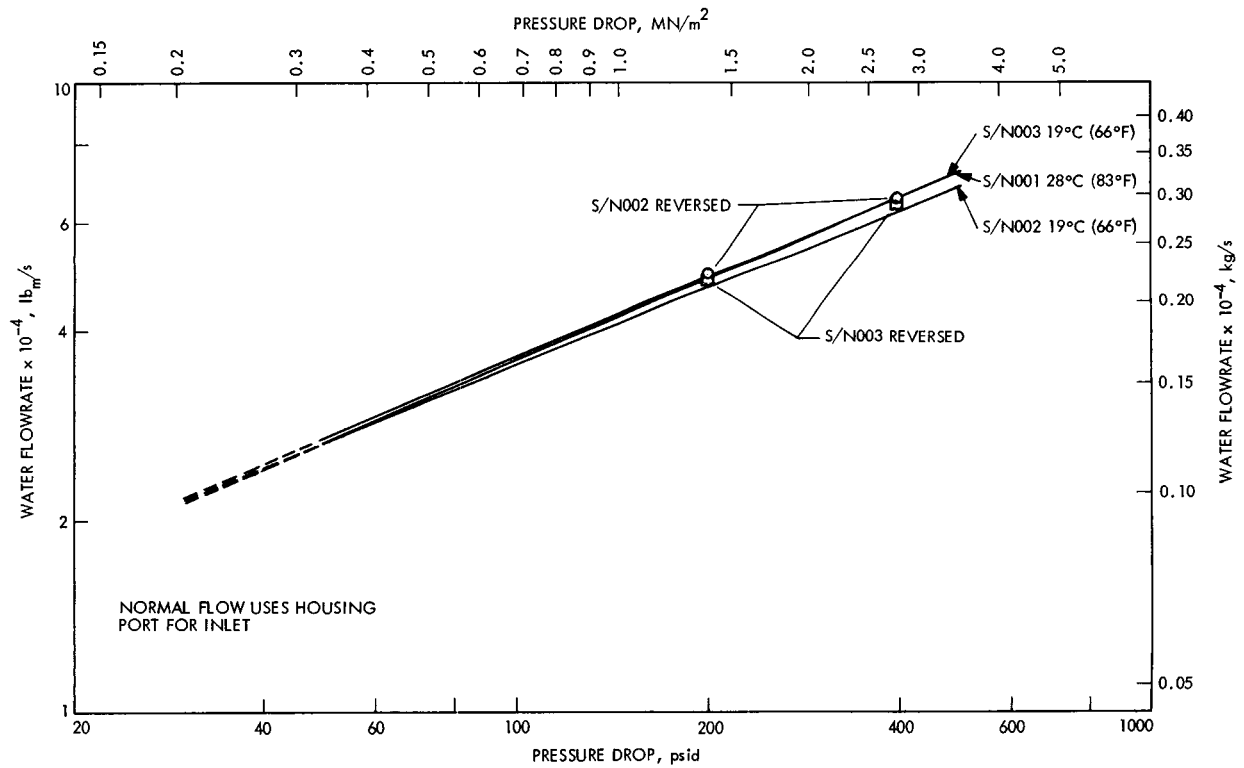
PRESSURE DROP, MN/m^2

Fig. 59. Viscojet waterflow data

Making metering devices adjustable requires additional effort. All devices investigated to date have provided constant flowrates with pressure drop, and desired flow is established by setting tank pressure. Flowrate trimming to compensate for variances in thruster-to-thruster variation has not been attempted with the Viscojet. However, the relationship between the number of discs and the pressure drop in stacked-disc-type filters was well established during the filter evaluation program. Minor variations in thruster performance could be "trimmed" to some constant level by adjusting the number of active discs in the filter stack. Pressure drop could be adjusted to the desired value by replacing the appropriate number of etched discs with blanks (no etched pattern). Trimming by this technique would result in matched filter-valve-metering device thruster assemblies. However, this technique would be of questionable value if the filter were to clog.

A final configuration for the TOPS metering device has not been established, but the following general design and performance criteria have been determined:

(1) Construction materials must be compatible with hydrazine; that is, they must have a minimum catalytic effect which would cause hydrazine decomposition. The material must be the same as that of the rest of the feed-system components to eliminate dissimilar metals and allow installation by welding to seal all external leak paths.

(2) Pressure drop at rated flow must be predictable and remain constant throughout useful life.

(3) The device must have minimum susceptibility to blockage by particulate contamination. Cleanliness should be verifiable by inspection of detail parts.

(4) It must be capable of being produced in quantity at a reasonable cost.

(5) It must either be adjustable or available in a range of sizes to enable tayloring for individual thrusters.

(6) Normal handling during installation and usage must not cause a change in metering characteristics.

3. Filters. The possibility of restricting or plugging the small-diameter passageways in the propellant-metering devices by particulate contamination is of concern in the operation of small thrusters. This requirement, plus the necessity of protecting the valve sealing surfaces, determined the filter criteria for the APS. Since the filtration requirements for the protection of the metering device

were not established, a decision was made to develop a 1-μm absolute-rated filter on the premise that this filtration capability was probably the minimum rating that would ever be required for the APS system. Thruster and valve tests with existing 5- and 15-μm (absolute) filters were conducted to evaluate component tolerance for the larger particles.

JPL specifications for stacked-disc-type filters (CS 505476 for a 1-μm and CS 505997 for a 15-μm absolute filter) were written and released for development only. Summaries of the design and performance requirements are shown in Table 19. These requirements can be met by the labyrinth-disc filter (Figs. 9 and 60). The Wintec Corporation is licensed to manufacture these filters from a JPL patent.

Five 1-μm filters were procured from Wintec and delivered to JPL on July 8, 1971. Acceptance data accompanying the filters indicated that all filters met the acceptance criteria of JPL Specification CS 505476. A sixth filter was tested by the vendor according to Table II of this specification. Reference 8 presents the results from the evaluation tests. In summary, the filter met or exceeded all of the test requirements. However, meeting the requirements as defined did not preclude all problems that were encountered. The filter was very sensitive to particulate contamination and required frequent cleaning to maintain the "clean element" flow capability. Since all tests were run with a Millipore 0.45-μm absolute filter upstream of the 1-μm filter, the clogging evidenced indicates that the element may have been filtering to a level below 1 μm absolute. This premise is substantiated by
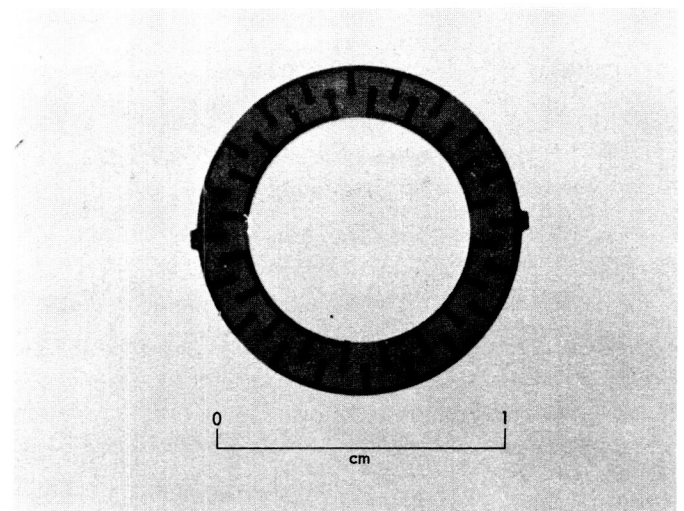

Fig. 60. Labyrinth filter disc

Table 19. Performance and design criteria, 1- and 15-μm (absolute) filters

Characteristic	Dimension	Requirement
Pressure, operating	N/m² (psig)	2.758×10^6 (400) (maximum)
proof	N/m² (psig)	5.516×10^6 (800) (minimum)
burst	N/m² (psig)	1.103×10^6 (1600) (minimum)
Leakage, external (He)	scc/s	10^{-7} (maximum) from 0 to 2.76×10^6 N/m² (400 psig)
Fluid, operating	—	N_2H_4 and GN_2
test	—	H_2O, He, and isopropynol
		15 μm: 6.8×10^{-2} (0.15) (nominal)
Flowrate (N_2H_4)	kg/s (lb$_m$/s)	1 μm: 1×10^{-3} (2.2×10^{-3}) (nominal)
		15 μm: 1.9 (4.1) (nominal)
(GN_2)	kg/s (scfm)	1 μm: 2.72×10^{-2} (6.0×10^{-2}) (nominal)
		15 μm: 3.4×10^4 (5.0) (maximum)
Pressure drop (N_2H_4, H_2O)	N/m² (psid)	1 μm: 5.86×10^5 (85) (maximum)
		15 μm: 6.9×10^4 (10) (maximum)
(isopropynol)	N/m² (psid)	1 μm: 1.034×10^6 (150) (maximum)
		15 μm: 1.4×10^4 (2) (minimum)
(GN_2)	N/m² (psid)	1 μm: 6.89×10^3 (1.0) (maximum)
Surge pressure (liquid)	N/m² (psi/s)	4.137×10^3 (600) (minimum)

the retention of all glass beads from the injected samples containing bead populations that were less than 2 μm in diameter.

Two aspects of the 1-μm filter performance indicate a need for improvement:

(1) The pressure drop across the assembled element was greater than desired and sensitive to the torque on the retaining screw. Test data indicate that the stack of discs was not at "solid height" at the final value of assembly torque (i.e., maximum disc compression).

(2) With the low torque value and allowable disc misalignment, fluid leakage across the inner and outer walls of the disc flow path probably accounted for much of the total flow. This premise is substantiated by some disc damage caused by erosion evident after evaluation testing. The damage was caused by relative motion between discs at high flowrates during pressure-drop and surge pressure testing.

When the 1-μm filter program was completed, several areas needed further effort to identify design criteria for the stacked-disc filters. These included evaluating a wide range of etch depths (5 to 40 μm) to establish relationships between

(1) Etch depth and glass bead rating.

(2) Etch depth and bubble point.

(3) Element assembly torque and absolute filtration rating (bubble point and glass beads).

(4) Element assembly torque and pressure drop.

The results of these tests are presented in Ref. 9. The etch pattern used for these tests was identical to that used for the 1-μm filter, except that the thickness of the inner and outer walls of the flow paths were increased from 2.54 $\times 10^{-4}$ to 1.52×10^{-3} m (0.010 to 0.060 in.) to reduce leakage across the walls and to provide sufficient support area to minimize distortions due to assembly torque. The thick-walled labyrinth filter is depicted in Fig. 61. Good data correlation was obtained for this four-reversal disc design for 10-, 20-, and 40-μm etch depths. However, the vendor had trouble etching 2- and 5-μm discs, and tests on these sizes were unsuccessful. Better etching methods are being investigated.

A photoetch process for titanium discs was investigated for the zero-flow-reversal pattern shown in Fig. 62. Discs with 10- and 20-μm etch depths were successfully developed. Preliminary flow tests performed on a final filter assembly indicated that the discs were orientation-sensitive. By assembling the discs so that all the non-etched lands were in line, the flow through the filter assembly increased by a factor of five for the same upstream pressure. This better orientation provided more
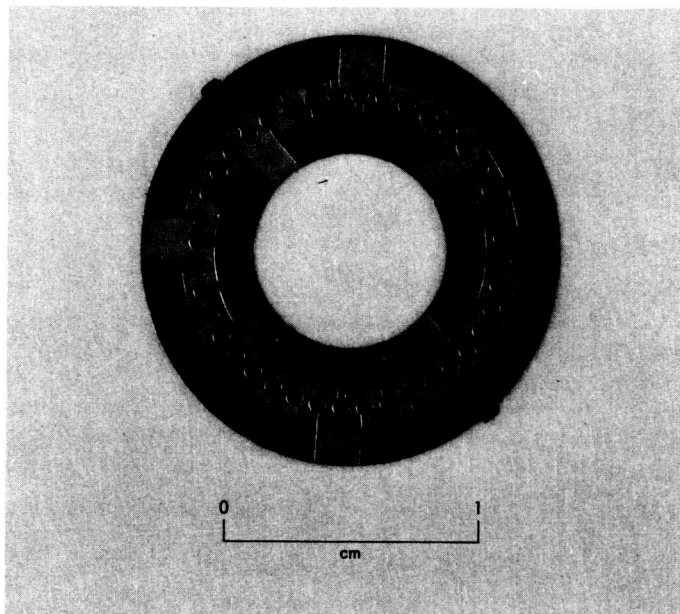
Fig. 61. Thick-wall labyrinth filter disc
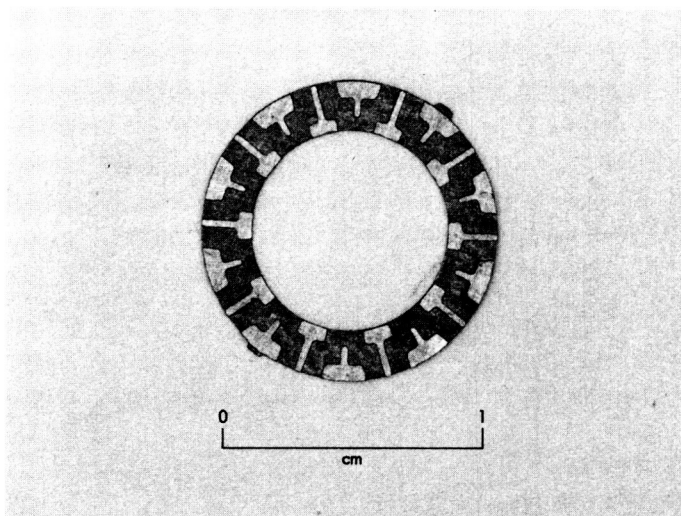
Fig. 62. "Zero—reversal" labyrinth filter disc

support and prevented disc deformation by compression loads. On the basis of these findings, future filter elements will be assembled with specially oriented discs.

K. Evaluation of Elastomeric Materials for Valve Seat Seals

TOPS requirements for reliable valves to control thruster operation during long-duration missions are more stringent than any specified for previous JPL spacecraft. Since the ability to meet these requirements had never been

verified by actual testing, and since scheduled launch dates would preclude real-time verification testing, component performance characteristics must have significant design margin to provide confidence in mission success. Because of the concern for propellant leakage during long-duration missions, a program to evaluate the performance of valve seat seals was implemented. This program consisted of accelerated testing of existing valves and evaluation of promising seat-seal materials.

Valve testing was reported in Section J of this report; Table 20 shows the kinds of "soft" seats tested. As indicated, only six materials were considered suitable for hydrazine usage. Of the six, the DuPont Teflons TFE and FEP, which represent aerospace standards, are readily available in many "off-the-shelf" valve designs. Ethylene propylene rubber (EPR) was considered the best of the commercially available elastomers. AF-E-102, a HYSTL-filled ethylene propylene terpolymer (EPT), was selected as the most promising of the recently developed elastomers and is more hydrazine-compatible than EPR. DuPont's new fluoroelastomer, a copolymer of TFE Teflon and perfluorovinylmethyl ether, which is known by various names ("new" teflon, LRV-448, ECD-006, and AF-E-124D), was the latest candidate for the seat-seal material evaluation program.

Table 20. Soft seat-seal material evaluated in valves

Material	Valves in which material was evaluated
Teflon (TFE)	Carleton P/N 2217-001-2-1
	Marquardt P/N 228683; 228684
	Marquardt P/N T-8700
	Marquardt P/N X24572
	Moog P/N 010-58176-1
	Moog P/N 010-58723-1
	Parker P/N 5696050
Teflon (FEP)	Rocketdyne P/N 407559; 409402
HYSTL-filled EPT (AF-E-102)	Marquardt P/N 228683
	Marquardt P/N X24572
	Marquardt P/N X28051
	Wright P/N 15548
DuPont "new" Teflon (LRV-448)	Marquardt P/N 228683
	Marquardt P/N X24572
	Wright P/N 15548
Fluoroelastomer (AF-E-124D)	Marquardt P/N X24572
	Marquardt P/N 228683
EPR (Parker E-515-8)	Allen P/N 13940-02
	Wright P/N 15548

The valve sealing material evaluation program was conducted in two phases. In the first phase, a short-term exposure (approximately 3 weeks) to hydrazine at ambient temperature was used to screen doubtful materials. Material samples and a quantity of hydrazine were sealed in a glass vial, which was instrumented with a gage to measure the autogenous vapor pressure of the propellant. These screening tests were adequate to eliminate unsatisfactory materials and to identify doubtful material properties which needed further evaluation. Measurements were made before and after exposure to determine

(1) Changes in weight and volume (swell).

(2) Loss of physical properties (strength, hardness, etc.).

(3) Degradation of surface characteristics (tackiness, flaking, blistering, etc.).

The second phase of the seat-seal evaluation program involved seat-seal design and processing, valve seat fabri-

cation, and testing of valves with candidate elastomeric seat seals in inert fluids and hydrazine (see Table 21). Valve seat designs utilize two kinds of seals—those cut from sheet-stock material and those which are molded and cured.

The Allen P/N 13940-02 and the Wright P/N 15543 valves, which incorporate sheet-stock EPR seals, were tested in hydrazine. The Marquardt P/N X24572 and Wright P/N 15548 valves were modified with seat seals from sheet-stock EPT and "new" Teflon and tested in inert fluids and hydrazine. Seat seals for the Marquardt R4D valves, P/N 228683, were molded from EPT and "new" Teflon. R4D valves were modified with these seals, and the EPT seat seals were tested in inert fluids and hydrazine. The "new" Teflon seals were unsatisfactory for use in the R4D valve seat design because they did not have sufficient strength to resist being drawn into the flow path by flow forces generated by high-velocity liquid passing the seal cavity. As shown in Table 20, many valves with TFE

Table 21. Valve seat design support test summary

Test series	Material	Configuration	Cycle/temperature history	Maximum GN$_2$ leakage at 414 × 10^3 N/m^2 (60 psig), scch		Observations and remarks
1	Grade 7 TFE	Constrained	25,000/ambient 25,000/149°C (300°F)	2.0 1.3		Excess leakage after cooldown from 149°C (300°F). Permanent set from 149°C (300°F) operation precludes seal.
2	Kel-F 81	Constrained	5,000/ambient 5,000/149°C (300°F)	0.0 0.0		Began leaking at 121°C (250°F) on cooldown. Leakage increased with decreasing temperature. Permanent set at 149°C (300°F) precludes seal.
3	Kel-F 81	Spring-loaded	25,000/ambient 25,000/149°C (300°F) 1,000/ambient	10 0.0 15		Imprint indicates out-of-parallel interface of seal with land. Depth of imprint not excessive.
4	AF-E-102 (ethylene propylene terpolymer)	Constrained	25,000/ambient 25,000/149°C (300°F) 1,000/−40°C (−40°F)	0.0 0.0		Began leaking at −1.1°C (30°F) on cooldown. Cycling did not recover seal. Excessive deformation load at 149°C (300°F).
				Sample		
				1	2	
5	AF-E-102 (2 samples)	Spring-loaded	26,000/ambient 30,000/−40°C (−40°F) 1,000/93°C (200°F) 5,000/121°C (250°F) 20,000/149°C (300°F) 19,000/−46°C (−50°F)	1.0 1.5 0.0 0.4 1.4 120[a]	1.0 1.5 0.0 0.4 0.0 1.7	
6	Grade 7 TFE	Spring-loaded	50,000/ambient 25,000/149°C (300°F) 25,000/−40°C (−40°F)	0.5 0.7 5.5		

[a]Reduced to 0.0 on warming to −12.2°C (+10°F). Subsequent check at −46°C (−50°F) indicated 0.0 scch.

and FEP Teflon seat seals were tested during the seal evaluation program. The performance of all valves with TFE and FEP Teflon seals over the TOPS temperature range of 4 to 32°C (40 to 120°F) was satisfactory.

1. Sheet-stock seals. Sheet-stock AF-E-124D, AF-E-102, and TFE Teflon seals were tested over a temperature range from −40 to +268°C (−40 to +300°F) during a comparative endurance test program which Marquardt conducted under JPL contract to select seal material for the P/N X28051 latching valve. These tests were conducted with modified seats in the Marquardt P/N X24572 valve. The dimensional stability of the AF-E-102 appeared superior to that of TFE and AF-E-124D, and this stability resulted in better sealing characteristics. The results of the endurance tests led to the AF-E-102 material becoming the prime candidate for TOPS valve seat seals. Table 21 presents a summary of the seal evaluation program showing test materials, conditions, and results. These test results were documented by Marquardt in an Internal Report, MIR 404, and will be included in the final report to Langley Space Flight Center on their Resistojet Program.

The long-duration hydrazine exposure tests for EPR (Parker Compound E-515-8) sheet-stock seals showed this material to be unsatisfactory as a valve seat because of excessive swelling of the seals. Short-term (21-day) exposure tests had shown some catalytic effect causing hydrazine decomposition (3.45×10^4 N/m² = 5-psid) pressure increase and a small weight gain (2%), which indicated that this material might not be satisfactory for long-term hydrazine service. These results also indicate that EPR should not be used for hydrazine control valve seats if the valve is being used to meter hydrazine. As indicated in an earlier section, in one 3-month test, the EPR seal swelled sufficiently to prevent flow through the valve when the armature was actuated. In the second 9-month test, seal swelling caused the pressure drop for a fixed flowrate to increase from 6.9×10^4 to 3.66×10^5 N/m² (10 to 53 psid).

With the exception of the problems with EPR seals, seat seals cut from sheet-stock material were satisfactory for use in small valve seats. Some method to limit the applied load appears to be needed to enhance seat durability during operation in the TOPS temperature range, and load-limiting is mandatory for high-temperature (above 71°C = 160°F) operation.

2. Molded seals. Techniques were derived for satisfactory in-place molding and curing of seat seals for the Marquardt R4D valve. This valve was selected for molded

seat-seal evaluations because of the wealth of valve performance data accrued during the Apollo program and the availability of several surplus valves which had completed the Apollo test program. The R4D valve seat uses TFE Teflon for the "soft" seal and depends on a metal-to-metal stop downstream of the TFE to limit the impact load during closing. The thin disc of TFE is almost completely encapsulated by metal. Only a small annulus around a hole through the center of the Teflon disc contacts the poppet and effects the seal when the valve is closed (Fig. 63). The primary objective in replacing the Teflon seal was to simplify seat fabrication by minimizing the number of critical dimensions and eliminating in-process precision machining and final matching of armature-seat pairs. Secondary objectives were to reduce the leakage rate, to decrease susceptibility to particulate contamination, and to improve radiation resistance.

A seal evaluation program was conducted under JPL contract to the Marquardt Corporation, during which an R4D valve was used as a test item. The R4D valve seat is not designed for a very high-velocity flow in the region of
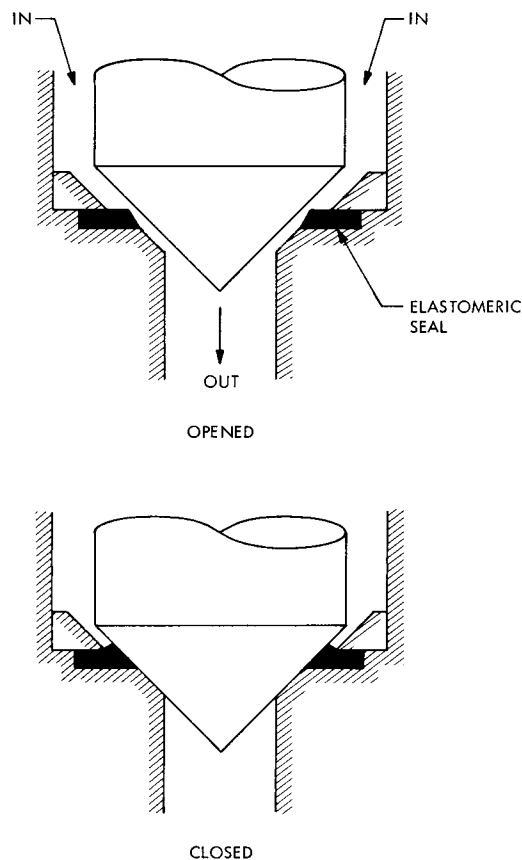

Fig. 63. Conical valve-seating configuration

the elastomer (Fig. 63), as sufficient dynamic forces can be generated to pull the elastomeric seal from its retention cavity and close the annulus around the poppet. Weaker elastomeric materials are also subject to erosion. This high-velocity-induced reduction in flow area is aggravated at higher temperatures.

A summary of the seal evaluation program and the elastomers tested is presented below:

"New" Teflon (Phase I). These seals were molded by Stillman Rubber Company from stock which JPL had procured from DuPont and furnished to Stillman. The Marquardt Corporation fabricated valve seats and tested two valves with water over the temperature range of 4 to 71°C (40 to 160°F). The results of these tests, reported in Ref. 10, indicated that the seats sealed well but the flow dynamic forces caused a significant reduction in seat area. The test was terminated because of excessive leakage after 7500 cycles. Examination of the disassembled valve revealed that portions of the seal had eroded, leaving a leak path across the seal. Although these seals apparently did not possess sufficient strength to perform properly in the R4D seat design, stock shelf-life and post-cure uncertainties of the seals indicated that the tests should be rerun to evaluate molded seals which had been properly processed.

AF-E-102 (inert fluids). These seals were molded by TRW Systems Group from stock which TRW supplied to the AF Materials Laboratory (LNE). Marquardt fabricated valve seats and tested two valves with water over a temperature range from 4.5 to 71°C (40 to 160°F). The test results, reported in Ref. 11, indicated that the seats sealed well and that flow reduction was evidenced only at the higher temperatures. Since these seals appeared satisfactory after 25,000 cycles, a decision was made to initiate testing with temperature-conditioned hydrazine.

AF-E-102 (hydrazine). The valves from the inert fluid tests were installed in a test setup which provided temperature-conditioned (4.5 to 49°C = 40 to 120°F) hydrazine as the test fluid. The test results, reported in Ref. 12, show that the seats sealed well and were not damaged by hydrazine testing. The earlier reduction in seat flow area under dynamic loading was the only difficulty evidenced with AF-E-102 seat seals. Proper design to minimize flow velocity effects should provide satisfactory seals for hydrazine flow-control valves. These valves are scheduled for future radiation-exposure testing to determine the comparative resistance between the AF-E-102 and the TFE seals.

"New" Teflon (Phase II). These seals were molded by DuPont using a JPL-furnished mold. The elastomer looked significantly different physically from the original one molded by Stillman in that the DuPont material was homogeneous and dark brown in color. Marquardt Corporation assembled these molded seats into two valves for testing. In both cases, the reduction in flow was so severe that valve testing with water could not be conducted. The test program was redirected to test sheet-stock seat seals rather than molded seals. The sheet-stock seals performed very well in hydrazine, indicating that a properly designed seat using "new" Teflon is satisfactory for hydrazine service. Marquardt will report the results of this testing in a future report.

L. Magnetic Field Constraints

The TOPS requirements for spacecraft magnetic field control were an order of magnitude more restrictive than those for previous JPL programs. The magnetometer (science magnetic field experiment) requires the minimum spacecraft-generated magnetic field at its location, which is 7.6 m (25 ft) from the propulsion bay, to be 10^{-11} tesla (0.01 gamma). The electrical actuators for the propellant control valves are among the worst offenders of this constraint in that, by design, relatively powerful magnetic fields are used to actuate the valve mechanisms when thruster operation is required.

Resources were not available to explore this problem in depth during the TOPS program, but the cursory examination which was accomplished indicated that this area requires a significant amount of investigation to ensure that effective control can be obtained. The magnetic fields of several existing valve designs were mapped at JPL, and the results applicable to the APS size are presented in Table 22. Attempts to correlate these data have not been completely successful because of the wide variance in valve operating conditions. In no case was the magnetic field of the energized solenoid low enough to meet the desired constraints without compensation. The unenergized field strength of some valves without permanent magnets did, however, approach the design goal. Since the valves operate only intermittently, scheduling of magnetometer observations during quiescent periods may be required to circumvent valve-induced magnetic field anomalies. The limited data available indicate that the most promising approach to minimizing valve-induced dynamic field interference involves limiting the strength of the generated fields by proper design rather than trying to shield or compensate an unnecessarily large field strength. The static magnetic fields from valve permanent

Table 22. Experimental data from valve magnetic field tests

Vendor and part number	Test number	Maximum field strength at 0.15 m (6 in.), nanoteslas		Valve type	Valve electrical conditions	Comments
		Energized	De-energized			
Allen 14011-01 (Material: Permendur)	1	2.16×10^4	1.9×10^2	Dual-coil in-line solenoid	24 V 0.1 A	7.6×10^4 m (0.030-in.) gap in housing
	2	1.35×10^4	—			Small gap
	3	1.0×10^4	54			No gap
Allen 13950 (Material: 430F S.S.)	1	2.1×10^4	2.97×10^3	Dual-coil in-line solenoid	24 V 0.05 A	
	2	2.86×10^4	2.97×10^3		31 V 0.1 A	
Wright 15548	1	2.98×10^3	1.0×10^3	In-line solenoid	26 V	
Marquardt X 28051	1	1.02×10^4	1.92×10^3	Magnetic latching	28 V	Opening coil
	2	1.0×10^4	1.41×10^3			Closing coil

magnets, however, can be sufficiently compensated on the spacecraft system level.

M. New Technology Requirements

As a result of this supporting research and advanced development effort, several items have been identified as being desired technological improvements of existing hardware and techniques. Some of these items are:

(1) All-titanium feed system components, specifically, the wetted surfaces (e.g., solenoid valves).

(2) Solenoid valves with very low magnetic fields during static state and minimal magnetic fields during actuation, as well as very low power during use.

(3) APS-size thrusters capable of operating with mono-methyl-hydrazine (MMH) and other blends for application of this attitude propulsion principle to spacecraft for which the primary on-board fuel is other than hydrazine.

(4) Flowmeter capable of steady-state and transient response at flowrates on the order of 4.5×10^{-4} kg/s (10^{-4} lb$_m$/s).

(5) Thrust-measuring stand capable of steady-state and transient response at very low thrust levels (on the order of 0.22 to 0.44 N = 0.05 to 0.1 lb$_f$); the stand must be isolated from outside perturbations.

(6) A very small (low thermal mass), very high (on the order of 1100°C = 2000°F) temperature-measuring device that does not interfere with the flowstream.

(7) A definition of limit-cycle capability for 0.44-N (0.1-lb$_f$) catalytic thrusters (i.e., the minimum impulse bit capability, minimum required start temperature, and maximum life expectancy).

(8) Determination of long-term materials compatibility with hydrazine for both metals and polymers.

(9) Combination of the best features of the catalytic and electrothermal thrusters for maximum reliability.

Nomenclature

A_t throat area

c^* characteristic velocity

C_F thrust coefficient, dimensionless

d differential operator

d_e effective passage diameter

F thrust

G superficial mass flux

I_{sp} specific impulse

$\dot{m}$ propellant mass flowrate

N_{PL} pressure loss modulus, dimensionless $\equiv \rho d_e^3 \Delta P / \mu^2 \lambda$

N_{Re} Reynolds number, dimensionless $\equiv 4\dot{m}/\pi d_e \mu$

p_a ambient pressure

P_c chamber total pressure

P_{ft} fuel tank pressure

T_c catalyst bed temperature

ΔT temperature difference

X ammonia dissociation fraction

α coefficient of thermal expansion

ΔP differential pressure

$\Delta P_c / \overline{P}_c$ relative chamber pressure roughness (peak to peak)

ϵ nozzle expansion-area ratio, dimensionless

η_{CF} thrust coefficient efficiency, dimensionless

λ effective length of passage

μ absolute viscosity

π 3.14159 . . .

ρ density

θ time

References

1. *Policies and Requirements for Thermoelectric Outer Planet Spacecraft Advanced Systems Technology Project,* TOPS Project Document No. 1, 701-24 (Internal Document), Jet Propulsion Laboratory, Pasadena, Calif., Feb. 14, 1969.

2. Nunz, G. J., "Experimental Evaluation of a Miniature Catalytic Hydrazine Thruster," AIAA Paper No. 71-706, AIAA/SAE 7th Propulsion Joint Specialist Conference, Salt Lake City, Utah, June 14–18, 1971.

3. Ferrera, J. D., and McKown, P. M., *A Method for Calculating Steady-State Thrust and Flow Rate Levels for Mariner IV Type Attitude Control Nitrogen Gas Jets,* Technical Report 32-1353, Jet Propulsion Laboratory, Pasadena, Calif., Dec. 1, 1968.

4. Schmitz, B. W., *et al., Development of Design and Scaling Criteria for Monopropellant Hydrazine Reactors Employing Shell 405 Spontaneous Catalyst,* Final Report RRC-66-R-76, (NASA Contract NAS7-372), Rocket Research Corp., Seattle, Wash., Jan. 18, 1967.

5. Drenning, C. K., *Post Test Analysis of TMC R-25A 0.1-lb Thrust Monopropellant Engine (P/N T-17412, S/N 002),* The Marquardt Company, Van Nuys, Calif., March 21, 1972 (Ref. –/52/19599).

References (contd)

6. Cannon, W. A., English, W. D., and Robson, J. H., *Pressurization Systems Design Guide, Vol. III, Pressurant Gas Solubility in Liquid Propellants*, Report DAC-60510-F1 (NASA Contract NAS7-548), National Aeronautics and Space Administration, Washington, D. C., July 1968.

7. Long, H. R., and Bjorklund, R. A., *Trajectory Correction Propulsion for TOPS*, Technical Report 32-1571, Jet Propulsion Laboratory, Pasadena, Calif., Nov. 1972.

8. *Evaluation Test Report Filter Assembly Fluid, 1 Micron Absolute, Disc Labyrinth Part No. 9-580*, Report No. 247, Wintec Corporation, Los Angeles, Calif., May 1971.

9. *Development Test Report, Etched Labyrinth Disc Filter Assembly, 2 Micron, 5 Micron, 10 Micron, 20 Micron, 40 Micron*, Test Report TR 254, Wintec Corporation, Los Angeles, Calif., Oct. 1971.

10. Lynch, R., *Test Report—Evaluation of DuPont LRU 488 as a Seat Seal Material in the Marquardt R4D Engine Valve*, Report S-991, TMC Program 7208-3, The Marquardt Company, Van Nuys, Calif., Jan. 1971.

11. Lynch, R., *Evaluation of AF-E-102 Elastomer as a Seat Seal Material for the Marquardt R4D Valve*, Report S-1012, The Marquardt Company, Van Nuys, Calif., July 1971.

12. Lynch, R., *Test Report—Evaluation of AF-E-102 Elastomer in N_2H_4 as a Seat Seal Material for the Marquardt R4D Valve*, Report S-1034, The Marquardt Company, Van Nuys, Calif., Jan. 1972.

Bibliography

Baughman, L. E., "TOPS Spacecraft Propulsion Subsystem," *Aeronautics and Astronautics*, pp. 77–82, Sept. 1970.

Chirivella, J. E., Moynihan, P. I., and Simon, W., "Small Rocket Exhaust Plume Data," *JPL Quarterly Technical Review*, Vol. 2, No. 2, Jet Propulsion Laboratory, Pasadena, Calif., July 1972.

Hagler, R., Jr., *Valve Assembly, Propellant Shutoff, Solenoid-Actuated, Bi-Stable, Detail Specification for*, Part Specification No. CS506226, Rev. A, Jet Propulsion Laboratory, Pasadena, Calif., Jan. 7, 1972.

Hagler, R., Jr., *Valve Assembly, Propellant Flow Control, Solenoid-Actuated, Detail Specification for*, Part Specification No. CS505999, Rev. C, Code I.D. 23835, Jet Propulsion Laboratory, Pasadena, Calif., Jan. 17, 1972.

Hagler, R., Jr., *Valve Assembly, Propellant Flow Control, Solenoid-Actuated, Detail Specification for*, Part Specification No. CS506221, Rev. B, Code I.D. 23835, Jet Propulsion Laboratory, Pasadena, Calif., Jan. 18, 1972.

Bibliography (contd)

Hagler, R., Jr., *Valve Assembly, Propellant Shutoff, Solenoid-Actuated, Bi-Stable, Detail Specification for*, Part Specification No. CS506087, Rev. D, Code I.D. 23835, Jet Propulsion Laboratory, Pasadena, Calif., Jan. 18, 1972.

Holcomb, L. B., *Satellite Auxiliary-Propulsion Selection Techniques*, Technical Report 32-1505, Jet Propulsion Laboratory, Pasadena, Calif., Nov. 1, 1970.

Moynihan, P. I., "TOPS Attitude Propulsion Subsystem Technology," *JPL Quarterly Technical Review*, Vol. 1, No. 3, Jet Propulsion Laboratory, Pasadena, Calif., Oct. 1971.

Moynihan, P. I., "Minimum Impulse Tests of 0.45-N Liquid Hydrazine Catalytic Thrusters," *JPL Quarterly Technical Review*, Vol. 2, No. 1, Jet Propulsion Laboratory, Pasadena, Calif., July 1972.

Simon, W., *Plume Backscatter Measurements Using Quartz Crystal Microbalances in JPL Molsink (Molecular Sink)*, Technical Memorandum 33-540, Jet Propulsion Laboratory, Pasadena, Calif., May 15, 1972.

Test Report—Evaluation of DuPont LRV 448 as a Seat Seal Material in the Marquardt R4D Engine Valve, Final Report, Report No. S-991, The Marquardt Company, Van Nuys, Calif., Jan. 1971.

Weiner, R. S., *Basic Criteria and Definitions for Zero Fluid Leakage*, Technical Report 32-926, December 15, 1966.